

UNIVERSIDAD DE COSTA RICA  
SISTEMA DE ESTUDIOS DE POSGRADO

**INTERACCIÓN DE *BRUCELLA* SP. CON PROTEÍNAS DEL SUERO  
DE SU HOSPEDERO**

**INTERACTION OF *BRUCELLA* SP. WITH HOST SERUM PROTEINS**

Tesis sometida a la consideración de la Comisión del Programa de Estudios de Posgrado en  
Microbiología, Parasitología, Química Clínica e Inmunología para optar al grado y título de  
Maestría Académica en Microbiología con Énfasis en Bacteriología

GABRIELA GONZÁLEZ ESPINOZA

Ciudad Universitaria Rodrigo Facio, Costa Rica

2018

## **DEDICATION**

Quiero dedicar todo este esfuerzo a mi madre Ana Lucía Espinoza, sin su apoyo no lo hubiese logrado---

## ACKNOWLEDGMENTS

En primer lugar, doy gracias infinitas a Dios, a mi madre y toda mi familia que **INCONDICIONALMENTE** me han amado y apoyado en este proceso de aprendizaje. Simplemente no lo hubiese logrado sin su apoyo.

A mi tutor, Carlos Chacón, por creer en mí y permitirme ser parte del “experimento”. Gracias por ser un modelo a seguir. Siempre agradeceré los sabios consejos académicos y de vida que compartió conmigo, así como su entusiasmo y su capacidad inagotable de soñar.

A Norman Rojas y Esteban Chaves por haber depositado su confianza en mí, enseñarme y aconsejarme durante todo este tiempo que hemos trabajado juntos.

A Bruno Lomonte por su indispensable ayuda en el análisis proteómico y su guianza en mi proceso de aprendizaje

A Edgardo Moreno por ser un gran maestro académico y brindarme buenas oportunidades.

Al Dr. Ignacio Moriyón, Dra. Raquel Conde y a los integrantes del Departamento de Microbiología y Parasitología de la Universidad de Navarra por abrirme las puertas de su laboratorio y recibirme como una compañera más. Forman parte de una experiencia inolvidable en mi vida.

Al equipo de Navarra Biomed por toda su colaboración en el análisis proteómico realizado en Pamplona.

A José Molina por su colaboración en el análisis de datos.

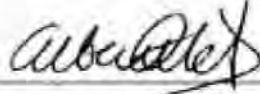
A la familia de Bacteriología Médica de la Facultad de Microbiología (Yeimy, Jhonatan, Juan y Neysa). Muchas gracias por ser excelentes compañeros de trabajo.

A Pamela Altamirano, más que una compañera de trabajo una amiga. Muchas gracias por escucharme en cada momento.

A todo el personal del Centro de Investigaciones en Enfermedades Tropicales, amigos fuera de la “U” y todos los compañeros de investigación que estuvieron conmigo durante este periodo (Ricardo Mora, Cristina Gutiérrez, Tatiana Murillo, Adriana Badilla, Jazmín Meza, Diana López, Elías Barquero).

A Ñukie por su fidelidad incondicional en cada desvelada.

“Esta tesis fue aceptada por la Comisión del Programa de Estudios de Posgrado en Microbiología, Parasitología, Química Clínica e Inmunología de la Universidad de Costa Rica, como requisito parcial para optar al grado y título de Maestría Académica en Microbiología con Énfasis en Bacteriología”



---

Dr. Alberto Alape Girón, *PhD*

**Representante del Decano  
Sistema de Estudios de Posgrado**



---

Dr. Carlos Chacón Díaz, *PhD*

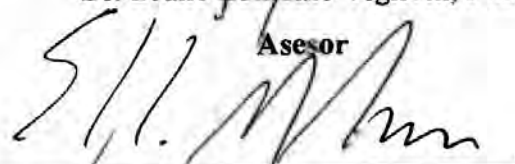
**Director de tesis**



---

Dr. Bruno Lomonte Vigliotti, *PhD*


**Asesor**



---

Dr. Edgardo Moreno Robles, *PhD*

**Asesor**



---

Dr. César Rodríguez Sánchez, *PhD*

**Director**

**Programa de Posgrado en Microbiología, Parasitología y Química Clínica**

---

Gabriela González Espinoza

**Candidata**

## TABLE OF CONTENTS

DEDICATION	ii
ACKNOWLEDGMENT	iii
APPROVAL	iv
TABLE OF CONTENTS	v
RESUMEN	vi
ABSTRACT	vii
LIST OF TABLES	viii
LIST OF FIGURES AND ILLUSTRATIONS	ix
ABBREVIATIONS	xii
1. INTRODUCTION.....	1
1.1 <i>Brucella</i> uses a furtive strategy to evade innate immunity.....	2
1.2 The complement system: activation and regulation.....	4
1.3 Complement evasion strategies used by pathogenic bacteria.....	6
1.4 Interaction between humoral innate components and <i>Brucella</i> .....	7
1.5 Proteomic quantification by mass spectrometry.....	9
2. JUSTIFICATION.....	11
3. HYPOTHESIS.....	12
4. OBJECTIVES.....	13
5. MATERIALS AND METHODS.....	14
5.1 Ethics.....	14
5.2 Serum samples collection and storage.....	14
5.3 Bacterial strains and growth conditions.....	14
5.4 Antibodies.....	15
5.5 Sensitivity to the bactericidal action of non-immune serum.....	17
5.6 Determination of complement consumption by <i>Brucella</i> .....	17
5.7 Adsorption of serum components by <i>Brucella</i> and protein identification.....	17
5.8 Label free data analysis.....	19
5.9 Immunodetection of complement factors.....	20
5.10 Prothrombin and Partial Thromboplastin Time determination.....	20
5.11 Statistics.....	20
6. RESULTS.....	22
6.1 Resistance to bactericidal action of serum is an intrinsic trait of <i>Brucella</i> organisms, regardless of the host preference.....	22
6.2 <i>Brucella</i> ability to bind serum proteins is species and host dependent.....	22
6.3 Adsorption of serum components by <i>Brucella</i> organisms.....	25
6.4 Identification of serum components adsorbed by <i>B. abortus</i> .....	25
6.5 Wild-type and LPS mutants show differences in the serum protein interaction profile.....	28
6.6 Label free quantitative proteomics analysis of sheep serum proteins eluted from wild-type <i>Brucella</i> and LPS mutants.....	36
7. DISCUSSION.....	48
8. CONCLUSIONS AND FUTURE PERSPECTIVES.....	55
9. REFERENCES.....	56
10. APPENDIXES.....	63

## RESUMEN

El género *Brucella* ha evolucionado como un patógeno furtivo capaz de evadir el reconocimiento y la activación de varios elementos de la inmunidad innata, entre ellos el sistema del complemento y los neutrófilos polimorfonucleares. Sin embargo, los mecanismos mediante los cuales estas bacterias logran modular la respuesta inmune innata han sido poco estudiados. Durante una brucelosis, los factores humorales presentes en el suero son la primera línea de defensa. Este trabajo pretende contribuir a comprender cómo estos elementos interactúan con *Brucella*. El objetivo de este estudio consistió en identificar y cuantificar las proteínas séricas del hospedero que interactúan con la superficie de *Brucella*. Por lo tanto, se desarrolló una estrategia para recuperar proteínas séricas que se unen a la superficie bacteriana de cepas silvestres y mutantes de membrana externa de *Brucella abortus* y *Brucella melitensis*. Por medio de un abordaje proteómico se determinó que existen diferencias cualitativas y cuantitativas en los perfiles de interacción de acuerdo a la composición de la membrana externa de la bacteria. Se identificaron 96 proteínas del suero que interactúan con la bacteria. La mayoría de las proteínas identificadas se encontraban relacionadas al sistema de complemento y de coagulación. Además, se detectaron proteínas reguladoras del sistema de complemento en la superficie de *Brucella*. Basándose en los resultados, se proponen una serie de modelos conceptuales para sustentar nuestra hipótesis que asocia la interacción con proteínas del suero como un evento clave en la modulación de la inmunidad innata en la brucelosis.

**Palabras clave:** *Brucella*, label-free, suero, sistema de complemento, respuesta innata, interacción.

## ABSTRACT

*Brucella* genus has evolved as a stealthy pathogen capable of avoiding, the recognition and activation of several elements of the innate immune response, including complement and PMNs. However, the mechanisms by which brucellae modulate the innate immune response are not fully understood. Since humoral factors are the first to confront the extracellular bacteria, we tried to understand in how these elements interact with the bacterium. The purpose of this study was to identify and quantify host serum proteins that interact with the surface of *Brucella* organisms. Therefore, we developed a strategy for the identification and quantitation of serum proteins that bind to surface of the bacteria and compared the interaction profiles between wild type and LPS mutants. Most of the identified proteins were related to the complement and coagulation systems. Complement system regulators proteins were identified in *Brucella* surface. Based on our results we propose a series of conceptual models to sustain our hypothesis that interaction with serum factors is a key event in the modulation of innate immunity in brucellosis.

**Keywords:** *Brucella*, label-free analysis, serum, complement system, innate response, interaction.

## LIST OF TABLES

	<b>Page</b>
<b>Table 1.</b> Examples of bacterial complement evasion proteins and their targets on host cells.	7
<b>Table 2.</b> Bacterial strains used in this work.	15
<b>Table 3.</b> Antibodies used to complement components, peroxidase-conjugated antibodies and others.	16
<b>Table 4.</b> Other non-complement sheep serum proteins eluted from <i>Brucella</i> surfaces.	32
<b>Table 5.</b> Other non complement human serum proteins eluted from <i>Brucella</i> surfaces.	34
<b>Table 6.</b> Sheep serum proteins eluted from <i>Brucella</i> surfaces in relation to <i>B. melitensis</i> 16M.	44
<b>Table 7.</b> Coagulation times in residual consumed plasma by <i>Brucella</i> .	46



## LIST OF FIGURES AND ILLUSTRATIONS

	<b>Page</b>
<b>Illustration 1.</b> Complement system activation.	5
<b>Illustration 2.</b> Complement evasion strategies used by human pathogens.	6
<b>Figure 1.</b> Resistance to killing action of serum is an intrinsic trait of <i>Brucella</i> species regardless to the host preference.	23
<b>Figure 2.</b> Complement consumption by <i>Brucella</i> .	24
<b>Figure 3.</b> Adsorption of serum components by <i>Brucella</i> cells.	26
<b>Figure 4.</b> Identification of serum components adsorbed by <i>B. abortus</i> .	27
<b>Figure 5.</b> Survival rate of <i>Brucella</i> and LPS mutants to the bactericidal action of sheep non-immune serum.	29
<b>Figure 6.</b> <i>Brucella</i> wild-type and LPS mutants show different serum protein interaction profiles.	30
<b>Figure 7.</b> Identification of sheep serum complement proteins interacting with wild-type and LPS defective <i>Brucella</i> surfaces.	31
<b>Figure 8.</b> Identification of human serum complement proteins interacting with wild-type and LPS defective <i>Brucella</i> surfaces.	33
<b>Figure 9.</b> Western blot analysis of complement proteins from <i>Brucella</i> surfaces.	35

<b>Figure 10.</b> Western blot analysis of complement regulator proteins eluted from <i>Brucella</i> surfaces.	37
<b>Figure 11.</b> Serum proteins interacting with wild-type <i>Brucella</i> and LPS defective mutants segregate based on protein abundance.	38
<b>Figure 12.</b> Proteomaps visualization of sheep serum proteins adsorbed to <i>Brucella</i> surfaces.	40
<b>Figure 13.</b> Proteomaps of sheep serum proteins adsorbed in (A) <i>B. melitensis</i> 16M and (B) <i>B. abortus</i> 2308 surfaces.	41
<b>Figure 14.</b> Proteomaps of sheep serum proteins adsorbed in (A) <i>B. melitensis</i> 16M $\Delta$ wadC and (B) <i>B. melitensis</i> 16M $\Delta$ per surface.	42
<b>Figure 15.</b> Sheep serum proteins differentially adsorbed by <i>B. abortus</i> and LPS mutants in relation to <i>B. melitensis</i> .	43
<b>Figure 16.</b> Complement (A) and coagulation (B) proteins adsorbed by <i>B. abortus</i> and LPS mutants in relation to <i>B. melitensis</i> .	45
<b>Figure 17.</b> Immune related (A) and iron transport (B) proteins adsorbed by <i>B. abortus</i> and LPS mutants in relation to <i>B. melitensis</i> .	47
<b>Figure 18.</b> Conceptual model: <i>Brucella</i> modulates immunity through sequestration of complement regulators.	49
<b>Figure 19.</b> Conceptual model: <i>Brucella</i> adsorption of pentraxin enhances recruitment of complement regulators.	51

**Figure 20.** Conceptual model: Interaction with coagulation proteins promotes low inflammatory response and favors inactivation of the complement system on *Brucella* surface. 52

**Figure 21.** Conceptual model: Conglutinin attachment on *Brucella* surface favors entry to host cells. 54

## **LIST OF ABBREVIATIONS**

**ACN:** Acetonitrile

**C1INH:** C1 inhibitor

**C4BP:** C4b-binding protein

**CFHL1:** Factor H-like protein 1

**FB:** Factor B

**FDR:** False Discovery Rate

**FH:** Factor H

**FI:** Factor I

**HMWK:** High Molecular Weight Kininogen

**KEGG:** Kyoto Encyclopedia of Genes and Genomes

**KO:** KEGG Orthology

**LPS:** Lipopolysaccharide

**MAC:** Membrane Attack Complex

**MS:** Mass Spectrometry

**PAMPs:** Pathogen Associated Molecular Patterns

**PBS:** Phosphate Buffered Saline

**PCA:** Principal Component Analysis

**PMNs:** Polymorphonuclear

**PRRs:** Pathogen Recognition Receptors

**PT:** Prothrombin Time

**PTT:** Partial Thromboplastin Time

**PVDF:** Polyvinylidene difluoride

**TSB:** Trypticase Soy Broth

## 1. INTRODUCTION

Brucellosis is a zoonotic disease caused by the facultative intracellular extracellular bacteria of the genus *Brucella*. *Brucella* species are classified according to differences in pathogenicity, host preference, supported by bacteriological methods and molecular taxonomy (Moreno and Moriyón, 2006). The genus is well adapted to its hosts and currently comprises different species: *B. melitensis* (from sheep and goats), *B. suis* (pigs), *B. abortus* (cattle), *B. ovis* (sheep), *B. canis* (dogs), *B. microti* (common voles), and *B. neotomae* which was isolated from wood rats and recently found to be zoonotic (Cutler et al., 2005; Moreno and Moriyón, 2006, Lucero et al., 2010; Moreno, 2014; Suárez-Esquivel et al., 2017). In the last decade, new species have been described: *B. pinnipedialis* from seals, *B. ceti* from cetaceans (Foster et al., 2007), and *B. innopinata*, whose preferred host is still unknown (Foster et al., 2007; Scholz et al., 2010). Recently, there has been a number of atypical *Brucella* strains isolated from amphibians and fish (Whatmore et al., 2015). The biology of these isolates is unknown, and they stand outside of the classical brucellae species (Fischer et al., 2012; Whatmore et al., 2015). *B. melitensis*, *B. abortus*, *B. suis*, and in less extent *B. canis*, are the most important species from an economic, animal, and public health perspective (Moreno and Moriyón, 2006).

*Brucella* is transmitted by direct contact or accidentally to secondary hosts, such as humans (Moreno, 2014). The bacterium is able to cross the epithelial mucosa to reach its replication niche within the reticuloendothelial system and reproductive organs (Moreno and Moriyón, 2006). In domestic animals, (such as cattle, sheep, goats, pigs and dogs) the major consequences of brucellosis are abortions and metritis in females, and orchiepididymitis and infertility in males (Moreno and Moriyón, 2006). In humans, clinical symptoms relate to undulating fever, accompanied with malaise, anorexia and prostration. Brucellosis in humans has been also associated with endocarditis, orchitis, spondylitis, osteomyelitis, arthritis and meningoencephalitis (Ko and Splitter, 2003).

The outer membrane of *Brucella* is composed of phospholipids, ornithine lipids, proteins, lipoproteins and lipopolysaccharides (LPS). *Brucella* LPS is a non-canonical molecule because it exhibits different physicochemical and biological properties in comparison to widely studied enterobacterial LPS (Moreno et al., 1981). These properties include low endotoxicity, high resistance to macrophage degradation and protection against

immune responses (Moreno et al., 1981, Forestier et al., 2000; Lapaque et al., 2005). The lipid A and oligosaccharide core possess a reduced number of negatively charged sugars (Barquero-Calvo et al., 2009; Moriyón, 2014). In addition, the O-chain consists of homopolymers of N-formyl perosamine that are longer than those present in other bacteria (Kubler-Kielb and Vinogradov, 2013). Altogether, these traits contribute to an overall reduction of negative net charges on the surface of *Brucella* that prevents its recognition by the innate immune system in early stages of infection (Barquero-Calvo et al., 2007; Conde-Álvarez et al., 2012).

*Brucella* LPS may occur as smooth (presence of O-antigen) and rough-like (absence of O-antigen) strains (Cardoso et al., 2006). Zoonotic relevant species, *B. melitensis*, *B. abortus*, and *B. suis*, possess the smooth phenotype, a feature required for full virulence (González et al., 2008). Rough mutants targeting genes related to the synthesis or O-chain transport to the bacterial surface (e.g. the perosamine synthetase gene, *per*) are attenuated in the murine model and more susceptible to cationic peptides and complement (Martirosyan and Gorvel, 2013). Although *B. ovis* and *B. canis* are considered rough-like they display virulent properties (Carmichael and Bruner, 1968; Jones et al., 1968; Monreal et al., 2003). Likewise, mutants in the LPS core that have an intact O-chain and lipid A (e.g. mutants in glycosyltransferase, *wadC*), are also attenuated in the murine model. These outer membrane alterations induce a greater proinflammatory response than wild-type *Brucella*, making their carriers to the bactericidal effect of serum and cationic peptides (Conde-Álvarez et al., 2012).

### **1.1 *Brucella* uses a furtive strategy to evade innate immunity**

Innate immunity plays a fundamental role in the defense against bacteria. In addition to the action of physical and chemical barriers, innate immunity relies directly on pathogen recognition receptors to be effective. This recognition is achieved by the host through Pathogen Associated Molecular Patterns (PAMPs) present in bacteria (Janeway and Medzhitov, 2002). Macrophages, polymorphonuclear (PMNs) and dendritic cells possess multiple Pathogen Recognition Receptors (PRRs). Specific PRRs are activated by bacterial PAMPs such as: lipopolysaccharide, lipoproteins, glycolipids, flagellum, peptidoglycan or DNA (Mogensen, 2009; Kumar et al., 2011). PAMPs recognition triggers transduction

signaling pathways that include the release of proinflammatory mediators activating the adaptive immune response (Kumar et al., 2011).

Previous works have investigated how *Brucella* interacts with specific components that relate to innate immunity (Barquero-Calvo et al., 2007, 2013, 2015; Martirosyan et al., 2011). *B. abortus* induces a weak proinflammatory response in comparison to other Gram-negative bacteria, such as *Salmonella*. This weak response is characterized by a low number of leukocyte recruitment at the site of infection, and low activation of humoral components and innate immune cells (Barquero-Calvo et al., 2007). Interestingly, at later times of infection in the murine model, *B. abortus* is killed more efficiently in the absence of PMNs cells than in their presence (Barquero-Calvo et al., 2013). This suggests that PMNs could exert a regulatory role in the adaptive immune response against *Brucella*. It may also strengthen the notion that PMNs actively participate in regulatory circuits shaping both innate and adaptive immunity (Barquero-Calvo et al., 2013).

In addition, *Brucella* is resistant to the bactericidal action of PMNs and does not stimulate the degranulation of these cells (Kreutzer et al., 1979, Buzgan et al., 2010). Moreover, it does not induce and exacerbate proinflammatory response at early times of infection (Barquero-Calvo et al., 2007). This bacterium is highly resistant to the bactericidal action of antimicrobial peptides and serum (Hoffmann and Houle, 1983; Eisenschenk et al., 1995, 1999; Martínez de Tejada et al., 1995; Freer et al., 1996; Velasco et al., 2000) and does not consume complement (Moreno et al., 1981, Barquero-Calvo et al., 2009). Therefore, it has been proposed that *Brucella* behaves as a furtive pathogen that evades the proinflammatory response at early times of infection, through PAMPs reduction or modification, ensuring that these are not recognized by the respective PRRs (Barquero-Calvo et al., 2007). This allows *Brucella* to open an “immunological window” and take an advantage to spread throughout the reticuloendothelial system, establishing itself in its replicative niche within the phagocytic cells (Barquero-Calvo et al., 2007; Martirosyan et al., 2011). It is just after this silent incubation period that a vigorous adaptive immunity is started and the chronic infection could be established (Martirosyan et al., 2011).

## 1.2 The complement system: activation and regulation

Complement is one of the most effective systems of innate immunity (Galvan, 2014). Therefore, the manner in which *Brucella* interacts with complement components may determine the fate of the infection. The host complement system consists of more than 30 proteins that are either present as soluble proteins in the bloodstream, lymph or are present as membrane-associated proteins on cell surfaces (Galvan, 2014). Complement proteins are mainly synthesized in the liver, although extra hepatic sites also contribute to the synthesis. Complement proteins are mostly present as inactive pro-enzymes or zymogens. Membrane-associated proteins comprise receptors and regulators of complement activation. Complement components are organized into a hierarchy of proteolytic cascades that start with the detection of pathogenic and foreign surfaces (Dunkelberger and Song, 2010; Kolev et al., 2014).

The complement cascade can be activated by three pathways: the classical, the alternative, and the lectin pathway (Illustration 1). These routes converge in a common pathway that leads to the generation of the C3 and C5 convertase enzyme complexes. C3 is cleaved into the anaphylatoxin C3a and the opsonin C3b, and C5 is cleaved into the anaphylatoxin C5a and C5b. Deposition of C5b onto the target initiates Membrane Attack Complex (MAC) formation. The opsonins and anaphylatoxins promote phagocytic uptake of pathogens by scavenger cells, and activate neutrophils, monocytes and mast cells, respectively (Galvan, 2014; Kolev et al., 2014).

A diversity of biological functions have been attributed to the complement system which are mainly dedicated to (i) pathogen recognition and clearance, (ii) phagocytosis of opsonized targets, (iii) promotion of humoral immune responses, (iv) modulation of cellular immune responses, (v) non-inflammatory clearance of self-antigens derived from apoptotic processes, (vi) and immune complex transport (Holers, 2014).



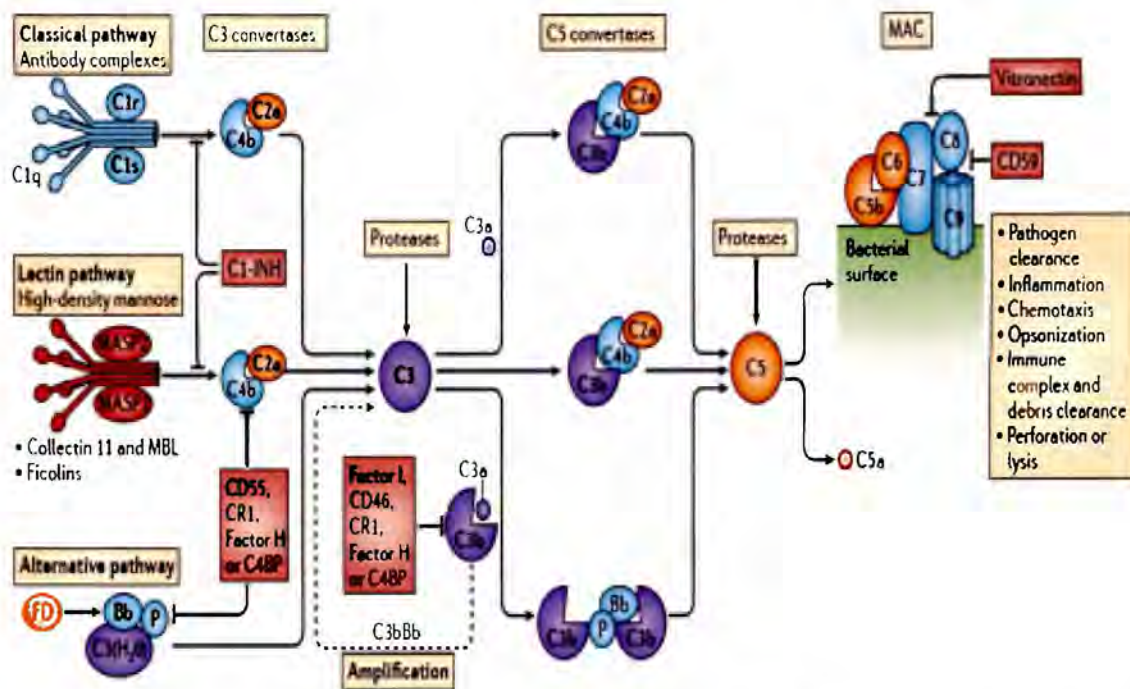


**Illustration 1.** Complement system activation. The three complement pathways, its regulation (red boxes) and their main functions are shown. Taken from (Kolev et al., 2014).

Activation of complement may lead to deleterious implications within the host. Therefore, complement activation requires proper regulatory mechanisms to be specifically effective over pathogenic surfaces. Complement regulatory proteins control activation of the cascade, preventing collateral damage to healthy host tissues (Zipfel and Skerka, 2009). Imbalances in complement regulation, can result in tissue damage, as seen in autoimmune diseases (Zipfel and Skerka, 2009).

Complement regulators can be classified in three categories: (i) fluid phase regulators, (ii) surface bound regulators, and (iii) complement effector receptors. Fluid phase complement regulators, such as Factor H (FH), complement Factor H-like protein 1 (CFHL1) and the activator protein properdin control different steps of the alternative activation cascade (Zipfel and Skerka, 2009). In turn, soluble regulators related to the classical and lectin pathway include complement component C1q, C1 inhibitor (C1INH) and C4b-binding protein (C4BP) (Merle et al., 2015). Soluble inhibitors of the terminal pathway include clusterin, vitronectin and CFHR1 (Zipfel and Skerka, 2009). Membrane bound regulators include CR1 (also known as CD35 or CDX), CD46 (also known as MCP), CD55 (also known

as Decaying Accelerating Factor, DAF), CD59 and complement receptor of the immunoglobulin superfamily CR1g; (also known as VSIG4). These receptors bind C3b or C4b deposited on the surface of the target and drive effector functions (Zipfel and Skerka, 2009; Noris and Remuzzi, 2013; Schmidt et al., 2016).

Complement regulatory proteins are also implicated in other cellular processes. They participate in intercellular adhesion, extracellular matrix adhesion and the coagulation cascade, which is tightly regulated with the complement system (Sundsmo and Fair, 1983; Markiewski et al., 2007; Amara et al., 2010).

### 1.3 Complement evasion strategies used by pathogenic bacteria

Some pathogenic microorganisms rely on their ability to evade immunity. The complement system is one of the first lines of defense. Consequently, several pathogens have developed mechanisms to counter complement activity (Illustration 2). Pathogens share common evasion strategies that relate to: (i) mimicking or sequestering molecules related to the natural regulation of the system, (ii) direct inhibition or modulation of complement effector molecules, and (iii) inactivation of the system through degradation of its proteins (Lambris et al., 2008). In addition, there are other structural and differential characteristics of microorganisms such as LPS composition, the presence of capsules, membrane proteins, or release of membrane components that promote complement activation away from the pathogen (Joiner, 1988). Table 1 summarizes some of the specific complement evasion proteins that have been described in different bacterial models.

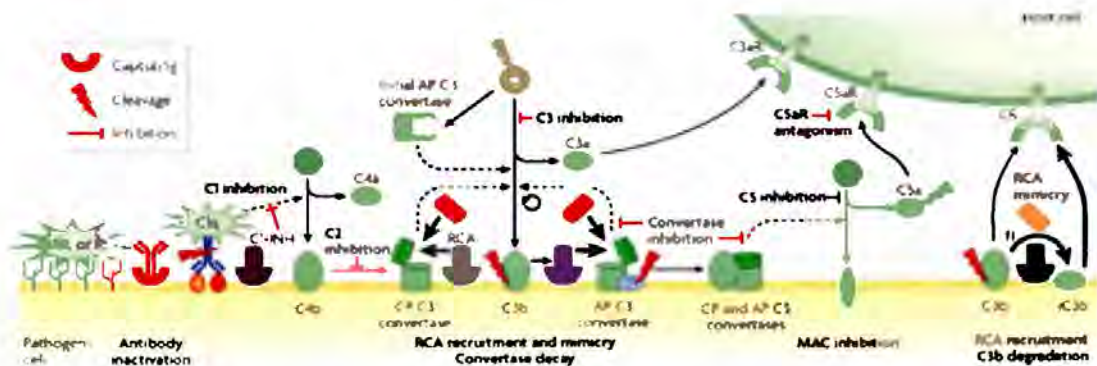


**Illustration 2.** Complement evasion strategies used by human pathogens. Taken from (Lambris et al., 2008).

**Table 1.** Examples of bacterial complement evasion proteins and their targets on host cells. Taken from (Rautemaa and Meri, 1999; Lambris et al., 2008; Blom et al., 2009).

<i>Antibody depletion</i>		
Staphylococcal protein A (SpA)	IgG	<i>Staphylococcus aureus</i>
<i>Direct complement inhibition</i>		
Extracellular fibrinogen-binding protein (Efb)	C3 and C3b-containing convertases	<i>Staphylococcus aureus</i>
Staphylococcal superantigen-like protein-7 (SSL-7)	C5	<i>Staphylococcus aureus</i>
Staphylococcus complement inhibitor (SCIN)	C3 convertases	<i>Staphylococcus aureus</i>
Chemotaxis inhibitory protein (CHIPS)	C5a receptor (C5aR)	<i>Staphylococcus aureus</i>
CD59 like protein	C8-C9b	<i>Borrelia burgdorferi</i>
<i>Mimicry or acquisition of complement regulators</i>		
Porin A	FH	<i>Neisseria meningitidis</i>
Yad A	FH	<i>Yersinia enterocolitica</i>
UspA and UspB	C4BP	<i>Moraxella catarrhalis</i>
<i>Regulators of complement activation recruitment</i>		
Complement-regulator-acquiring protein (CRASP)	FH, CFHL1 and C4BP	<i>Borrelia</i> ssp
M protein family	FH, CFHL1 and C4BP	
<i>Proteolytic degradation</i>		
Staphylokinase	C3b and IgG (by activation of plasmin)	<i>Staphylococcus aureus</i>
<i>Pseudomonas</i> elastase (PaE)	C3, C5a	<i>Pseudomonas</i> ssp
<i>Structural strategy</i>		
Capsule	Inhibition of alternative pathway	<i>Streptococcus pneumoniae</i>

#### 1.4 Interaction between humoral innate components and *Brucella*

*Brucella* mainly replicate inside host cells. However, part of their life cycle is extracellular. Indeed, free *Brucella* cells are the vehicles that infect new hosts and naïve cells. During the first stages of infection, the bacterium confronts humoral factors of the immune system of the hosts. Likewise, after *Brucella* organisms have reached high numbers within cells, they are released (Starr et al., 2012) and become in contact with complement, antibodies and other soluble components. Moreover, after infection and replication in placental trophoblast, and other organs, large numbers of bacteria are detected extracellularly, as singlets or in groups (Anderson et al., 1986; Gidlewski et al., 2000; González-Barrientos et al., 2010). Features that relate to the interaction between *Brucella* and innate immunity have been previously described, emphasizing in cellular components such as neutrophils and macrophages (Barquero-Calvo et al., 2007, 2013). However, little is known about the interaction between this pathogen and the complement system. In addition, there is no

information regarding the interaction of *Brucella* and the coagulation cascade or other serum components. Previous studies have focused mainly on the role of the *Brucella* LPS as a determinant factor for innate immune evasion (Lapaque et al., 2005; Barquero-Calvo et al., 2009; Conde-Álvarez et al., 2012).

Eisenschenck et al. (1999) observed that both rough and smooth strains of *B. abortus* could bind C1 and C1q in their outer membrane. They concluded that the classical complement pathway was therefore involved in activation. However, the bactericidal effect was only observed in mutant rough strains (Eisenschenk et al., 1999). Thereafter, Fernandez-Prada et al. (2000) described that both the classical and the lectin pathways were involved in complement activation. They related deposition of factors belonging to those pathways to the bactericidal action of the complement. These authors supported that the alternative pathway was not activated, but at the same time, they proposed that the amount and strength of interaction of complement factors with the bacterial surface could determine their ability to resist the complement (Fernandez-Prada et al., 2001).

Recently, a protein called BtaF belonging to a family of autotransporters was described in *B. suis*. Orthologs have been found in other *Brucella* species. *B. suis* BtaF mutants show a 53% reduction in their survival rate compared to the parental strain in serum resistance assays (Ruiz-Ranwez et al., 2013). In addition, it was found that some regions of this protein showed structural similarities with UspA1 from *Moraxella catarrhalis*. UspA1 together with UspA2 have been characterized as C4BP regulator sequesters (Nordstrom et al., 2004; Attia et al., 2005, Attia et al., 2006). Previously, the same research group had described BtaE, an adhesin required for full virulence in *B. suis*. This protein possesses a C-terminal domain similar to the YadA protein described in *Yersinia enterocolitica*, which sequesters the complement regulator FH, conferring the ability to resist serum (China et al., 1993). In the context of a furtive strategy, recruitment of regulators of the complement cascade could be a mechanism employed by *Brucella*. Nevertheless, this has not been studied yet.

*Brucella* resists the lytic and microbicidal effect of serum. Which are the serum proteins that specifically mediate these phenomena are still unknown. Our proposal is to identify and quantify serum proteins that interact with *Brucella* using a biological and proteomic approach. These tools have been widely used to identify proteins in complex

biological mixtures and to explore their differential abundance pattern. We aim to gain a better perspective of the interaction of *Brucella* with serum proteins and understand the way *Brucella* modulates them.

### 1.5 Proteomic quantification by mass spectrometry

Historically, the interaction of the host complement system with pathogens has been studied through functional assays of the complement system (complement fixation assays). Another method used is to specifically detect complement components through radioimmune techniques, immunofluorescence, flow cytometry, or western blot (Corbeil et al., 1988; Eisenschenk et al., 1999; Ferguson et al., 2004; Nordstrom et al., 2004; Berends et al., 2013). Recently, proteomics has been widely used to analyze a wide spectrum of biological samples, identifying proteins in complex biological mixtures, and to explore their differential pattern of abundance (Higgs et al., 2005; Wilm, 2009). It is not an exception that this tool would be useful to understand interactions between complement system and bacterial pathogens.

It must be emphasized that not only the presence or absence of a protein is an indicator of a biological condition, but also the abundance of that protein in relation with another (Higgs et al., 2005; Wilm, 2009). Quantitative proteomics comes to merge these two concepts. The quantification of proteins by Mass Spectrometry (MS) can be absolute or relative. Absolute quantification determines abundance of protein amount based on a certified concentration of an internal standard control. Relative quantification determines the presence of an increased or decreased protein in comparison to another biological condition. Choosing between absolute or relative quantification will depend on the need to know the precise concentration of a protein, or the ratio between several biological conditions. Ultimately, an absolute concentration remains relative in regards to the concentration of an internal standard (Elliott et al., 2009).

In relative quantification-based proteomics, there are two methodologies employed. The first one is dependent on isotope labeling or metabolic labeling. The second methodology is independent of protein labeling, therefore usually called “label-free”. Label-free methods are finding broad applications. Current label-free approaches are based on a single MS feature of abundance, such as spectral or peptide count or chromatographic peak area or height, which are obtained individually and then compared directly with the other repetitions.

The advantage of this technique is that it minimizes the number of steps in sample processing by conserving a greater number of quantifiable peptides and eliminating the need for costly isotope labeling reagents (Wilm, 2009; Zhu et al., 2010).

## 2. JUSTIFICATION

*Brucella* organisms are intracellular bacteria displaying an extracellular stage in their life cycle. Since humoral factors are the first to confront the extracellular bacteria, it becomes necessary to understand the elements that interact with the bacterium and the nature of these interactions. Therefore, it was justified to develop a strategy for the identification and quantitation of serum proteins from different animals that bind to the *Brucella* surface. In turn, this will help elucidating the mechanisms by which *Brucella* resists the antimicrobial activity of host serum factors and modulate the innate immune response.

### 3. HYPOTHESIS

In accordance to their furtive strategy, *B. abortus* and *B. melitensis* selectively interact with serum host proteins to resist bactericidal action and to modulate the immune response.



#### **4. OBJECTIVES**

##### **General objective**

To identify and quantify host serum proteins that interact with the surface of *Brucella* cells, to propose a model for their resistance to the microbicidal action of humoral substances and for the modulation of the innate immune response.

##### **Specific objectives**

1. To identify animal and human serum proteins that selectively interact with wild-type *B. abortus*, *B. melitensis* and *B. canis* cell surfaces.
2. To compare the interaction profiles of sheep serum proteins with wild-type and LPS-mutant *Brucella* to understand how surface alterations modulate their interaction.
3. To establish conceptual models that explain the modulation of the innate immune response by *Brucella*

## **5. MATERIALS AND METHODS**

### **5.1 Ethics**

Human blood samples were collected from volunteer healthy donors at Centro de Investigación de Enfermedades Tropicales (CIET), Universidad de Costa Rica. To maintain anonymity, serum samples were pooled. Samples were taken following the procedures dictated by the Costa Rican National Health system (Ley 9234, Costa Rica, La Gaceta 79, 2014) and the World Medical Association Declaration of Helsinki: Ethical Principles for Medical Research Involving Human Subjects, General Assembly, Seoul, October 2008, regarding the use of blood samples. The use of human serum in this research did not required additional permission by the "Comité Ético Científico, Universidad de Costa Rica" (VI-4277-2016) (see Appendix 1).

Dog, sheep, guinea pig and bovine serum samples were obtained from a sera collection stored at the Hospital de Especies Menores, Escuela de Veterinaria, Universidad Nacional. Mouflon, deer and buck serum samples were obtained from sera collection from healthy animals stored at Universidad de Navarra, Pamplona, Spain.

### **5.2 Serum samples collection and storage**

Whole blood samples were collected from human, sheep, cow bovine, mouflon, deer, buck, dog and mice. Non-immune serum was recovered by centrifugation, pooled and frozen immediately at  $-80^{\circ}\text{C}$ . Rose Bengal test was used as screening test to discard positive immune sera (Lucero et al., 2010).

### **5.3 Bacterial strains and growth conditions**

The bacterial strains used are listed in Table 2. All strains were grown in tryptic soy broth for 18 hours at  $37^{\circ}\text{C}$  and stored at  $-80^{\circ}\text{C}$  in Brain Heart Infusion broth supplemented with 20% glycerol.

**Table 2.** Bacterial strains used in this work.

Bacterial strains	Abbreviation	Description	LPS type	Source-Origin
<i>B. melitensis</i> 16M Biovar 1	<i>B. melitensis</i>	Reference strain	Smooth LPS	(González et al., 2008)
<i>B. melitensis</i> 16M $\Delta$ <i>per</i>	<i>Bm</i> $\Delta$ <i>per</i>	LPS O-chain defective mutant	Rough LPS	(Fontana et al., 2016; González et al., 2008)
<i>B. melitensis</i> 16M $\Delta$ <i>wadC</i>	<i>Bm</i> $\Delta$ <i>wadC</i>	LPS core-defective mutant	Smooth LPS	(Fontana et al., 2016)
<i>B. abortus</i> 2308 Biovar 1	<i>Ba</i>	Reference strain	Smooth LPS	(Sangari and Agüero, 1991)
<i>B. abortus</i> :: <i>per</i>	<i>Ba</i> :: <i>per</i>	LPS O-chain defective mutant	Rough LPS	(Conde-Álvarez et al., 2012)
<i>B. abortus</i> $\Delta$ <i>wadC</i>	<i>Ba</i> $\Delta$ <i>wadC</i>	LPS core-defective mutant	Smooth LPS	(Conde-Álvarez et al., 2012)
<i>B. canis</i> <i>beanCR12</i>	<i>Bc</i>	Wild-type strain	Rough LPS	(Chacón-Díaz et al., 2015)
<i>Salmonella enterica</i> <i>sv. typhimurium</i> Strain SL1344	<i>Se</i>	Wild-type strain	Smooth LPS	(Barquero-Calvo et al., 2009)
<i>O. anthropi</i> LMG 3331	<i>Oa</i>	Wild-type strain	Smooth LPS	(Velasco et al., 1998)

#### 5.4 Antibodies

The antibodies used in this project are listed in Table 3.

**Table 3.** Antibodies used to complement components, peroxidase-conjugated antibodies and others.

Name	Immunogen	Molecular weight	Description	Dilution used	Commercial name
<b>Common pathway</b>					
Anti C3	Human C3 protein	187 kDa	Chicken polyclonal antibodies	WB*: 1/500	Abcam ab14232
<b>Alternative pathway</b>					
<b>Anti-Factor B (M13/12)</b>	Factor B/Bb	86kDa	Monoclonal antibodies in mouse	WB:1/50	Abcam-ab106139
<b>Final pathway</b>					
Anti C9	Purified, full length native human complement C9	Is not specified	Mouse monoclonal antibodies	WB:1/500	Abcam ab17931
Anti C9	Synthetic peptide from residues 1-100 of human C9	75 kDa	Rabbit polyclonal antibodies	WB:1/500	Abcam ab 71330
<b>Regulators</b>					
Anti-Factor H	Purified Human FH	155 kDa	Sheep polyclonal antibodies	WB: 1/500	Abcam-ab8842
Anti-Vitronectin	Internal region of Human vitronectin synthetic peptide	54 kDa	Rabbit polyclonal antibodies	WB:1/500	Abcam-ab135913
Anti-C4BP	Human C4BP synthetic peptide (1100-1200 residues)	90,180kDa	Rabbit polyclonal antibodies	WB: 1/500	Abcam-ab66791
<b>Others</b>					
Anti-Mouse	Mouse IgG, whole molecule	-	Rabbit polyclonal Secondary antibodies to Mouse IgG-(H+L)	WB:1/1000	Abcam-ab6728
Anti-rabbit	Rabbit IgG, whole molecule	-	Rabbit polyclonal Mouse Secondary antibodies to Rabbit IgG-(H+L)	WB:1/1000	Abcam-ab6721
Anti-Sheep	Sheep IgG, whole molecule	-	Dunkey polyclonal Secondary antibodies to Sheep IgG-(H+L)	WB:1/1000	Abcam-ab97125

\*WB: western blot.

### **5.5 Sensitivity to the bactericidal action of non-immune serum**

Survival to bactericidal action of non-immune serum was determined by two methods: (1) Plate counts: exponentially growing bacteria were adjusted to  $10^4$  CFU/mL and incubated with fresh non-immune serum from different species (ovine, bovine, mouflon, deer, bulk, human, murine) at 37°C. After 45 minutes of incubation, aliquots were streaked on trypticase soy agar plates. Results were expressed as the percentage of the average CFU with respect to heat-inactivated serum (control). (2) Direct count viability assays: exponentially growing bacteria were adjusted to  $10^8$  CFU/mL and incubated during 90 minutes with fresh, non-immune serum from sheep. After incubation, bacteria were washed twice with Phosphate Buffered Saline (PBS) and stained for 30 min with 1.5  $\mu$ L of SYTO<sup>®</sup> 9 green-fluorescent nucleic acid stain and 1.5  $\mu$ L of red-fluorescent nucleic acid stain, propidium iodide (LIVE/DEAD BacLight, Life Technologies). Stained bacterial suspensions were placed onto a coverslip and analyzed on a fluorescence microscope (Nikon Eclipse 80i). Imaging analysis were performed using the Cell Profiler software (<http://cellprofiler.org/>) and the results were expressed as the percentage of live bacteria with respect to the untreated control.

### **5.6 Determination of complement consumption by *Brucella***

Complement consumption was estimated as the reduction of the hemolytic activity of serum complement incubated with live bacteria, as described elsewhere (Manterola et al., 2005). Briefly, human or guinea pig serum was incubated with live packed bacteria for 15 - 30 min at 37°C. After incubation, the complement activity on the serum was monitored as its ability to lyse 2% sheep erythrocytes pre-sensitized with guinea pig antibodies to sheep erythrocytes. For bovine serum, human erythrocytes sensitized with anti-D antibody were used as target, due to conglutinating activity of bovine serum with sheep erythrocytes. Incubation was carried out for 45 min, and the hemolysis was determined at 540 nm after removal of cells and debris by centrifugation.

### **5.7 Adsorption of serum components by *Brucella* and protein identification**

Reference strains and LPS mutants ( $5 \times 10^9$  UFC/mL) were grown overnight in 80 mL of Trypticase Soy Broth (TSB) in glass flasks at 200 rpm and washed two times with PBS

(1X, NaCl 137mM, KCl 2.7mM, Na<sub>2</sub>HPO<sub>4</sub> 10mM, KH<sub>2</sub>PO<sub>4</sub> 1,8 mM, pH 7.2). The bacterial pellet was resuspended in 3 mL of ovine or human fresh normal serum and incubated at 37°C for 45 min under mild agitation. Control bacteria were incubated with PBS. Bacteria were washed three times with barbital buffer (1.02 mM NaCl, 13 mM sodium diethylbarbiturate, 62.5 mM diethylbarbituric acid, 2.18 mM MgCl<sub>2</sub>, 440 mM CaCl<sub>2</sub>, pH 7,6). All bacterial preparations were treated for 30 min with 800 µL of 0.1 M glycine-HCl (pH 2.0) to remove adsorbed proteins or with PBS for control purposes. The eluted supernatants were neutralized with 160 µL of 1 M Tris-HCl (pH 9.0) and proteins were concentrated by methanol-chloroform precipitation as described previously (Friedman, 2006). Eluted proteins from the bacterial surface, were analyzed using two different procedures:

**5.7.1 Qualitative protein identification:** eluted proteins were separated in 7.5 or 10% SDS-PAGE under reducing conditions, and stained with Coomassie blue. Stained protein bands were excised and subjected to in-gel reduction, alkylation, and tryptic digestion, using an automated workstation (DigestPro MSi, Intavis, Germany). The resulting peptides were analyzed by MALDI-TOF-TOF mass spectrometry on a Proteomics Analyzer 4800 Plus instrument (Applied Biosystems), as described elsewhere (Lomonte et al., 2014). The resulting fragmentation spectra were searched against the global and species-specific UniProt databases ([www.uniprot.org](http://www.uniprot.org)) using ProteinPilot, version 4.0, and the Paragon algorithm (ABSciex) for protein identification at ≥95% confidence.

**5.7.2 Quantitative protein identification:** eluted proteins were redissolved in 7 M Urea, 2 M Thiourea and 2% CHAPS, 50 mM DTT with vigorous agitation in a vortex for 30 min at room temperature. Trypsinization was performed in total protein without fractionation. Samples (10 µg) were loaded on SDS-PAGE gels and separated by electrophoresis allowing the sample to enter the gel. Gels were fixed (50 % methanol/ 10 % acetic acid), stained with Coomassie (Simply Blue Safe Stain, Invitrogen). Gel band was excised and trypsinized. Briefly, the band was destained twice with 100 µl acetonitrile (ACN) for 5 minutes at 40°C removing liquid to complete dryness. Proteins were reduced and alkylated with 10 mM DTT / 100 mM ammonium bicarbonate and 28 mM iodoacetamide / 100 mM ammonium bicarbonate, respectively, for 10 minutes at 40°C. Subsequently, the gel pieces were dried with 100 µl ACN for 5 minutes at 40°C removing the supernatant to complete dryness. Proteins were digested with trypsin (Promega) using a 1:20 trypsin/protein

ratio overnight at 37°C. Peptide extraction was performed with consecutive incubations (30 minutes, room temperature) with: 1 % formic acid / 2 % ACN; 05% formic acid / 50 % ACN; 100 % ACN. All supernatants were combined and taken to dryness in a speed-vac. Peptides were solubilized in 1 % trifluoroacetic acid and further extracted using a C18 reverse phase solvent (Pierce C18 Spin Tips) following the manufacturer protocol. Extracted peptides were dried in a speed-vac and redissolved in 5 µL of 2% ACN, 0.1% formic acid. Samples (2 µL) were subjected to mass spectrometry analysis in a TripleTOF 5600 (ABSciex) coupled to a nanoflow high performance HPLC (Eksigent) equipped with a nanoelectrospray ion source. The mobile phases used were A (100% H<sub>2</sub>O and 0.1% formic acid) and B (100% ACN and 0.1% formic acid) in a 4.5h gradient. Obtained data were analyzed with the software search engine ProteinPilot (ABSciex), using the global Uniprot database ([www.uniprot.org](http://www.uniprot.org)). Quantification was performed with the Progenesis IQ software for Proteomics (Nonlinear Dinamix, Waters). This software implements the automatic alignment of the chromatograms, and the correct assignment of the same peptides along the different samples to allow the quantification based on the ion intensities of the MS data. Each sample quantification was done by triplicate. To guarantee correct quantifications only identifications with False Discovery Rate (FDR) below than 1% were used.

## 5.8 Label free data analysis

**5.8.1 Principal Components Analysis (PCA):** To determine the similarity of the protein patterns between strains and replicates, a PCA was carried out. The complexity of the diversity of proteins measured was reduced by grouping and automated algebraic construction of components or variables ranked by contained variation, according to the usual specifications of the algorithm. For this, the procedure was done with the functions established in the Wolfram Mathematica program (<https://www.wolfram.com/mathematica/>).

**5.8.2 Proteomaps:** Proteins identified and quantified in the label-free analysis were categorized and classified according to a Protein Functional Hierarchy and Category Assignment of Kyoto Encyclopedia of Genes and Genomes (KEGG) ([www.genome.jp/kegg/](http://www.genome.jp/kegg/)). Proteins were assigned to functions via KEGG Orthology (KO) Identifications, which makes them comparable between organisms. Protein identity was

associated with their function, and normalized abundance obtained in the label-free quantitation analysis using Proteomaps software ([www.proteomaps.net/](http://www.proteomaps.net/)) (Liebermeister et al., 2014).

**5.8.3 Heat maps:** To determine the differential relative abundance of a protein, two-fold changes compared to the control strain *B. melitensis* was considered as different abundance of a protein (see Appendix 4, 5, 6). Intensity values per serum protein eluted from bacteria were normalized against *B. melitensis* and displayed in log fold change between strains in a heat map. The analysis was performed with a 95% statistical significance using a negative binomial distribution to estimate the probability of extreme events (the fold change) with a small number of replicates. The adjusted p-value statistic (q value) was considered for selection. This procedure was made on the Galaxy platform (<https://usegalaxy.org/>).

## 5.9 Immunodetection of complement factors

Eluted serum proteins from *Brucella* surface and bacterial lysates after serum incubation were separated by SDS-PAGE, electrotransferred to Polyvinylidene difluoride (PVDF) membranes and probed with antibodies to complement factors (see Table 3). Membranes were further incubated with peroxidase-conjugated antibodies and the detected bands were visualized by an enhanced chemiluminescence reaction (Roche).

## 5.10 Prothrombin and Partial Thromboplastin Time determination

A qualitative biologic assay by duplicate was performed to corroborate the interaction of coagulation proteins with the *Brucella* outer membrane. Exponentially growing bacteria were incubated with human heparinized plasma at 37°C. After 45 minutes of incubation, residual plasma was analyzed for Prothrombin Time (PT) and Partial Thromboplastin Time (PTT) and compared to non-consumed plasma. Results were expressed in seconds with respect to the non-consumed control.

## 5.11 Statistics

Values were expressed as means  $\pm$  standard deviation, and compared using Student's *t*-test for determining the statistical significance between two samples in the different assays. Values of  $p < 0.05$  were considered statistically significant. The Kolmogorov-Smirnov test was applied to assess the normal distribution of data obtained in each experiment. Thereafter,



means were statistically compared by a Student's *t*-test. Kruskal-Wallis and Mann-Whitney tests were used for experiments with non-normal data distribution. The SPSS statistical software was used in all cases.

## 6. RESULTS

### 6.1 Resistance to bactericidal action of serum is an intrinsic trait of *Brucella* organisms, regardless of the host preference.

*Brucella* cells are markedly resistant to the bactericidal action of normal serum (Eisenschenk et al., 1999; Fernandez-Prada et al., 2001). To assess whether this resistance is an intrinsic trait, independent of the source of animal serum, we determined survival of wild-type *Brucella* (*B. abortus*, *B. melitensis* or *B. canis*) after incubation with non-immune serum from rodents, hominids, canids, bovine, caprine, and cervids. In all conditions, wild-type brucellae showed survival rates above 70% independently from the source of serum (Figure 1). *B. abortus* showed a resistant phenotype to serum from hosts phylogenetically distant to bovines. We also assayed *B. canis*, a species that although considered zoonotic, is tightly associated to dogs (Moreno and Moriyón, 2006). These results support the concept that resistance to bactericidal action of serum is an innate trait of members of the *Brucella* genus, independently from the host preference.

### 6.2 *Brucella* ability to bind serum proteins is species and host dependent.

*Brucella* cells are poor complement activators in comparison with other bacteria such as *Salmonella* (Eisenschenk et al., 1999; Barquero-Calvo et al., 2007). To determine whether complement fixation relates to species and host, we explored the ability of *B. abortus* and *B. canis* to consume complement from guinea pig, human, and cow serum. In the conventional assay using guinea pig serum (Moreno et al., 1981), *B. canis* did not consume complement, as expected for *B. abortus* (Figure 2A). In contrast, other bacteria such as *O. anthropi* and *S. enterica* completely abrogated the lytic activity, demonstrating complement consumption of serum components (Figure 2A). Interestingly, *B. abortus* activates human components, as evidenced by partial reduction of hemolysis (Figure 2B), while *B. canis*, possessing a natural rough-like LPS phenotype, barely consumes human components (Figure 2B).

To assess complement binding using bovine serum, we had to modify the erythrocyte sensitized system due to conglutinating activity of bovine serum with sheep erythrocytes. For this purpose, we used human erythrocytes sensitized with an anti-D antibody. *B. abortus* and *B. canis* consumed at some extent bovine serum components (Figure 2C). These results suggest that the bacterial interaction with specific host proteins could be related to the

*Brucella* furtive strategy.

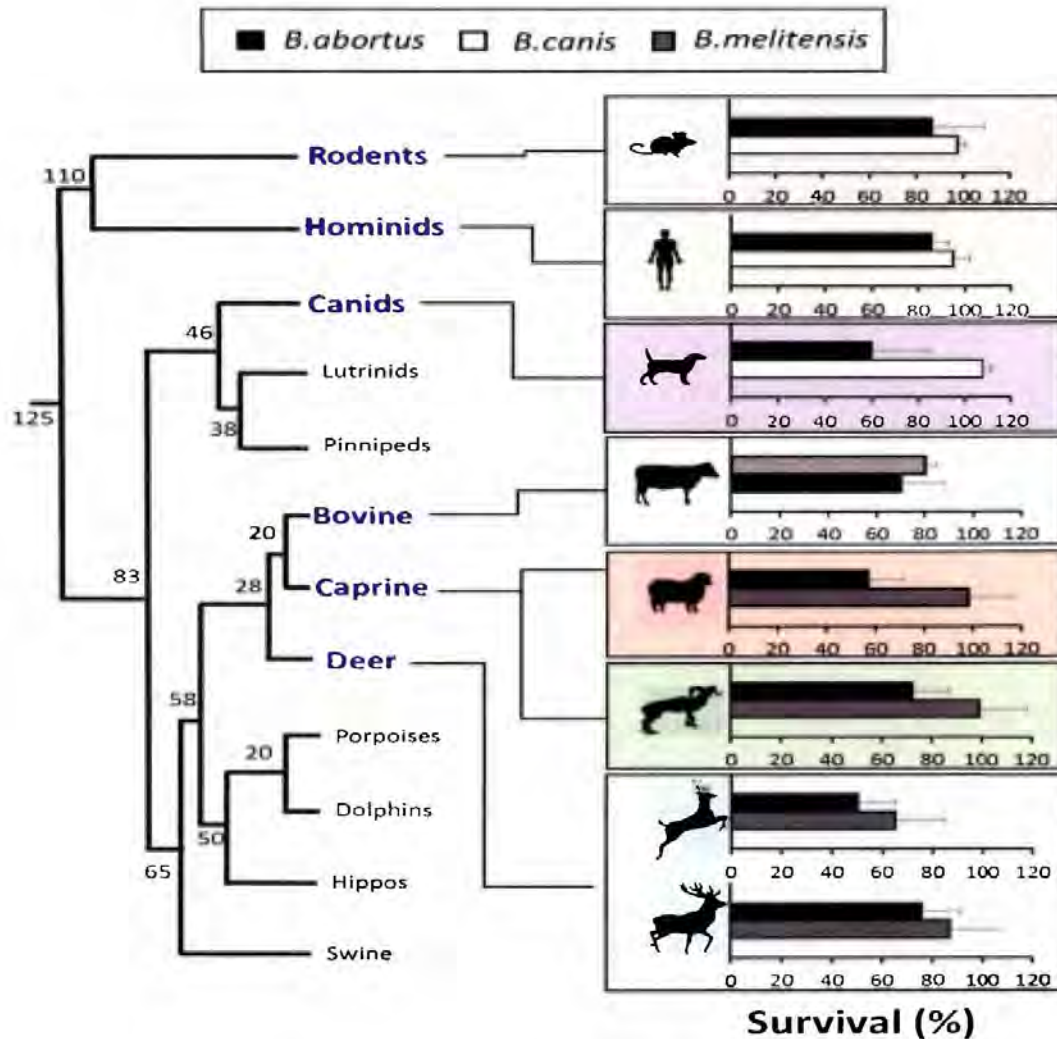


**Figure 1. Resistance to killing action of serum is an intrinsic trait of *Brucella* species regardless to the host preference.** Survival of wild-type *Brucella* after incubation with non-immune serum from rodents, hominids, canids, bovine, caprine (sheep and mouflon) and deer (red deer and buck). Phylogeny and time calibration of mammal evolution was adapted from (Kumar and Hedges, 1998; Bininda-Emonds et al., 2007). The numbers in the mammal phylogenetic tree represent millions of years. The survival rate was estimated as the % of CFU after serum incubation in relation to controls. Each bar is the mean  $\pm$  standard deviation of an experiment. The results are representative of at least three independent experiments. Statistical significance was calculated by Student's *t*-test,  $P < 0,05$ .

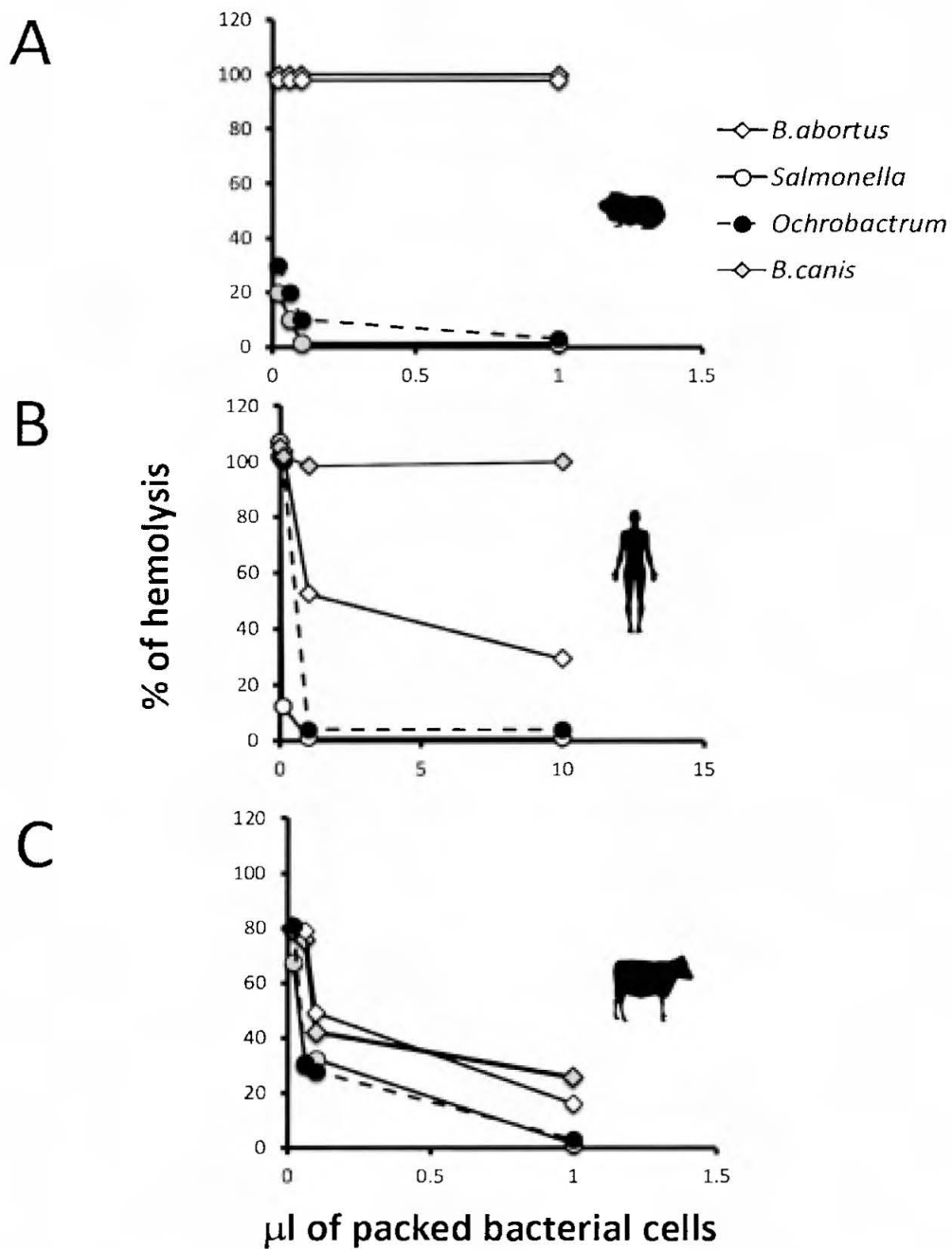


**Figure 2. Complement consumption by *Brucella*.** Packed bacteria were incubated with (A) non-immune guinea pig, (B) human serum and (C) cow serum. Residual complement measured was the hemolytic activity using an erythrocyte-antibody system. The results are representative of at least three independent experiments.

### 6.3 Adsorption of serum components by *Brucella* organisms.

It has been shown that bacteria are able to modulate and evade innate immunity through selective interaction with host proteins (Lambris et al., 2008, Blom et al., 2009). We have hypothesized that *Brucella*, in accordance with its furtive strategy, modulates in part the innate immune response through selective interaction with host serum proteins. Our first approach was to assess if adsorbed proteins vary within hosts. We determined the profiles of *B. abortus* interaction with serum proteins from mice, cow and human under same experimental conditions (10µg of protein/well). *B. abortus* barely adsorbed mouse serum proteins. In the case of bovine serum, *B. abortus* adsorbed moderately amount of proteins, which are concentrated in a few specific bands. *B. abortus* adsorbed a significant amount of human serum proteins (Figure 3A).

Then, compared the adsorbed human serum protein profiles of *B. abortus*, *B. canis*, *O. anthropi* and *S. enterica* different profiles of adsorbed proteins were seen for each species, suggesting an idiosyncratic interaction with host serum proteins (Figure 3B). Differences were also observed within *Brucella* species such as *B. abortus* and *B. canis* and non-related bacteria such as *S. enterica* and *O. anthropi* (Figure 3B).

### 6.4 Identification of serum components adsorbed by *B. abortus*.

Most of the adsorbed human serum proteins in *Brucella* surface, correspond to the complement system (Figure 4A). Human C3 was present in the majority of the analyzed bands, indicating proteolytic degradation of C3. Complement system regulator proteins such as properdin, clusterin and vitronectin, were also detected (Figure 4A). A few other proteins related to transport, (serotransferrin, haptoglobin, hemoglobin and apolipoproteins), protease inhibition (alpha-1-antitrypsin, alpha-1-acid glycoprotein) and coagulation (beta-2-glycoprotein) were also detected (Figure 4A).

Bovine serum proteins adsorbed to *B. abortus* corresponded to complement related components such as conglutinin and properdin, involved in the recognition of pathogens and casein protein (Figure 4B).

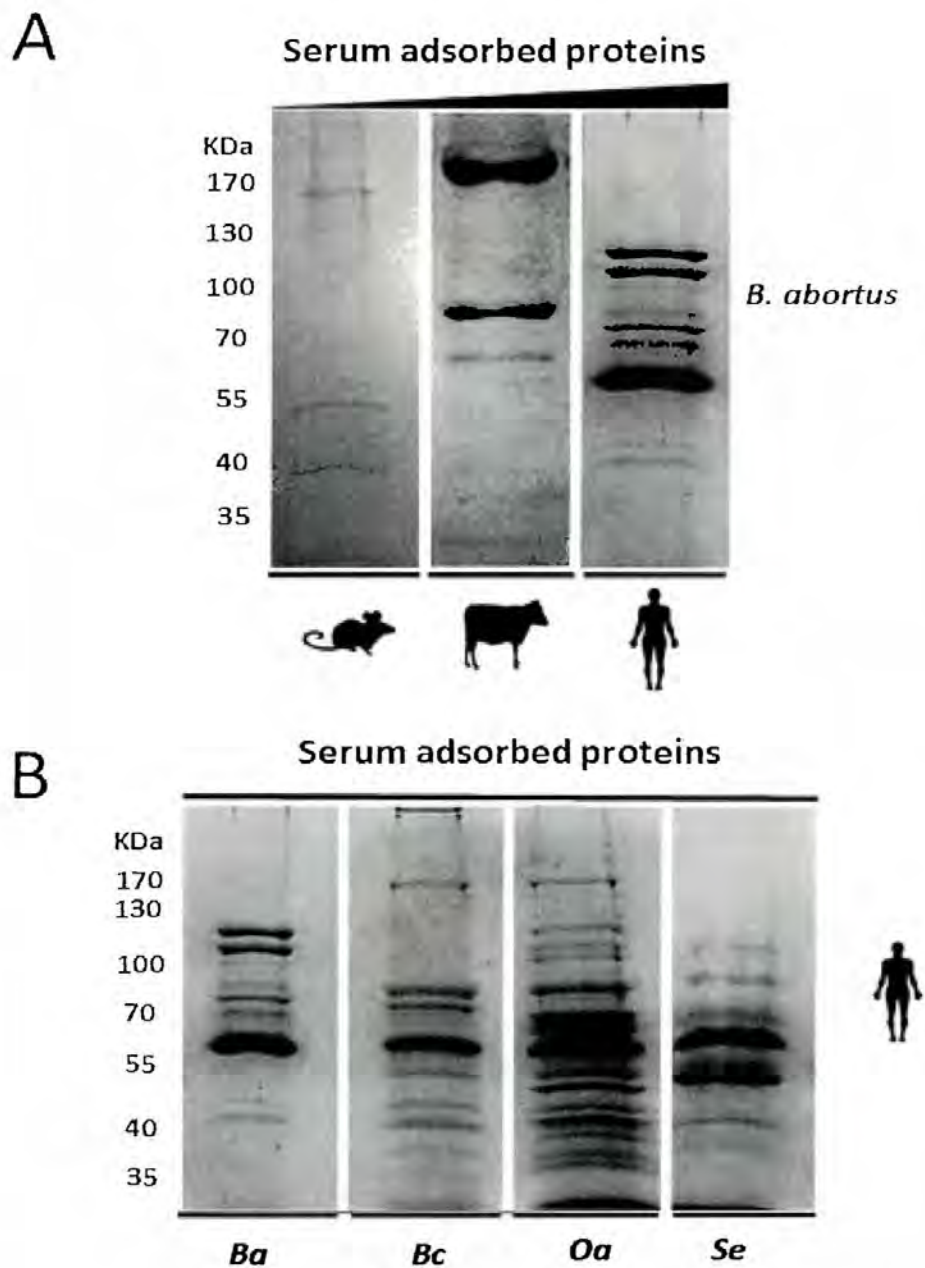


**Figure 3. Adsorption of serum components by *Brucella* cells.** (A) Coomassie blue stained gel of mouse, bovine and human serum proteins (10 $\mu$ g/well) eluted from *B. abortus* surface after incubation with serum. (B) Coomassie blue stained gel of human proteins eluted from the surface from viable bacterial cells after incubation with serum. Ba: *B. abortus*, Bc: *B. canis*, Oa: *O. anthropi*, Se: *S. enterica*.

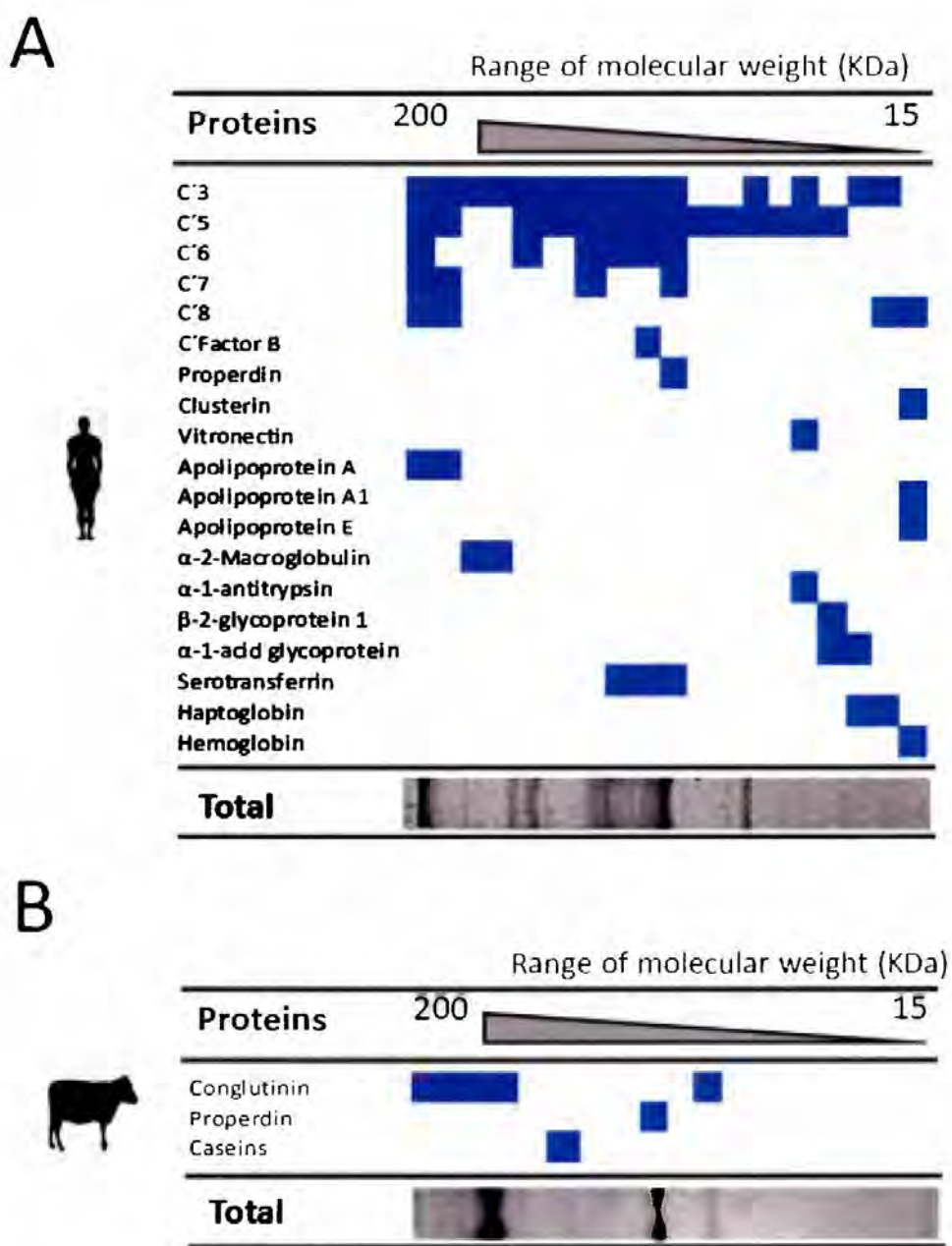


**Figure 4. Identification of serum components adsorbed by *B. abortus*.** (A) Coomassie blue stained gel of human and (B) bovine serum proteins (10 $\mu$ g/well) eluted from the surface of *B. abortus* after incubation of the respective serum with viable bacterial cells. Individual lines, correspond to the different eluted fractions, that were identified by proteomic analysis. Experiments were repeated two times.

### 6.5 Wild-type and LPS mutants show differences in the serum protein interaction profile.

It has been shown that *Brucella* LPS O-chain and core-defective mutants are more sensitive to bactericidal action of serum and cationic peptides (Moreno et al., 1981; Corbeil et al., 1988; Martínez de Tejada et al., 1995; Eisenschenk et al., 1995; Lapaque et al., 2005; Conde-Álvarez et al., 2012). When bacterial survival to non-immune sheep serum was measured, wild-type strains were more resistant to serum killing activity than LPS defective O-chain *B. abortus::per* and core *B. abortus ΔwadC* mutants (Figure 5A and 5B). Interestingly, the rough-like strain *B. canis* was very resistant to the microbicidal action of sheep serum (Figure 5B).

Then, we wanted to explore the major complement proteins and other related serum proteins from humans and ovine that attach to the surface of *Brucella* cells. For this, we performed a semi quantitative estimation through SDS-PAGE and proteomics. The wild-type and LPS defective strains showed differentiated protein interaction profiles and that matched to the host serum used (Figure 6). Indeed, *B. abortus ΔwadC* binds fewer sheep and human serum proteins than other bacteria (Figure 6), demonstrating the role of core determinants in the interaction. In contrast, both *B. abortus::per* and *B. canis*, lacking O-chain, bind more sheep protein serum; though they display a similar protein binding pattern. In spite of this, *B. abortus::per* is more sensitive to the microbicidal action of serum (Figure 5B). This demonstrates that binding of serum proteins to the surface of *Brucella* organisms, although relevant, is insufficient to display antimicrobial action (Figure 5B). Moreover, the O-chain is not the only component involved in complement bactericidal resistance.



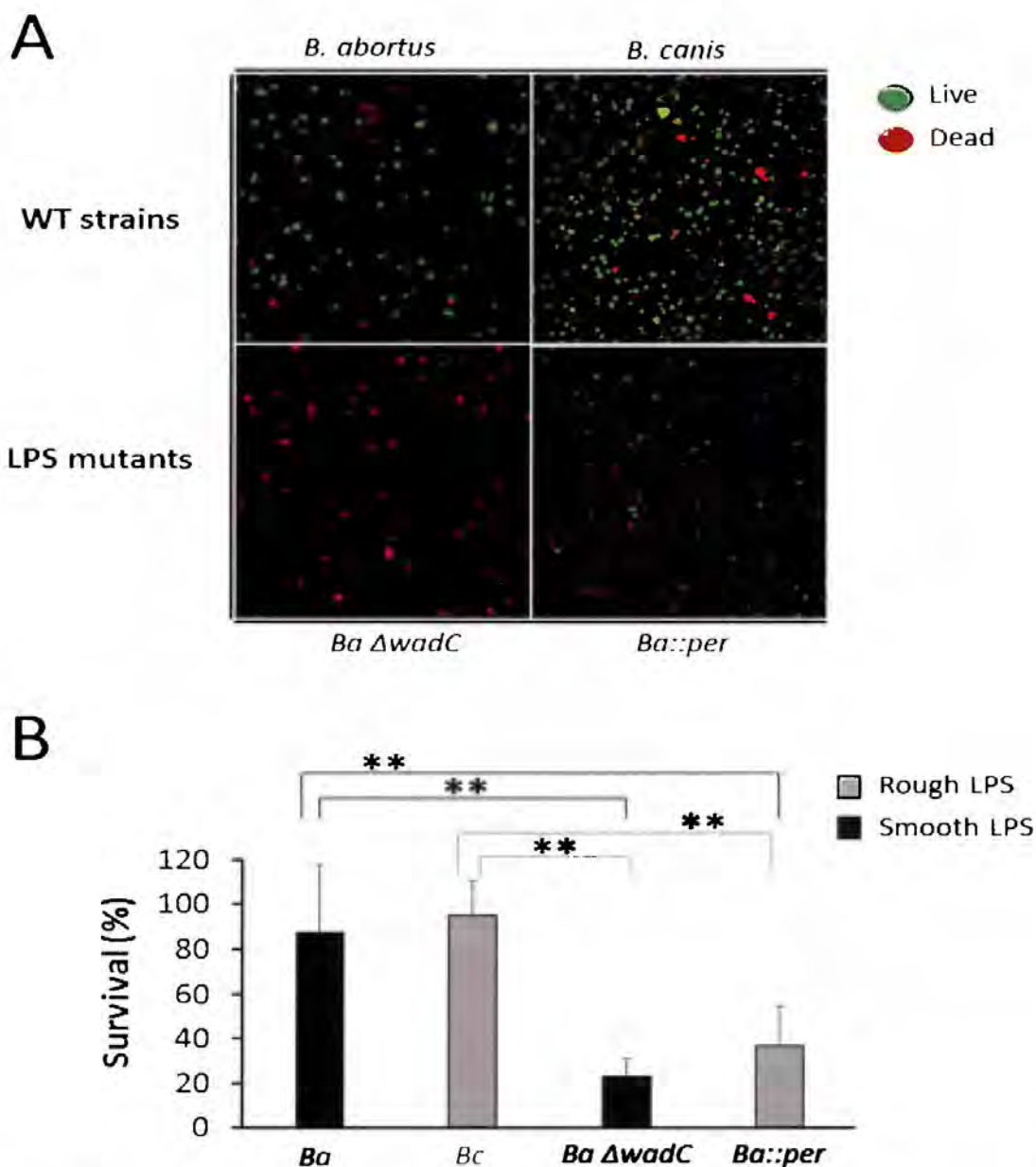
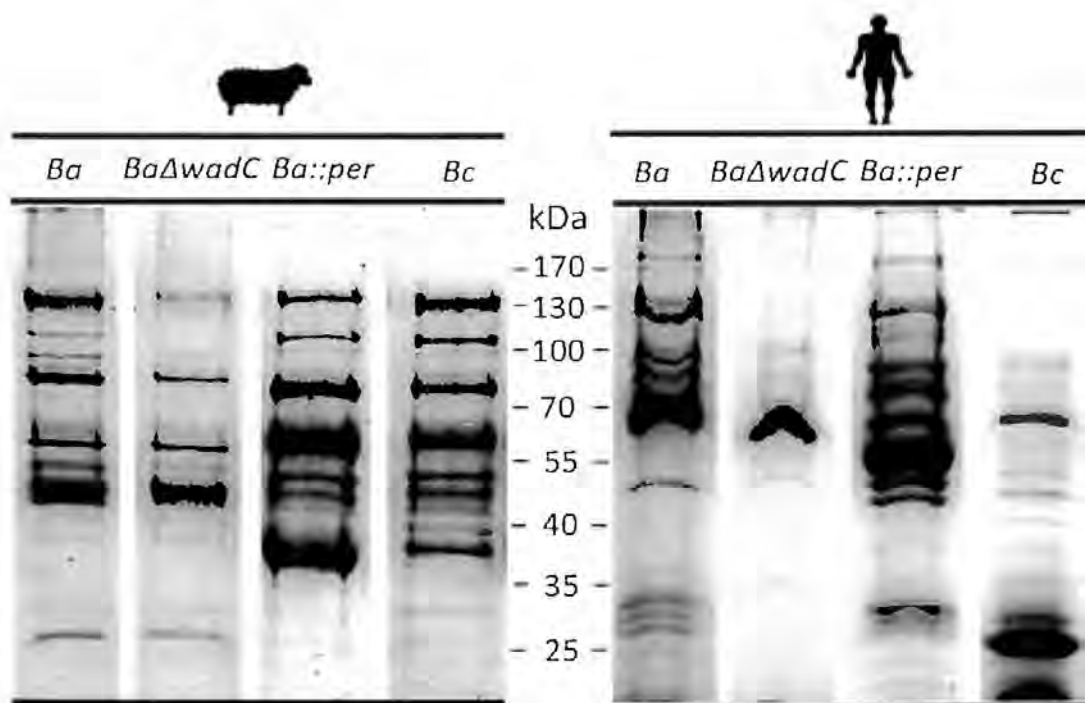


**Figure 5. Survival rate of *Brucella* and LPS mutants to the bactericidal action of sheep non-immune serum.** (A) Survival to non-immune sheep serum was estimated using a microscopy-based vital stain technique. *Brucella* strains were incubated with sheep serum and then, live bacteria (green) and dead bacteria (red) were counted under the fluorescent microscope. (B) Proportion of live/dead cells were determined by counting 2000 bacteria with the Cell Profiler Image software. Assays were repeated at least three times.  $p < 0.05$  values are indicated to the respective control using (\*). Magnification of images is 600x.



### Serum eluted proteins

**Figure 6. *Brucella* wild-type and LPS mutants show different serum protein interaction profiles.** (A) Coomassie blue stained gel of sheep and (B) human serum proteins (15  $\mu$ g/well) eluted from the surface of viable bacterial cells after incubation with the respective serum.

Considering that LPS structural modifications induce differential susceptibility to bactericidal action of serum (Figure 5), the implicated proteins in the serum susceptibility phenotype were identified. From sheep serum, *B. abortus* adsorbs conglutinin, C3 components, and terminal C5, C6, C8 proteins and complement system regulator FH. *B. abortus*  $\Delta$ wadC also binds proteins from the classical (conglutinin), common (C3), and terminal (C5 and C6) complement pathway (Figure 7). *B. canis* binds C1q, C3, conglutinin and properdin; while *B. abortus*::per, binds only C3 and FH (Figure 7). Apart from complement components, other proteins were identified (Table 4), mostly in *B. abortus*::per. One significant example is pentraxin, a protein that participates in host defense acting as an opsonin through activation of the complement pathway and through binding to Fc gamma receptors (Du Clos, 2013).

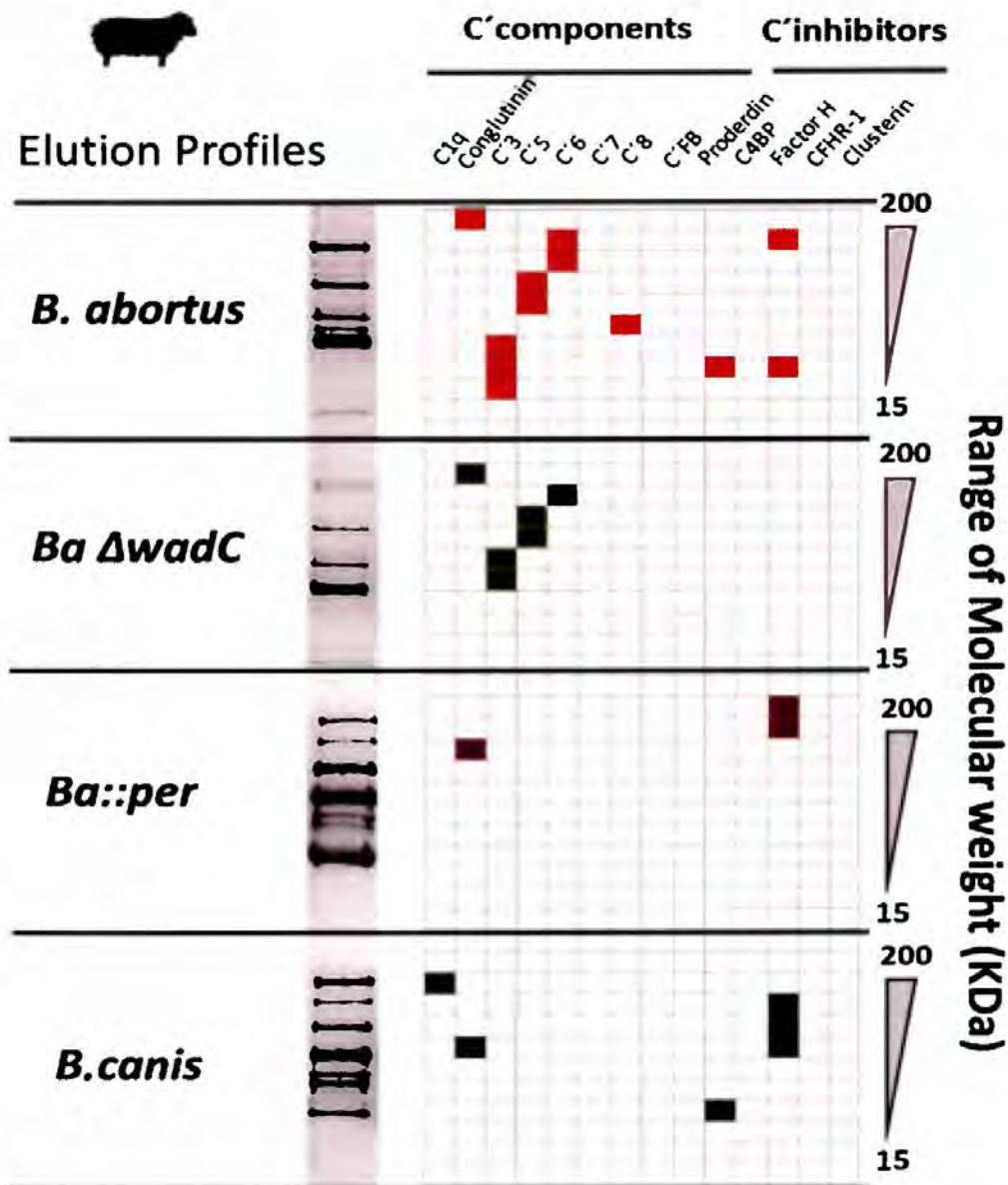


**Figure 7. Identification of sheep serum complement proteins interacting with wild-type and LPS defective *Brucella* surfaces.** Wild-type and LPS defective mutants were incubated with non-immune sheep serum. Afterwards, adsorbed host proteins were eluted with acid glycine solution and visualized in a gel stained with Coomassie Blue. Individual bands were identified by MS-MS. Experiments were repeated two times. Ba: *B. abortus*.

**Table 4.** Other non-complement sheep serum proteins eluted from *Brucella* surfaces.

Strain	Protein identified	kDa range
<i>B. abortus</i>	Serum albumin	100-70
	Globin H	70-55
	Pentraxin	25-15
<i>Ba<math>\Delta</math>wadC</i>	Pulmonary surfactant assoc protein	170-130
	Pentraxin	25-15
	C-X-C motif chemokine	25-15
<i>Ba::per</i>	Thrombospondin-1	170-130
	Ig gamma 1-chain	130-110
	Ig mu chain C	100-70
	Serum albumin	70-55
	Ig gamma chain	40-35
	C-reactive protein	25-15
	C-X-C motif chemokine	25-15
Ig J chain	25-15	
<i>B. canis</i>	Dipeptidyl peptidase 10	100-70
	Ig mu chain secretory	100-70
	Serum albumin	70-55
	Methionine synthase reductase	70-55
	Ig gamma chain	70-55
	Pentraxin	25-15

Human serum proteins bind more readily to *Brucella* cells than sera from other species. *B. abortus* binds most of the major complement proteins, as well as regulators such as clusterin and vitronectin (Figure 4 and 8). In contrast, *B. abortus*  $\Delta$ wadC binds only C3 and properdin. *B. abortus*::per and *B. canis* adsorbed complement regulators such as C4BP and FH. In addition to complement components, a few other serum proteins were also identified (Table 5).

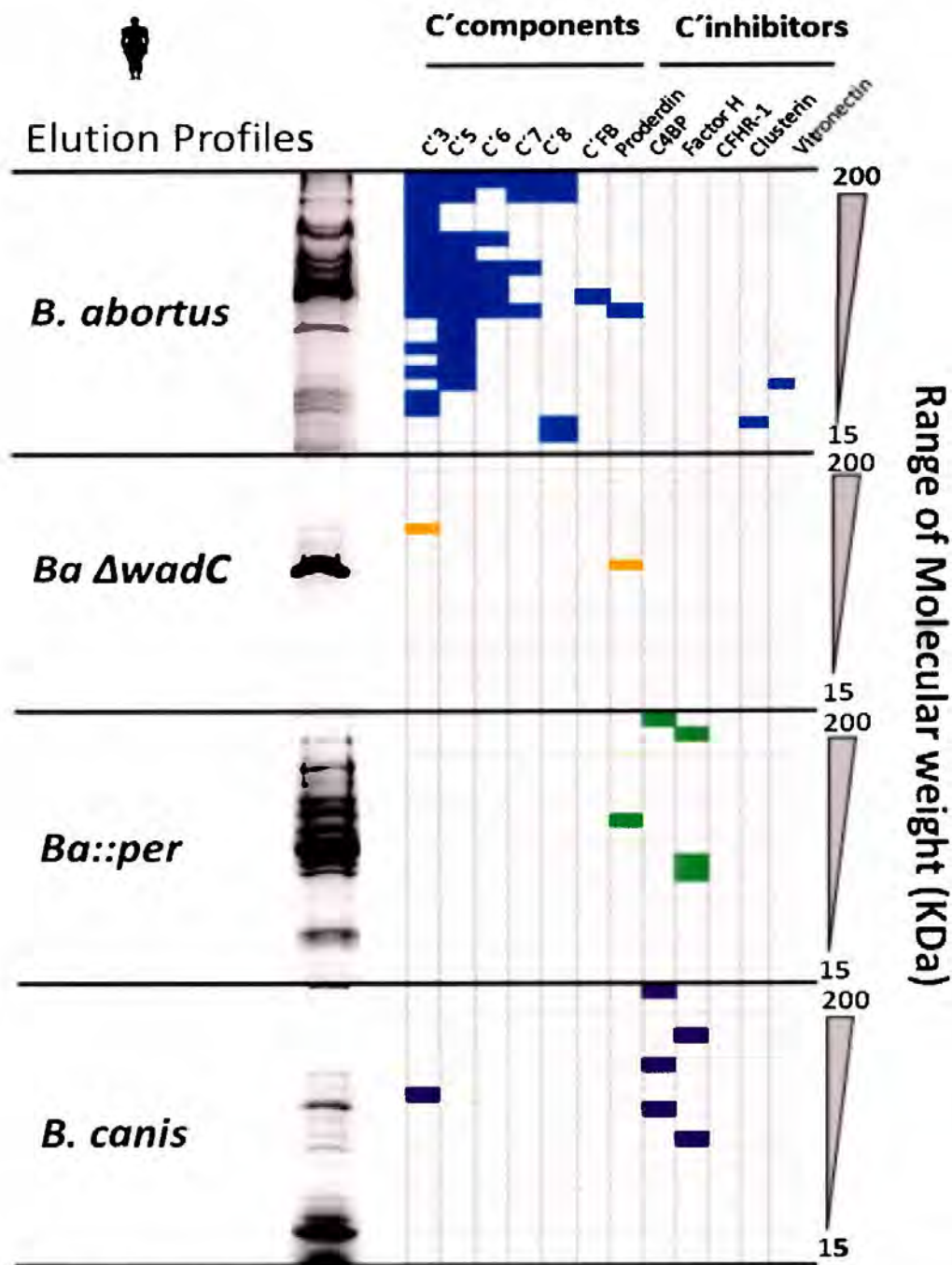


**Figure 8. Identification of human serum complement proteins interacting with wild-type and LPS defective *Brucella* surfaces.** Wild-type and LPS defective mutants were incubated with non-immune human serum. Afterwards adsorbed host proteins were eluted with acid glycine solution and visualized in a gel stained with Coomassie Blue. Individual bands were identified by proteomics. Experiments were repeated two times.

**Table 5.** Other non-complement human serum proteins eluted from *Brucella* surfaces.

Strain	Protein identified	kDa range
<i>B.abortus</i>	None	-
<i>BaΔwadC</i>	Ig heavy constant mu	100-70
	Unidentified	55-40
<i>Ba::per</i>	Inter-alpha-trypsin inh. heavy chain H4	100-70
	Ig gamma-1 heavy chain	100-70
	Ig heavy constant mu	100-70
	Serum albumin	70-55
	Ig heavy constant mu	70-55
	Beta-2-glycoprotein	55-40
	Serum amyloid P-component	35-25
<i>B.canis</i>	Ig heavy constant	100-70
	Alpha globin chain	15-10

Factor B, C3 and C9 were also identified by western blot (Figure 9A). *B. abortus::per* showed a different interaction pattern in regards to Factor B (FB). C3 and proteolytic C3 fragments, as well as C9, were detected in all strains. In order to determine the profile of eluted C9 from the surface of the bacteria and presence of C9 inserted into the outer membrane, we compared the C9 detection profile in eluted proteins and membrane lysates (Figure 9B). In *B. abortus* a single band was observed in the eluates but was undetectable in the lysate, suggesting interference in MAC assembly (Figure 9B). In contrast, a multiple band pattern was observed in the eluate and the lysate of C9 in *B. abortus::per*, implying the assembly of MAC on the bacterial surface (Figure 9B), in accordance with its susceptible phenotype (Figure 5). Although, *B. canis* shows the same pattern, it is resistant to the antimicrobial activity of serum. In *B. abortus ΔwadC*, C9 was detected in the eluates but hardly observed in the lysate, suggesting the possibility that *B. abortus ΔwadC*'s death is not fully dependent on complement activation, but on other bactericidal substances.

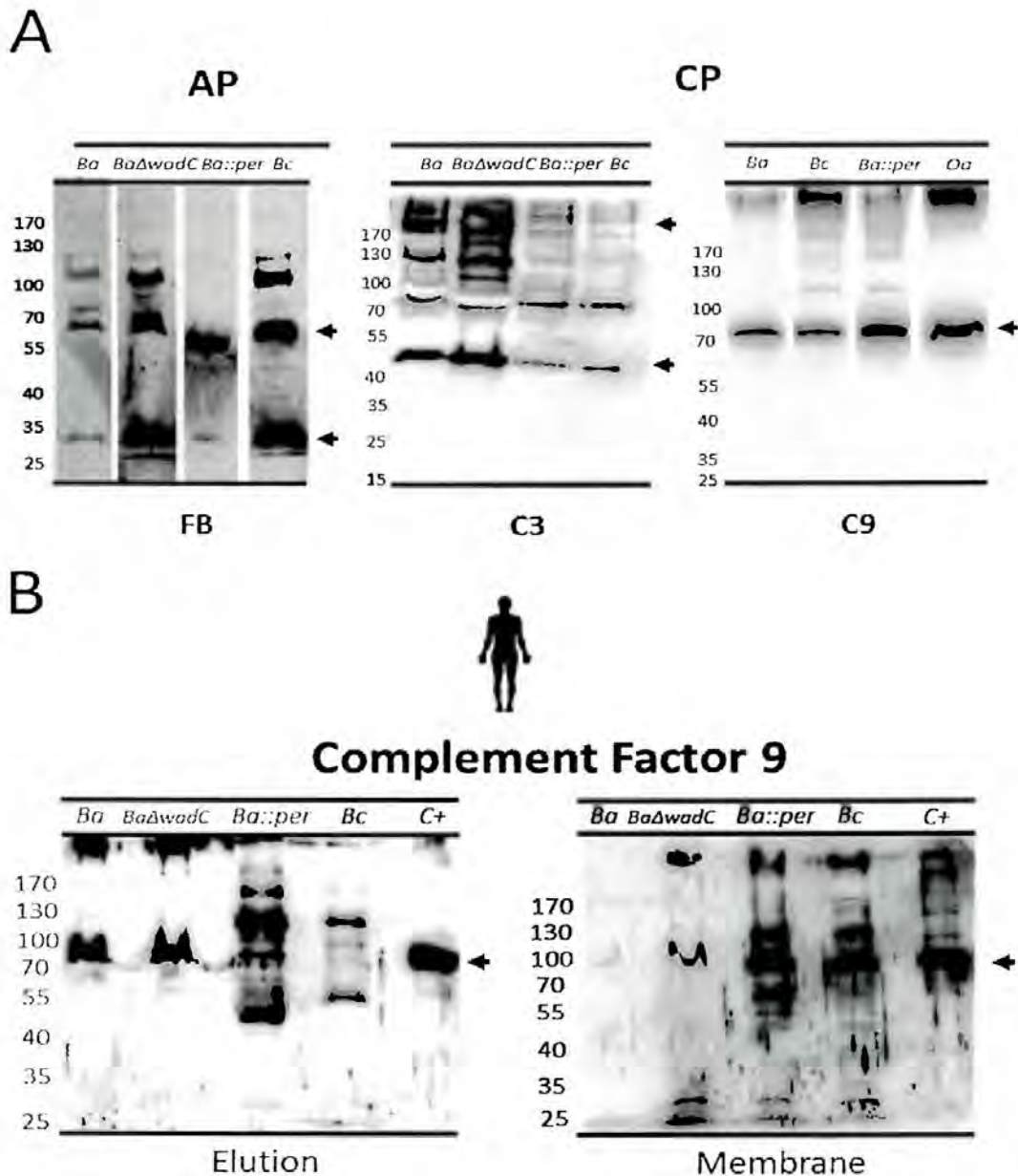


**Figure 9.** Western blot analysis of complement proteins eluted from *Brucella* surfaces. *Brucella* viable cells were incubated with non-immune human serum. Afterwards, adsorbed host serum proteins were separated in a SDS-PAGE gel and revealed with antibodies against (A) Factor B, C3, C9, (B) eluted and outer membrane attached C9. Arrows indicate the corresponding protein. AP, Alternative Pathway; CP, common pathway, C+, human serum control.

Complement regulators were determined by western blot (Figure 10). C4BP, vitronectin and FH were eluted from surface of *B. canis* after interaction with bovine and human serum (Figure 10 A, B and C), C4BP and vitronectin were not found in serum-susceptible bacteria such as *S. enterica* (Figure 10 A and C). The presence of C4BP on the surface of *Ochrobactrum* (Figure 10A) and FH in *B. abortus::per* (Figure 10B), seems not sufficient to counteract serum killing activity (Figure 5).

#### **6.6 Label free quantitative proteomics analysis of sheep serum proteins eluted from wild-type *Brucella* and LPS mutants.**

The amounts of serum proteins adsorbed to the surface of *Brucella* cells was evaluated by label-free quantitative proteomics. A total of 96 serum proteins were identified in all samples. Their function is cited in Appendix 2. To evaluate the correlation between replicates within each strain, a multivariate analysis was carried out by untargeted principal component analysis (PCA) (Figure 11). The PCA revealed the presence of four groups, corresponding to each bacterium tested. A significant correlation between the three replicates from each strain was attained; though *B. melitensis*  $\Delta wadC$  was the strain that displayed more variance. The clustering pattern correlates with the expected biologic significance: *B. melitensis* and *B. abortus* clusters were very close due to their structural similarity (Cardoso et al., 2006). Likewise, LPS defective susceptible mutants (*B. melitensis*  $\Delta per$  and *B. melitensis*  $\Delta wadC$ ) were far apart.



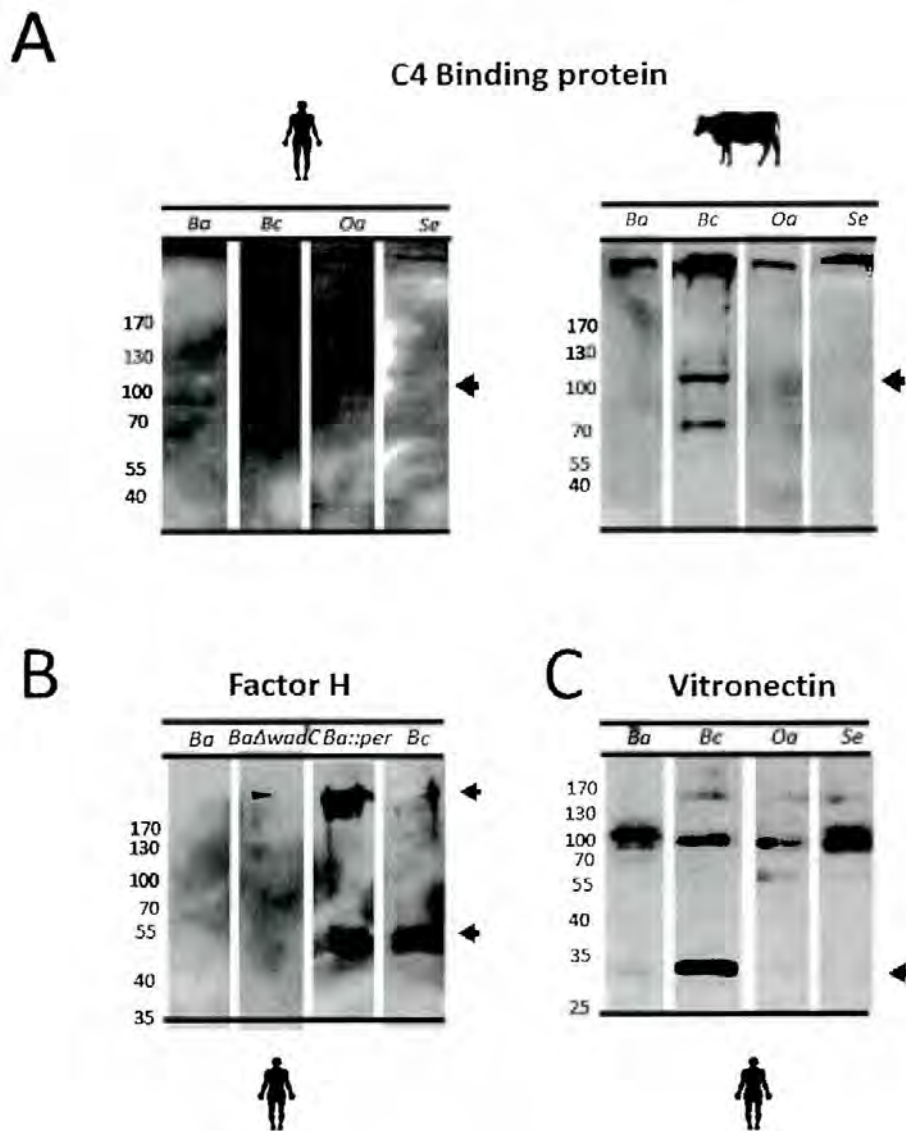


**Figure 10.** Western blot analysis of complement regulator proteins eluted from *Brucella* surfaces. *Brucella* viable cells were incubated with non-immune human serum. Afterwards adsorbed host serum proteins were separated in a SDS-PAGE gel and revealed with antibodies against (A) C4BP, (B) FH, (C) Vitronectin. Arrows indicate the corresponding protein.

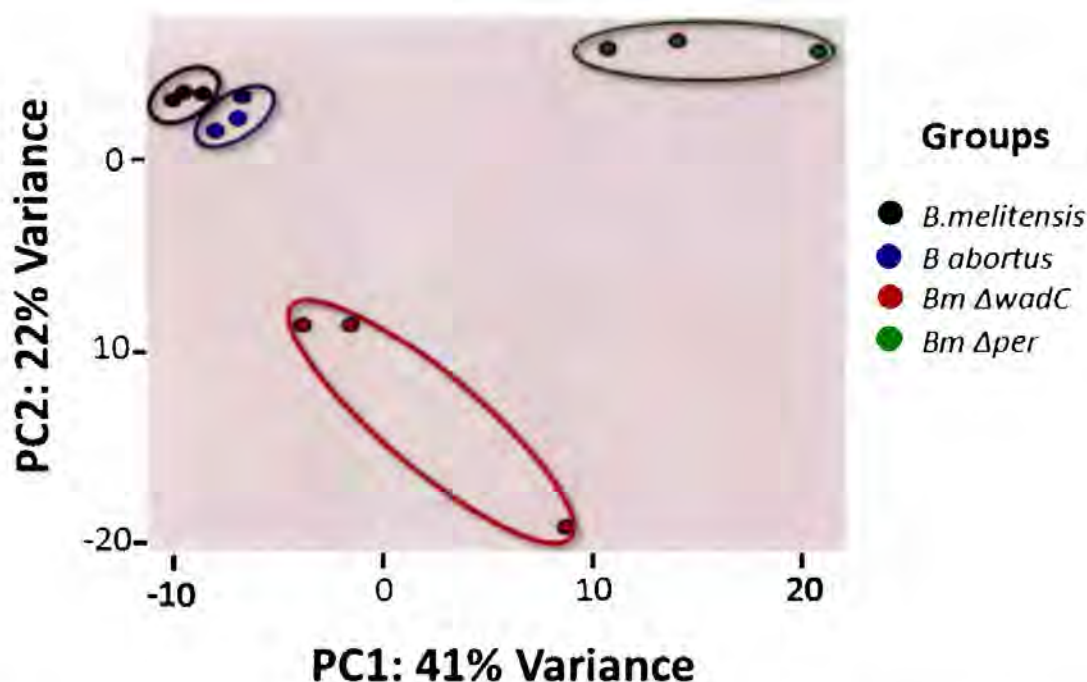


**Figure 11. Serum proteins interacting with wild-type *Brucella* and LPS defective mutants segregate based on protein abundance.** Viable bacteria were incubated with sheep serum, washed and then serum proteins were eluted from surface. Proteins were quantified by MS-MS label free spectrometry analysis. Multivariate analyses were carried out by untargeted Principal Component Analysis, using the intensity-abundance value from each protein detected.

To estimate the interactions with serum proteins bound to the bacterial surface, Proteomaps were constructed for each *Brucella* species. At the broadest level, all *Brucella*-host serum proteomes shared the same categories, suggesting that small shifts in protein abundance trigger significant changes on the interaction (Figure 12 A, B and C) (Appendix 3). *B. melitensis* and *B. abortus* share similar dimensions in relation to proteins in the immune system category (light brown polygon), mainly complement proteins (Figure 13 A and B). In contrast, in *B. melitensis ΔwadC*, C3 polygon-shape tile increases in size while other complement proteins decrease in the same category (Figure 14 A). In *B. melitensis Δper*, immune system category proteins were reduced but other proteins, such as coagulation factor V, coagulation factor VII, plasma kallikrein, C1q and FH were abundant (Figure 14B).

Moreover, an increase in the total amount of other non-immune proteins category was observed, generating a different visual insight of the *Brucella*-host serum interaction proteome (Figure 14B). This result is also consistent with the SDS-PAGE-proteomics and western blot proteomic pattern previously shown in Figure 7 and Table 4.

To further study how structural modifications in LPS influence interaction with host serum proteins, all profiles were normalized against *B. melitensis* (Appendix 4, 5, 6). As shown in Figure 15, *B. abortus* displays the least differences in fold-changes among proteins. In contrast, a large number of proteins are increased or decreased in *B. melitensis*  $\Delta$ wadC and *B. melitensis*  $\Delta$ per, indicating that structural similarities in the outer membrane in *Brucella* are in accordance with the expected protein interaction profile (Figure 15 and Table 6).

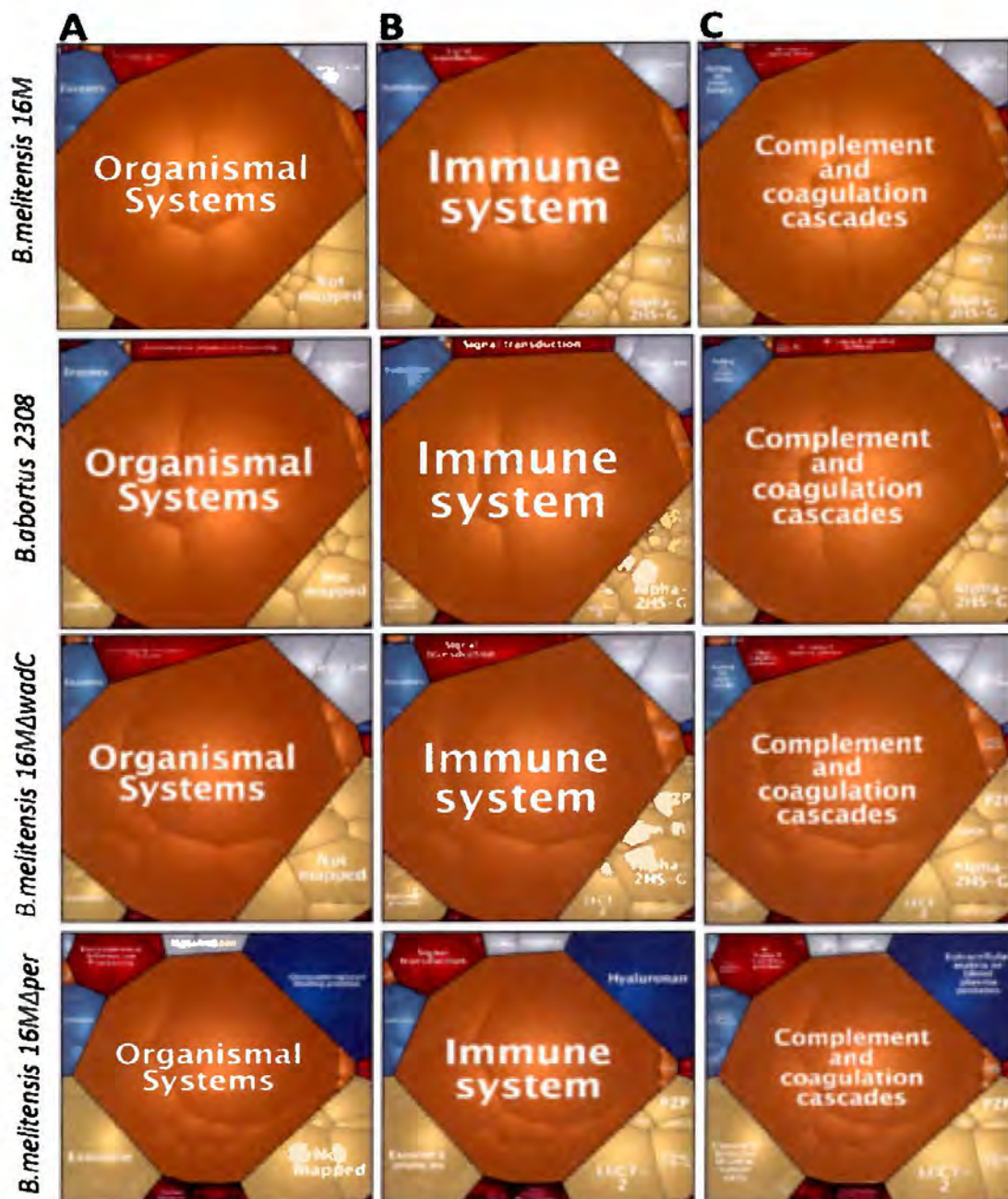


**Figure 12. Proteomaps visualization of sheep serum proteins adsorbed to *Brucella* surfaces.** Hierarchical classification of proteins according to KEGG Orthology function was performed (Appendix 3). Abundance and function of each protein were represented as a polygon-shape using Proteomaps software. Polygon sizes represent protein abundances obtained by MS-MS. Blue, enzymes; red, environmental information processing, light gray, metabolism; light brown, organismal systems. (A) Category level 1; (B) Category level 2; (C) Category level 3. Color code is according to category level 1 classification.

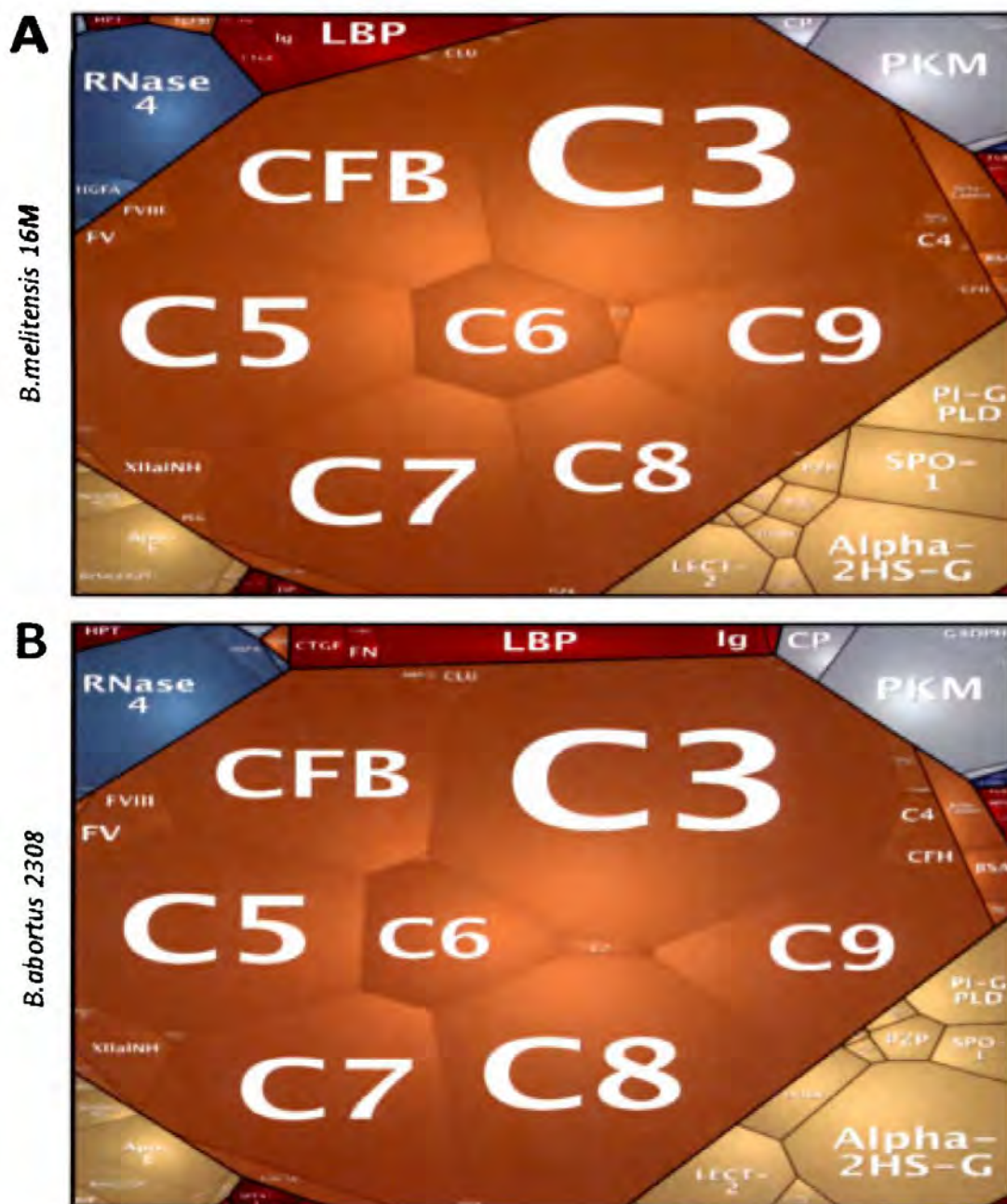


**Figure 13.** Proteomaps of sheep serum proteins adsorbed in (A) *B. melitensis* 16M and (B) *B. abortus* 2308 surface. Hierarchically classification of proteins according to their KEGG Orthology function (Appendix 3). Category level 4. Abundances and function of each protein were represented as a polygon-shape using Proteomaps software. Polygon size represent protein abundances obtained by MS-MS. Color code is according to category level 1 classification.

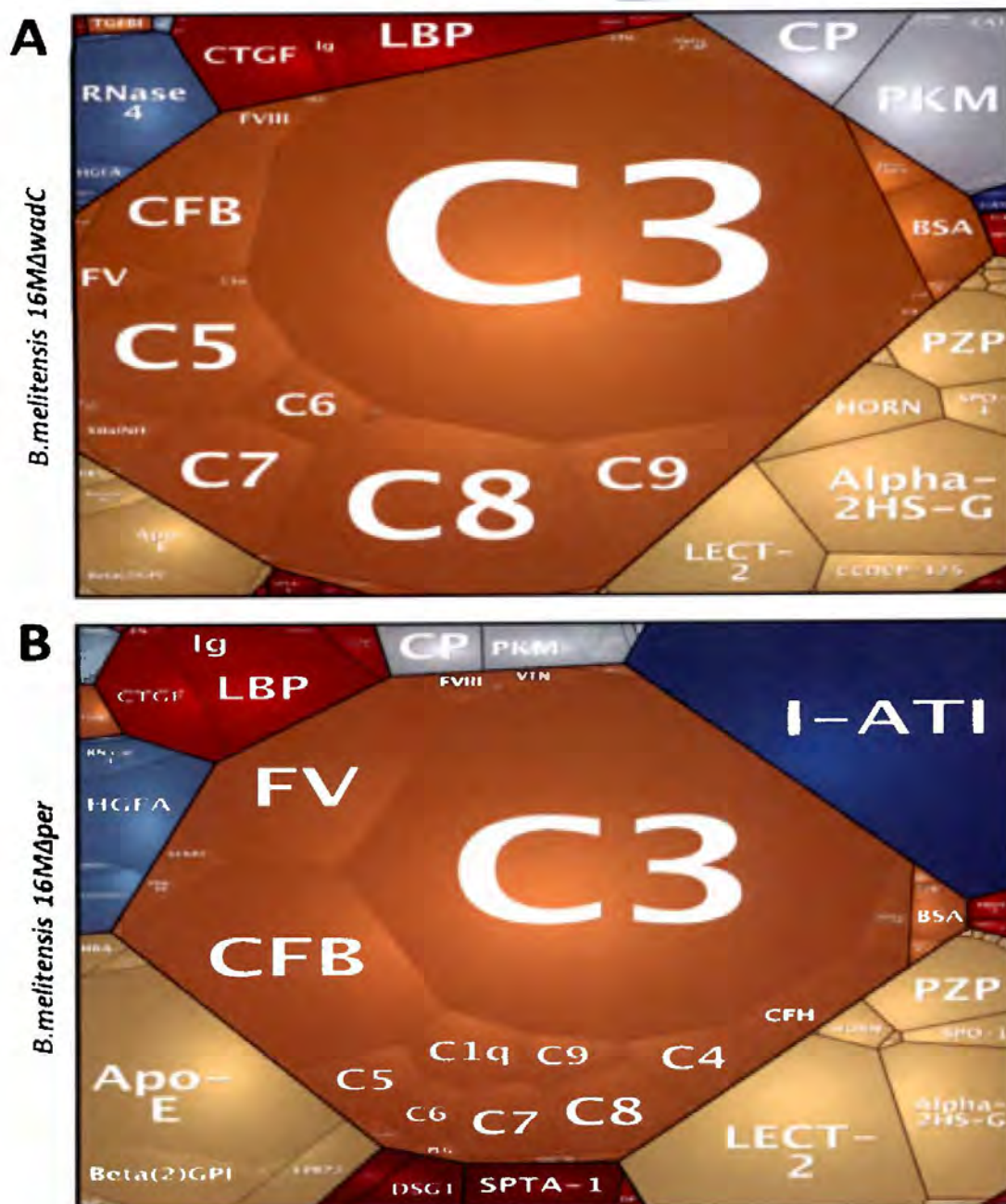


**Figure 14.** Proteomaps of sheep serum proteins adsorbed in (A) *B. melitensis* 16M $\Delta$ wadC and (B) *B. melitensis* 16M $\Delta$ per surface. Hierarchical classification of proteins according to their KEGG Orthology function (Appendix 3). Category level 4. Abundances and function of each protein were represented as a polygon-shape using Proteomaps software. Polygon size represent the protein abundances obtained by MS-MS. Color code is according to category level 1 classification.

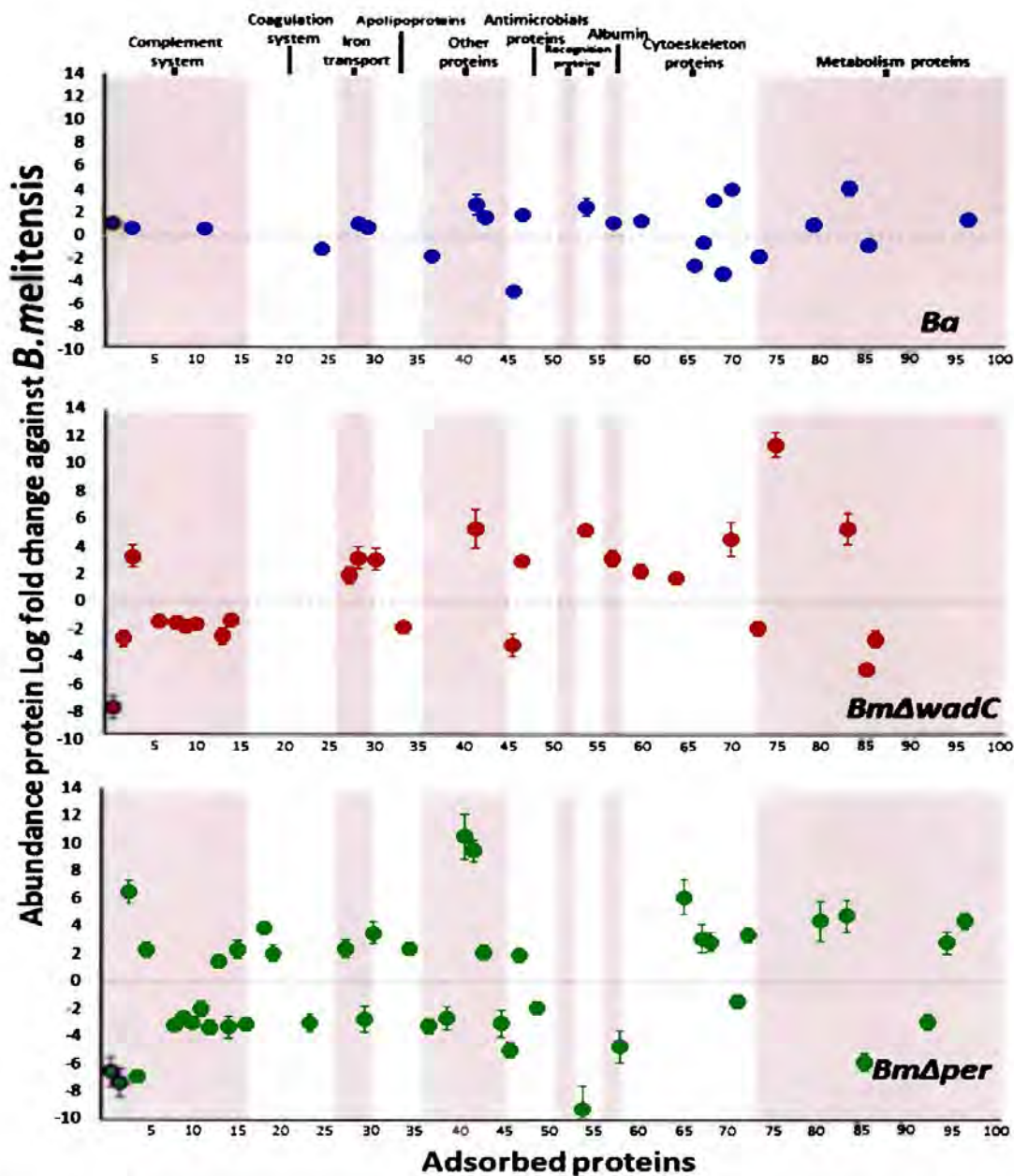


Figure 15. Sheep serum proteins differentially adsorbed by *B. abortus* and LPS mutants in relation to *B. melitensis*. Intensity values per protein eluted from *B. abortus* and LPS mutants were normalized against *B. melitensis* and displayed in Log fold change between strains (y-axis). Protein enumeration (x-axis) follows the numbering indicated in Appendix 4, 5, 6. From a total proteome, only significantly statistical different abundance of proteins were represented. Median and standard deviations of three independent replicates are shown. Protein function was assigned according to an arbitrary classification.

**Table 6.** Sheep serum proteins eluted from *Brucella* surfaces in relation to *B. melitensis* 16M.

	Number of proteins in relation to <i>B. melitensis</i> 16M		
	Common	Increased	Decreased
<i>B. abortus</i>	72	16	8
<i>B. melitensis</i> Δ <i>wadC</i>	70	13	13
<i>B. melitensis</i> Δ <i>per</i>	53	21	22

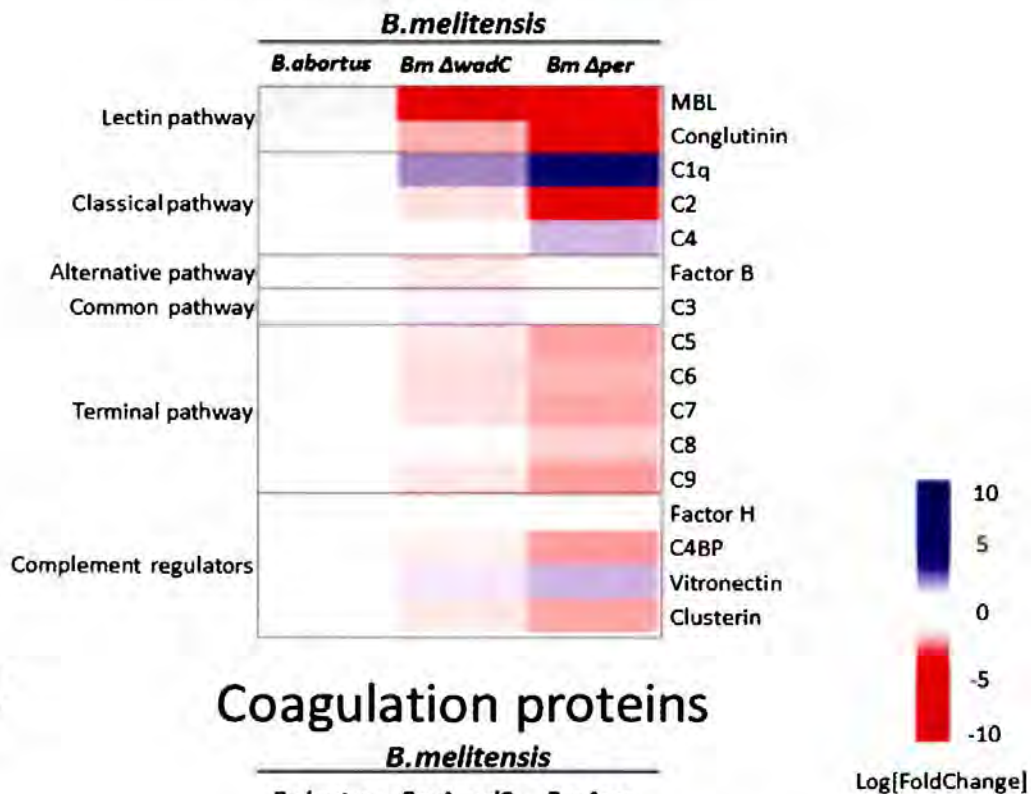
First, we determined the relative abundance of complement and complement-regulators proteins (Figure 16A). Except for mannose binding lectin (MBL), *B. abortus* and *B. melitensis* display similar adsorption profiles. In contrast, lectin pathway proteins (MBL and conglutinin) were reduced in *B. melitensis* Δ*wadC* and *B. melitensis* Δ*per*, but classical pathway proteins such as C1q and C4 were increased. Terminal complement factors showed a significant decrease in the LPS defective mutants except for FH, most of the complement regulators were decreased in both LPS mutants; little changes in abundance in vitronectin were observed (Figure 16A).

A total of eleven coagulation proteins were detected in the label free analysis (Figure 16B). From these, only four showed some differences in *B. abortus*. The LPS mutants displayed a more dissimilar pattern; though *B. melitensis* Δ*per* was the most distant. These experiments suggest that wild-type *Brucella* strains interact with coagulation factors modulating its activation. Coagulation functional assays were performed complementary to the label free analysis. Residual plasma consumed after incubation with *B. abortus*::*per* exhibits extended values in Prothrombin Time (PT) and Partial Thromboplastin Time (PTT) compared to control plasma, demonstrating a reduction in coagulation factors and augmented factors activated to the bacterial surface. Plasma incubated with *B. canis* did not display significant changes in PT and PTT (Table 7).



A

## Complement system



B

## Coagulation proteins

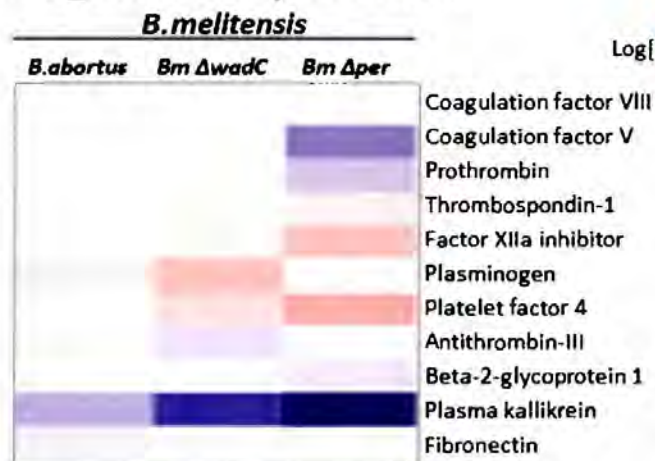


**Figure 16. Complement (A) and coagulation (B) proteins adsorbed by *B. abortus* and LPS mutants in relation to *B. melitensis*.** Colored squares indicate abundances level over log 2 (blue) and below log 2 (red) compared to *B. melitensis*. Arbitrary functional protein classification was assigned. Sample abundance quantification was done by triplicate.

**Table 7.** Coagulation times in residual consumed plasma by *Brucella*.

	Consumed Plasma	
	Prothrombin Time (s)	Parcial Thromboplastine Time (s)
<i>B. abortus</i>	12.5 ± 0.7	43.5 ± 0.5
<i>B. abortus</i> Δ <i>wadC</i>	14.0 ± 0.1	44.0 ± 1.4
<i>B. abortus</i> :: <i>per</i>	29.0 ± 0.1	98.5 ± 4.9
<i>B. canis</i>	18.0 ± 0.1	58.0 ± 0.1
Plasma control	14.0 ± 0.1 (12-15*)	42.5 ± 0.7 (20-40*)

\*Reference values.

Of particular interest was the differential profile of proteins involved in anti-inflammatory, proinflammatory and antimicrobial actions. *B. melitensis* Δ*wadC* and *B. melitensis* Δ*per* showed an increased fold change in pregnancy zone protein, hemopexin, alpha-1-antiproteinase, inter-alpha-trypsin inhibitor, plasma serine protease inhibitor, lysozyme, myeloperoxidase, lactotransferrin and catalase. Haptoglobin, protein S100-A8, and cathelicidin are increased in eluates from wild-type *B. abortus* and *B. melitensis* (Figure 17A). Except for haptoglobin, all the other iron transport proteins detected were augmented in LPS mutants (Figure 17B).

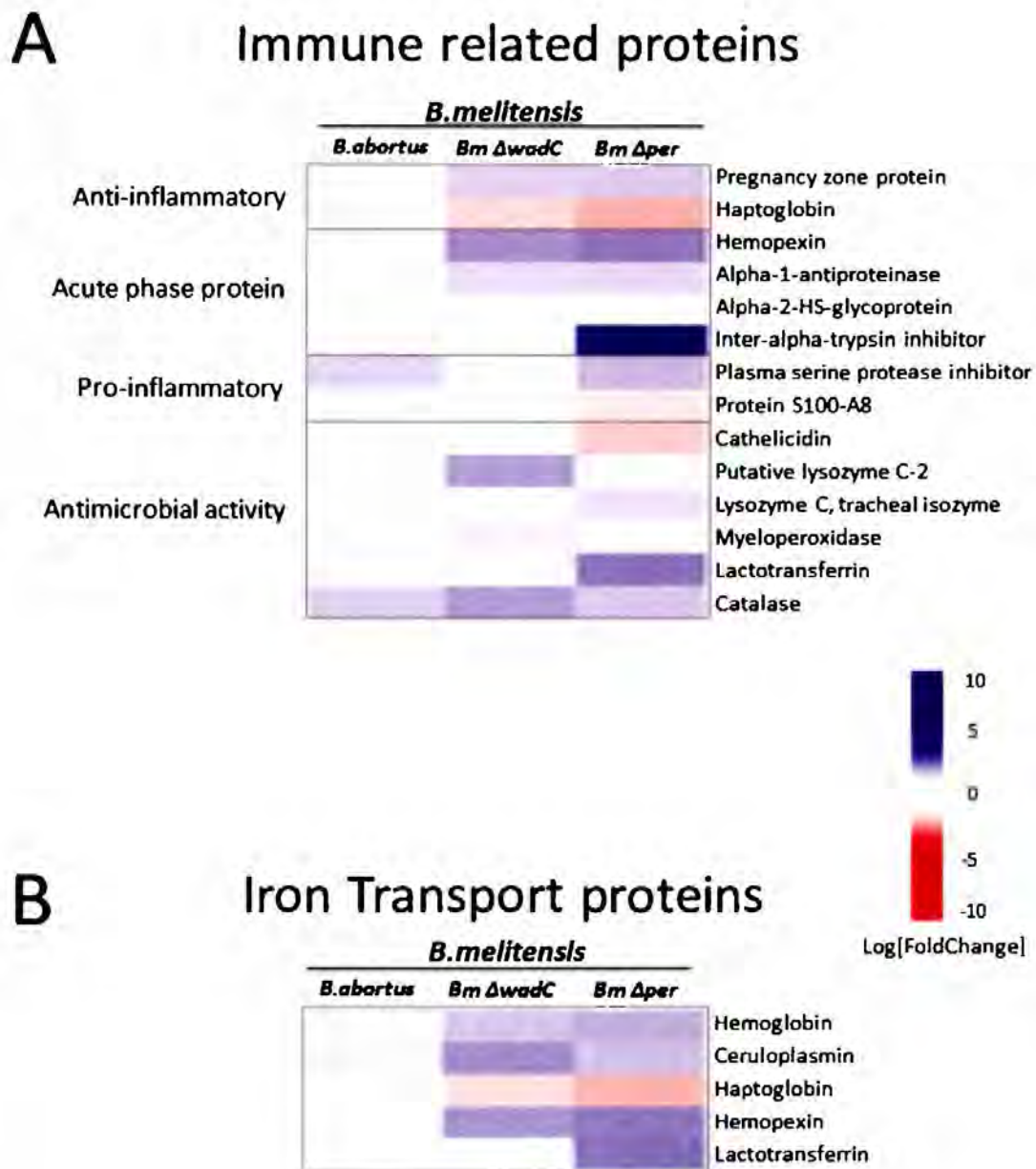


**Figure 17. Immune related (A) and iron transport (B) proteins adsorbed by *B. abortus* and LPS mutants in relation to *B. melitensis*.** Colored squares indicate abundances level over log 2 (blue) and below log 2 (red) compared to *B. melitensis*. Arbitrary functional protein classification was assigned. Sample abundance quantification was done by triplicate.

## 7. DISCUSSION

*Brucella* is capable of counteracting the host immune response. At the onset of the infection, *Brucella* (i) circumvents a strong activation of the innate immune system (Barquero-Calvo et al., 2007); (ii) evades the direct action of complement, coagulation and other bactericidal substances (Eisenschenk et al., 1999; Barquero-Calvo et al., 2007); (iii) resists and evades the bactericidal action of PMNs, macrophages and dendritic cells (Enright et al., 1990; Pizarro-Cerdá et al., 1999) and; (iv) prolongs the viability of infected host cells in order to establish long lasting infections (Gross et al., 2000). In this regard, it has been well accepted that *Brucella* evolved as a stealthy strategy which involves absence, modification or inaccessibility of classical PAMPs (Barquero-Calvo et al., 2007, 2009). During this process, *Brucella* avoids the recognition and activation of several elements of the innate immune response generating an “immunological window” that allows the bacterium to invade host cells of the reticuloendothelial system and replicate (Barquero-Calvo et al., 2007; Martirosyan et al., 2011). However, the mechanisms by which brucellae modulate these events are not fully understood. One striking feature is the *Brucella* outer membrane, which evolved to confront the host immune response (Velasco et al., 2000; Barquero-Calvo et al., 2007, 2009). In this work we have unveiled some of the humoral serum factors that interact with the *Brucella* cell envelope that appear to determine the fate of extracellular bacteria during the first moments of host invasion and after being released from cells.

Based on our results we propose the following conceptual models to illustrate how *Brucella* modulates innate immunity through interaction with serum proteins.

### **Conceptual model 1. *Brucella* modulates immunity through sequestration of complement regulators (Figure 18)**

Sequestration of complement regulators has been related to complement evasion in other pathogens to avoid direct killing, opsonization and chemotaxis (Kraiczy et al., 2001; Alitalo et al., 2001; Barbosa et al., 2009; Hallström et al., 2010; Laarman et al., 2011). In *Brucella* it has been proposed that the O-chain LPS molecule is the main responsible for resistance to bactericidal action of serum (Freer et al., 1996). However, we have demonstrated that other factors may be relevant in this resistance. For instance, rough-like *B. canis* devoided of O-chain is strongly resistant to the bactericidal action of sera, despite the

fact that the bacterium binds relatively large amounts of serum proteins. Moreover, the particular high resistance of rough-like *B. canis* against the bactericidal action of serum proteins may be linked to the higher quantities of different complement regulators adsorbed. It may be that through this mechanism, *B. canis* is capable of bypassing the requirements of an O-chain.

We propose that *Brucella* organisms are sequestering complement inhibitor regulators (Figure 18).

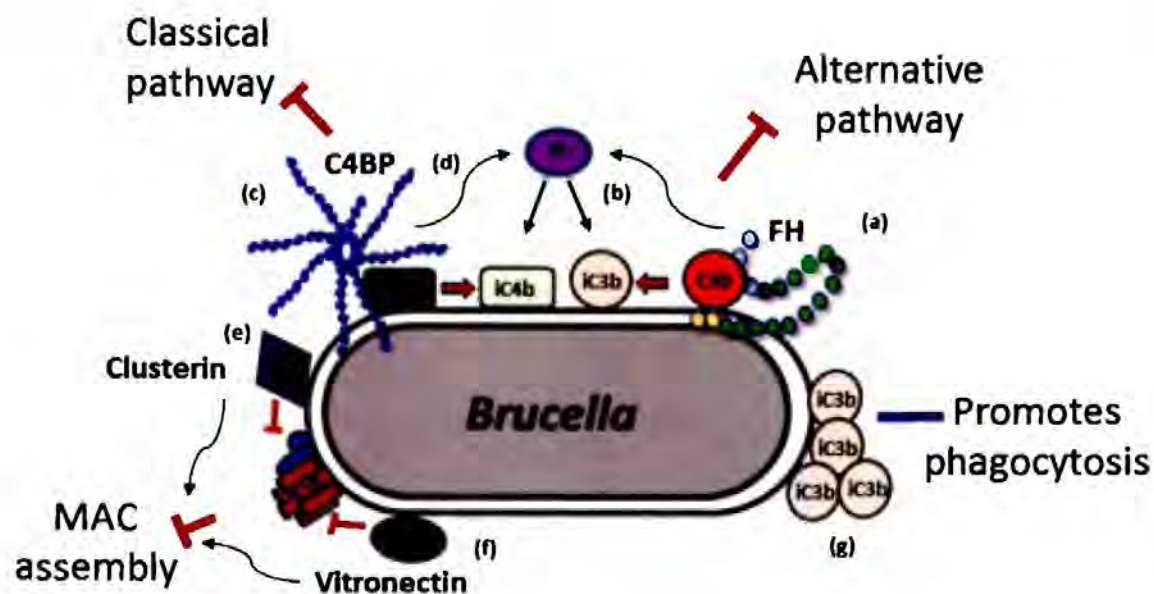


**Figure 18. Conceptual model: *Brucella* modulates immunity through sequestration of complement regulators.** (a) The deposition of C3b onto *Brucella* surface favors the recruitment of FH, (b) promoting the subsequent factor I-mediated (FI) conversion of C3b to iC3b blocking the activation of the alternative pathway. Concomitantly, (c) C4BP binds to the bacterial surface and becomes active; degrading C4b to iC4. This will inhibit the formation of C3 convertase of the classical pathway. (d) C4BP also promotes the FI-mediated conversion of C4b to iC4b, blocking the classical pathway activation. (e) Clusterin and (f) Vitronectin inhibit C5b-7 complex and C9 polymerization at the bacterial membrane-binding site, hampering MAC formation. (g) Complement regulators favor deposition of inactive complement molecules such as iC3b on *Brucella* surface, promoting its phagocytosis. As a

result, *Brucella* would evade complement bactericidal action, preventing the proinflammatory response and promoting its opsonization for phagocytosis of PMNs and other phagocytic cells.

This hypothesis is sustained by *i)* binding of several complement regulators on the bacterial surface of wild-type *Brucella* species; *ii)* presence of regulators on the surface of *B. canis* independent of the type of serum. *iii)* absence of regulators in serum-susceptible bacteria such as *S. enterica*. *iv)* the presence of regulators in LPS mutants and on the surface of *Salmonella* and *Ochrobactrum*, respectively, that were not sufficient to counteract serum killing activity. Independently of the host serum type (human and sheep), complement regulators bound to the *Brucella* surface.

*Brucella* circumvents several of the functions of complement such as the induction of anaphylotoxins, and probably, the resistance to direct killing of complement through the interaction with specific regulatory proteins. Complement regulators favor deposition of inactive complement molecules such as iC3b on *Brucella* surface, promoting its phagocytosis (Figure 18). According to the *Brucella* life cycle, opsonization favors the phagocytosis of *Brucella* for replication in host cells and opens a window for the bacterium to spread within the host through PMNs, macrophages and dendritic cells at the onset of the infection. It is striking that despite deposition of complement factors on the *Brucella* surface the proinflammatory response is abrogated (Barquero-Calvo et al., 2007; Chacón-Díaz et al., 2015).

It is worth noting that in other pathogens, MAC complexes can occur in inactivated forms or incomplete complex assemblies without compromising bacterial viability (Berends et al., 2013). It seems that in *Brucella*, MAC complexes are not assembled correctly. Usually, inactive MAC consists of only two or three C9 in which the completion of the C9 ring is stopped by acquisition of vitronectin or clusterin as seems the case in resistant *Brucella*. Indeed, we eluted significant quantities of C5, C6, C7, C8, C9 proteins in resistant bacteria in contrast to susceptible strains. Therefore, in the susceptible strains, MAC complement factors were covalently linked and immersed on the bacterial membrane in contrast to the resistant counterparts.

**Conceptual model 2: *Brucella* adsorption of pentraxin enhances complement regulators recruitment** (Figure 19).

Pentraxins are highly conserved components of innate immunity, involved in host defense against pathogen infection or in the regulation of the scavenger activity of macrophages and dendritic cells. They include the short pentraxins C-reactive protein and serum amyloid P component, and the long pentraxin PTX3 (Du Clos, 2013).

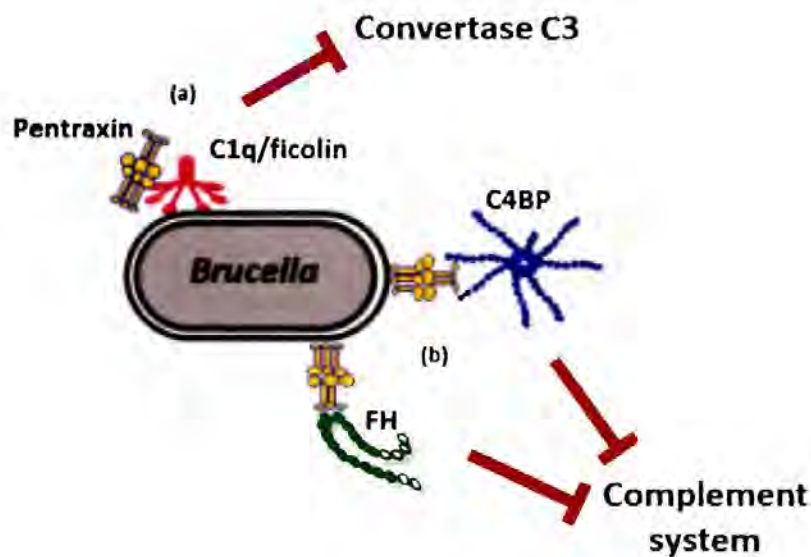


**Figure 19. Conceptual model: *Brucella* adsorption of pentraxin enhances recruitment of complement regulators.** (a) Pentraxin attached on the surface of *Brucella* may interact with C1q and ficolins. The C1q-pentraxin or ficolin-pentraxin ligand complex would not lead to the C3 convertase formation. (b) Pentraxin direct recruitment of FH and C4BP inhibitory proteins would limit C3 and C5 convertase activation. These would result in low complement activation and MAC formation as seen in *Brucella*.

*Brucella* adsorbed the acute-phase protein pentraxin. Pentraxins bind C1q and ficolins and thereby activate classical and lectin complement pathways. Concomitantly, pentraxins interact with the complement regulators C4BP and FH. The simultaneous binding of both, complement activators and inhibitory proteins, likely ensures an optimal opsonization of

target surfaces without detrimental effects or overwhelming complement activation (Braunschweig and Józsi, 2011).

**Conceptual model 3: *Brucella* interaction with FXIIa inhibitor promotes a low proinflammatory response and favors inactivation of the complement system on the *Brucella* surface** (Figure 20).

The interaction of *Brucella* surface with components of the coagulation cascade is also intriguing. Coagulation related proteins were the second most abundant proteins detected in the label free analysis. It is known that the complement and coagulation systems are two inter-related proteolytic cascades (Appendix 7)(Conway, 2015) that play important roles in host defense and hemostasis (Markiewski et al., 2007). Brucellosis does not induce coagulopathies and in contrast to other bacteria, it does not promote the generation of free fibrin peptides (Chen, 2004; Kwak et al., 2006; Barquero-Calvo et al., 2007). Our results show that *B. melitensis* and *B. abortus*, target-bind FXII inhibitor (Figure 20).

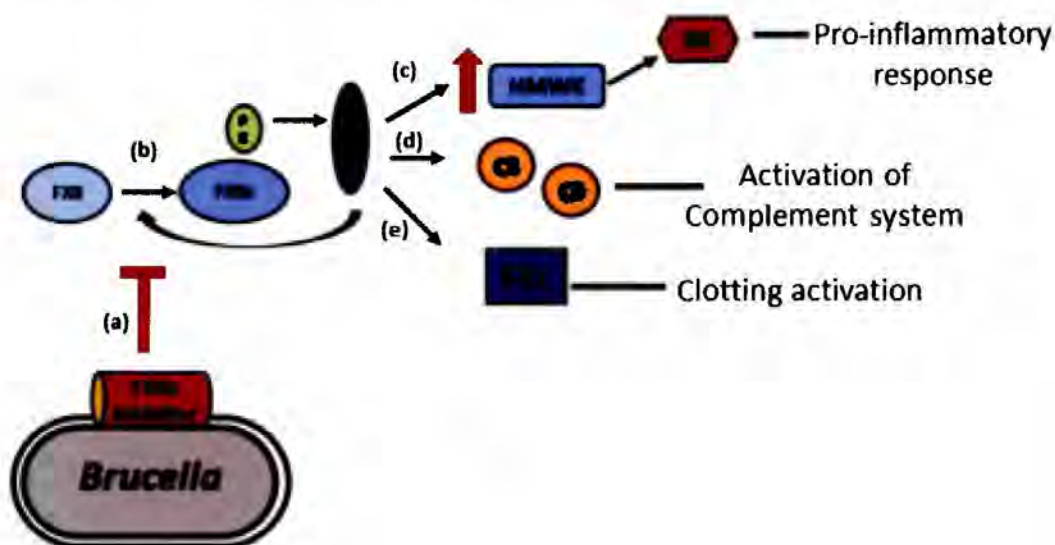


**Figure 20. Conceptual model: Interaction with coagulation proteins promotes low inflammatory response and favors inactivation of the complement system on *Brucella* surface.** The contact-intrinsic coagulation pathway is activated on negatively charged structures, such as the *Brucella* outer membrane. (a) Target-binding of FXII through factor XIIa inhibitor sequestration, as an evasion strategy, would result in low-level activation into



FXIIa, thus inhibiting the biological functions described. (b) Activated factor XII (XIIa) activates kallikrein. Production of kallikrein results in: (c) increased production of factor XII and High Molecular Weight Kininogen (HMWK) that releases the proinflammatory and vasoactive peptide bradykinin. (d) activates the complement alternative pathway, (e) and clotting pathway via activation of factor XI. PK, pre-kalikein; K, kalikein; HMWK, high molecular weight kininogen; BK, bradykinin.

Target binding of FXII through factor XIIa inhibitor as an evasion strategy would induce low-levels of autoactivation of FXIIa and reduction of active plasma kallikrein. In course, this may hamper complement and clotting activation and the subsequent recruitment of phagocytes (Sato et al., 1996; Schmaier, 2016). Further experiments are required to elucidate the specific role that components of the coagulation system may play during brucellosis.

**Conceptual model 4: Ruminant conglutinin attachment on *Brucella* surface would favor entry to host cells (Figure 21).**

The composition of serum proteins differ among various animal species (Moore, 1945). Of particular interest is conglutinin, a characteristic protein of ruminants, such as cows and sheep (Śliwa-Dominiak et al., 2010), absent in other animal species, including humans. Little is known about the physiological role of conglutinin. Previous works have determined that conglutinin decreases in pregnant cows four weeks before term and persists up to two weeks after delivery (Ingram and Mitchell, 1970). A decrease in conglutinin serum concentration has been also determined during or between the 2<sup>nd</sup> and 4<sup>th</sup> week after infectious abortion (Ingram and Mitchell, 1971). Both events are related with *Brucella* physiopathology. Further studies are required to understand how *Brucella* interaction with conglutinin may favor the bacteria in its interaction with the host.

According to our results, we propose the following conceptual model (Figure 21).

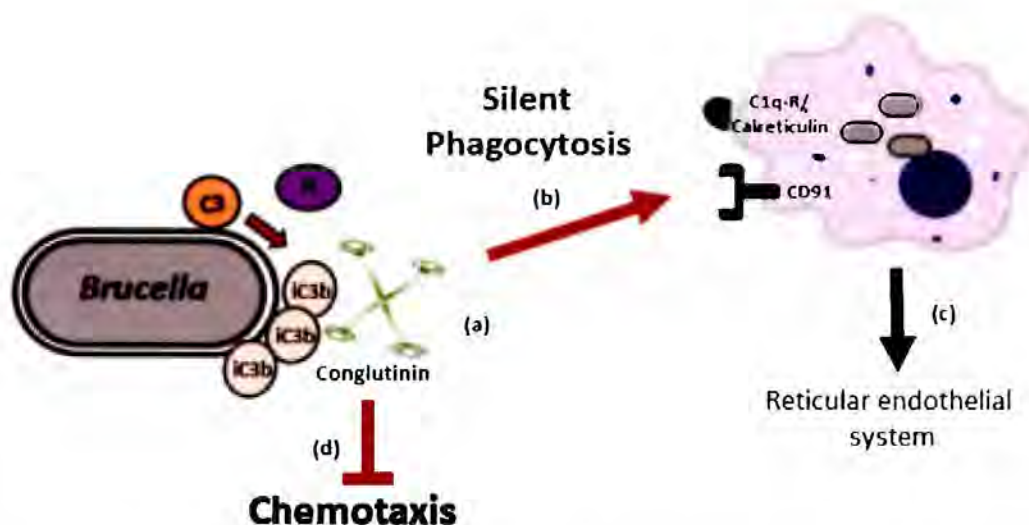


**Figure 21. Conceptual model: Conglutinin attachment on *Brucella* surface favors entry to host cells.** (a) Conglutinin binds to oligosaccharides in iC3b molecule previous deposited on *Brucella* surface. (b) Conglutinin-iC3b complex would mediate contact between bacteria and host phagocytic cell through calreticulin and CD91 receptor (silent apoptotic uptake). It results in a non-phlogistic bacterial phagocytosis. (c) Then the infected phagocytes may serve as “Trojan Horse” for transporting *Brucella* to regional lymph nodes and thereafter to the entire reticular endothelial system. (d) Moreover, conglutinin does not have chemotactic properties for bovine peripheral blood leucocytes.

Attached conglutinin to *Brucella* surface would be advantageous in bacterial dispersion within the host, since its receptor (C1q-R or calreticulin) has been shown to be expressed on the surface of macrophages and neutrophils (Malhotra et al., 1990, Raghavan et al., 2013). Moreover, calreticulin is also functionally associated with macrophage receptor CD91 or alpha-2-macroglobulin receptor related to apoptotic cell clearance. Thus, the recognition of C1q or conglutinin-opsonized *Brucella* by calreticulin would induce phagocytosis through silent and non-inflammatory CD91-dependent mechanisms (Vandivier et al., 2002). Attaching conglutinin could acts as opsonin and mediate biological functions by further interactions with phagocytic cells, allowing modulation of host innate response (Figure 21)(Dec et al., 2012).

## **8. CONCLUSIONS AND FUTURE PERSPECTIVES**

Our findings reveal how *Brucella* interaction with specific host serum proteins such as complement may have a role in pathogenesis. However, the interaction of *Brucella* with serum is not limited to a few proteins. In this regard, our approach opens new research areas that have never been studied with *Brucella* and open the possibility to explore the function of some serum proteins during brucellosis. Finally, experimental strategies are required to approved conceptual models proposed in this work.

## 9. REFERENCES

- Alitalo, A., Meri, T., Ramo, L., Jokiranta, T.S., Heikkilä, T., Seppälä, I.J.T., Oksi, J., Viljanen, M., and Meri, S. (2001). Complement evasion by *Borrelia burgdorferi*: serum-resistant strains promote C3b inactivation. *Infect. Immun.* 69, 3685–3691.
- Amara, U., Flierl, M.A., Rittirsch, D., Klos, A., Chen, H., Acker, B., Bruckner, U.B., Nilsson, B., Gebhard, F., Lambris, J.D., Huber-Lang, M. (2010). Molecular intercommunication between the complement and coagulation systems. *J. Immunol.* 185, 5628–5636.
- Anderson, T.D., Chevillat, N.F., and Meador, V.P. (1986). Pathogenesis of placentitis in the goat inoculated with *Brucella abortus*. II. Ultrastructural studies. *Vet. Pathol.* 23, 227–239.
- Attia, A.S., Lafontaine, E.R., Latimer, J.L., Aebi, C., Syrogiannopoulos, G.A., and Hansen, E.J. (2005). The UspA2 protein of *Moraxella catarrhalis* is directly involved in the expression of serum resistance. *Infect. Immun.* 73, 2400–2410.
- Attia, A.S., Ram, S., Rice, P.A., and Hansen, E.J. (2006). Binding of vitronectin by the *Moraxella catarrhalis* UspA2 protein interferes with late stages of the complement cascade. *Infect. Immun.* 74, 1597–1611.
- Barbosa, A.S., Abreu, P.A.E., Vasconcelos, S.A., Morais, Z.M., Goncalves, A.P., Silva, A.S., Dahan, M.R., and Isaac, L. (2009). Immune evasion of *Leptospira* species by acquisition of human complement regulator C4BP. *Infect. Immun.* 77, 1137–1143.
- Barquero-Calvo, E., Chaves-Olarte, E., Weiss, D.S., Guzmán-Verri, C., Chacón-Díaz, C., Rucavado, A., Moriyón, I., and Moreno, E. (2007). *Brucella abortus* uses a stealthy strategy to avoid activation of the innate immune system during the onset of infection. *PLoS ONE* 2, e631.
- Barquero-Calvo, E., Conde-Alvarez, R., Chacón-Díaz, C., Quesada-Lobo, L., Martirosyan, A., Guzmán-Verri, C., Iriarte, M., Mancek-Keber, M., Jerala, R., Gorvel, Moriyón, I., Moreno, E., and Chaves-Olarte, E. (2009). The differential interaction of *Brucella* and *Ochrobactrum* with innate immunity reveals traits related to the evolution of stealthy pathogens. *PLoS ONE* 4, e5893.
- Barquero-Calvo, E., Martirosyan, A., Ordoñez-Rueda, D., Arce-Gorvel, V., Alfaro-Alarcón, A., Lepidi, H., Malissen, B., Malissen, M., Gorvel, J.-P., and Moreno, E. (2013). Neutrophils exert a suppressive effect on Th1 responses to intracellular pathogen *Brucella abortus*. *PLoS Pathog.* 9, e1003167.
- Barquero-Calvo, E., Mora-Carín, R., Arce-Gorvel, V., de Diego, J.L., Chacón-Díaz, C., Chaves-Olarte, E., Guzmán-Verri, C., Buret, A.G., Gorvel, J.-P., and Moreno, E. (2015). *Brucella abortus* induces the premature death of human neutrophils through the action of its lipopolysaccharide. *PLOS Pathog.* 11, e1004853.
- Baumler, A., and Fang, F.C. (2013). Host specificity of bacterial pathogens. *Cold Spring Harb. Perspect. Med.* 3, a010041–a010041.
- Berends, E.T.M., Dekkers, J.F., Nijland, R., Kuipers, A., Soppe, J.A., van Strijp, J.A.G., and Rooijackers, S.H.M. (2013). Distinct localization of the complement C5b-9 complex on Gram-positive bacteria: localized C5b-9 deposition on Gram-positive bacteria. *Cell. Microbiol.* 15, 1955–1968.
- Bininda-Emonds O. R. P., Cardillo M., Jones K. E., MacPhee R. D. E., Beck R. M. D., Grenyer R., Price S. A., Vos R. A., Gittleman J. L., Purvis A. (2007). The delayed rise of present-day mammals. *Nature* 446, 507–512.

- Blom, A.M., Hallström, T., and Riesbeck, K. (2009). Complement evasion strategies of pathogens: acquisition of inhibitors and beyond. *Mol. Immunol.* *46*, 2808–2817.
- Braunschweig, A., and Józsi, M. (2011). Human Pentraxin 3 binds to the complement regulator C4b-binding protein. *PLoS ONE* *6*, e23991.
- Buzgan, T., Karahocagil, M.K., Irmak, H., Baran, A.I., Karsen, H., Evirgen, O., and Akdeniz, H. (2010). Clinical manifestations and complications in 1028 cases of brucellosis: a retrospective evaluation and review of the literature. *Int. J. Infect. Dis.* *14*, e469–e478.
- Cardoso, P.G., Macedo, G.C., Azevedo, V., and Oliveira, S.C. (2006). *Brucella* spp noncanonical LPS: structure, biosynthesis, and interaction with host immune system. *Microb. Cell Factories* *5*, 13.
- Chacón-Díaz, C., Altamirano-Silva, P., González-Espinoza, G., Medina, M.-C., Alfaro-Alarcón, A., Bouza-Mora, L., Jiménez-Rojas, C., Wong, M., Barquero-Calvo, E., Rojas, N., Guzmán-Verri, C., Moreno, E., and Chaves-Olarte, E. (2015). *Brucella canis* is an intracellular pathogen that induces a lower proinflammatory response than smooth zoonotic counterparts. *Infect. Immun.* *83*, 4861–4870.
- China, B., Sory, M.P., N'Guyen, B.T., De Bruyere, M., and Cornelis, G.R. (1993). Role of the YadA protein in prevention of opsonization of *Yersinia enterocolitica* by C3b molecules. *Infect. Immun.* *61*, 3129–3136.
- Conde-Álvarez, R., Arce-Gorvel, V., Iriarte, M., Mančák-Keber, M., Barquero-Calvo, E., Palacios-Chaves, L., Chacón-Díaz, C., Chaves-Olarte, E., Martirosyan, A., von Bargen, K., Grilló, M.J., Jerala, R., Branderburg, k., Llobet, E., Bengoechea, E., Moreno, E., Gorvel, J.P. Moriyón, I. (2012). The lipopolysaccharide core of *Brucella abortus* acts as a shield against innate immunity recognition. *PLoS Pathog.* *8*, e1002675.
- Conway, E.M. (2015). Reincarnation of ancient links between coagulation and complement. *J. Thromb. Haemost.* *13*, S121–S132.
- Corbeil, L.B., Blau, K., Inzana, T.J., Nielsen, K.H., Jacobson, R.H., Corbeil, R.R., and Winter, A.J. (1988). Killing of *Brucella abortus* by bovine serum. *Infect. Immun.* *56*, 3251–3261.
- Cutler, S.J., Whatmore, A.M., and Commander, N.J. (2005). Brucellosis - new aspects of an old disease. *J. Appl. Microbiol.* *98*, 1270–1281.
- David Eckersall, P. (2008). Proteins, proteomics, and the dysproteinemias. In *Clinical Biochemistry of Domestic Animals*, (Elsevier), pp. 117–155.
- Dec, M., Wernicki, A., Puchalski, A., Urban-Chmiel, R., and Radej, S. (2012). Effect of conglutinin on phagocytic activity of bovine granulocytes. *Pol. J. Vet. Sci.* *15*, 455–462.
- Du Clos, T.W. (2013). Pentraxins: structure, function, and role in inflammation. *ISRN Inflamm.* *2013*, 1–22.
- Dunkelberger, J.R., and Song, W.-C. (2010). Complement and its role in innate and adaptive immune responses. *Cell Res.* *20*, 34–50.
- Eisenschenk, F.C., Houle, J.J., and Hoffmann, E.M. (1995). Serum sensitivity of field isolates and laboratory strains of *Brucella abortus*. *Am. J. Vet. Res.* *56*, 1592–1598.

- Eisenschenk, F.C., Houle, J.J., and Hoffmann, E.M. (1999). Mechanism of serum resistance among *Brucella abortus* isolates. *Vet. Microbiol.* 68, 235–244.
- Elliott, M.H., Smith, D.S., Parker, C.E., and Borchers, C. (2009). Current trends in quantitative proteomics. *J. Mass Spectrom.* 12, 1637–1660.
- Enright, F.M., Araya, L.N., Elzer, P.H., Rowe, G.E., and Winter, A.J. (1990). Comparative histopathology in BALB/c mice infected with virulent and attenuated strains of *Brucella abortus*. *Vet. Immunol. Immunopathol.* 26, 171–182.
- Ferguson, J.S., Weis, J.J., Martin, J.L., and Schlesinger, L.S. (2004). Complement protein C3 binding to *Mycobacterium tuberculosis* is initiated by the classical pathway in human bronchoalveolar lavage fluid. *Infect. Immun.* 72, 2564–2573.
- Fernandez-Prada, C.M., Nikolich, M., Vemulapalli, R., Sriranganathan, N., Boyle, S.M., Schurig, G.G., Hadfield, T.L., and Hoover, D.L. (2001). Deletion of *wboA* enhances activation of the lectin pathway of complement in *Brucella abortus* and *Brucella melitensis*. *Infect. Immun.* 69, 4407–4416.
- Fernandez-Prada, C.M., Zelazowska, E.B., Nikolich, M., Hadfield, T.L., Roop II, R.M., Robertson, G.L., and Hoover, D.L. (2003). Interactions between *Brucella melitensis* and human phagocytes: bacterial surface O-Polysaccharide Inhibits phagocytosis, bacterial killing, and subsequent host cell apoptosis. *Infect. Immun.* 71, 2110–2119.
- Fischer, D., Lorenz, N., Heuser, W., Kämpfer, P., Scholz, H.C., and Lierz, M. (2012). Abscesses associated with a *Brucella inopinata*-like bacterium in a big-eyed tree frog (*Leptopelis vermiculatus*). *J. Zoo Wildl. Med.* 43, 625–628.
- Fontana, C., Conde-Álvarez, R., Stähle, J., Holst, O., Iriarte, M., Zhao, Y., Arce-Gorvel, V., Hanniffy, S., Gorvel, J.-P., Moriyón, I., Widmalm, G. (2016). Structural studies of lipopolysaccharide-defective mutants from *Brucella melitensis* identify a core oligosaccharide critical in virulence. *J. Biol. Chem.* 291, 7727–7741.
- Forestier, C., Deleuil, F., Lapaque, N., Moreno, E., and Gorvel, J.P. (2000). *Brucella abortus* lipopolysaccharide in murine peritoneal macrophages acts as a down-regulator of T cell activation. *J. Immunol. Baltim. Md 1950* 165, 5202–5210.
- Foster, G., Osterman, B.S., Godfroid, J., Jacques, I., and Cloeckert, A. (2007). *Brucella ceti* sp. nov. and *Brucella pinnipedialis* sp. nov. for *Brucella* strains with cetaceans and seals as their preferred hosts. *Int. J. Syst. Evol. Microbiol.* 57, 2688–2693.
- Freer, E., Moreno, E., Moriyón, I., Pizarro-Cerdá, J., Weintraub, A., and Gorvel, J.P. (1996). *Brucella-Salmonella* lipopolysaccharide chimeras are less permeable to hydrophobic probes and more sensitive to cationic peptides and EDTA than are their native *Brucella* sp. counterparts. *J. Bacteriol.* 178, 5867–5876.
- Friedman, D.B. (2006). Quantitative proteomics for two-dimensional gels using difference gel electrophoresis. In *Mass Spectrometry Data Analysis in Proteomics*, (New Jersey: Humana Press), pp. 219–240.
- Galvan, M. (2014). The complement system. In *Molecular Life Sciences*, R.D. Wells, J.S. Bond, J. Klinman, B.S.S. Masters, and E. Bell, eds. (New York, NY: Springer New York), pp. 1–10.
- González, D., Grilló, M.-J., De Miguel, M.-J., Ali, T., Arce-Gorvel, V., Delrue, R.-M., Conde-Álvarez, R., Muñoz, P., López-Goñi, I., Iriarte, M., et al. (2008). Brucellosis vaccines: Assessment of *Brucella*

- melitensis* lipopolysaccharide rough mutants defective in core and O-polysaccharide synthesis and export. *PLoS ONE* 3, e2760.
- González-Barrientos, R., Morales, J.-A., Hernández-Mora, G., Barquero-Calvo, E., Guzmán-Verri, C., Chaves-Olarte, E., and Moreno, E. (2010). Pathology of striped dolphins (*Stenella coeruleoalba*) infected with *Brucella ceti*. *J. Comp. Pathol.* 142, 347–352.
- Gidlewski, T., Cheville, N.F., Rhyan, J.C., Miller, L.D., and Gilsdorf, M.J. (2000). Experimental *Brucella abortus* induced abortion in a Llama: Pathologic Effects. *Vet. Pathol.* 37, 77–82.
- Hallström, T., Resman, F., Ristovski, M., and Riesbeck, K. (2010). Binding of complement regulators to invasive nontypeable *Haemophilus influenzae* isolates is not increased compared to nasopharyngeal isolates, but serum resistance is linked to disease severity. *J. Clin. Microbiol.* 48, 921–927.
- Higgs, R.E., Knierman, M.D., Gelfanova, V., Butler, J.P., and Hale, J.E. (2005). Comprehensive label-free method for the relative quantification of proteins from biological samples. *J. Proteome Res.* 4, 1442–1450.
- Hoffmann, E.M., and Houle, J.J. (1983). Failure of *Brucella abortus* lipopolysaccharide (LPS) to activate the alternative pathway of complement. *Vet. Immunol. Immunopathol.* 5, 65–76.
- Holers, V.M. (2014). Complement and its receptors: new insights into human disease. *Annu. Rev. Immunol.* 32, 433–459.
- Ingram, D.G., and Mitchell, W.R. (1970). Conglutinin levels in dairy cattle: changes associated with parturition. *Am. J. Vet. Res.* 31, 487–492.
- Ingram, D.G., and Mitchell, W.R. (1971). Conglutinin level in dairy cattle: changes associated with disease. *Am. J. Vet. Res.* 32, 875–878.
- Janeway, C.A., and Medzhitov, R. (2002). Innate immune recognition. *Annu. Rev. Immunol.* 20, 197–216.
- Joiner, K.A. (1988). Complement evasion by bacteria and parasites. *Annu. Rev. Microbiol.* 42, 201–230.
- Ko, J., and Splitter, G.A. (2003). Molecular host-pathogen interaction in brucellosis: current understanding and future approaches to vaccine development for mice and humans. *Clin. Microbiol. Rev.* 16, 65–78.
- Kolev, M., Friec, G.L., and Kemper, C. (2014). Complement: tapping into new sites and effector systems. *Nat. Rev. Immunol.* 14, 811–820.
- Kraicz, P., Skerka, C., Kirschfink, M., Brade, V., and Zipfel, P.F. (2001). Immune evasion of *Borrelia burgdorferi* by acquisition of human complement regulators FHL-1/reconnectin and Factor H. *Eur. J. Immunol.* 31, 1674–1684.
- Kreutzer, D.L., Dreyfus, L.A., and Robertson, D.C. (1979). Interaction of polymorphonuclear leukocytes with smooth and rough strains of *Brucella abortus*. *Infect. Immun.* 23, 737–742.
- Kubler-Kielb, J., and Vinogradov, E. (2013). The study of the core part and non-repeating elements of the O-antigen of *Brucella* lipopolysaccharide. *Carbohydr. Res.* 366, 33–37.
- Kumar, H., Kawai, T., and Akira, S. (2011). Pathogen recognition by the innate immune system. *Int. Rev. Immunol.* 30, 16–34.

- Kumar S., Hedges S. B. (1998). A molecular timescale for vertebrate evolution. *Nature* 392, 917–920.
- Laarman, A.J., Ruyken, M., Malone, C.L., van Strijp, J.A.G., Horswill, A.R., and Rooijackers, S.H.M. (2011). *Staphylococcus aureus* metalloprotease aureolysin cleaves complement C3 to mediate immune evasion. *J. Immunol.* 186, 6445–6453.
- Lambris, J.D., Ricklin, D., and Geisbrecht, B.V. (2008). Complement evasion by human pathogens. *Nat. Rev. Microbiol.* 6, 132–142.
- Lapaque, N., Moriyon, I., Moreno, E., and Gorvel, J.-P. (2005). *Brucella* lipopolysaccharide acts as a virulence factor. *Curr. Opin. Microbiol.* 8, 60–66.
- Lapaque, N., Takeuchi, O., Corrales, F., Akira, S., Moriyon, I., Howard, J.C., and Gorvel, J.-P. (2006). Differential inductions of TNF-alpha and IIGP, IIGP by structurally diverse classic and non-classic lipopolysaccharides. *Cell. Microbiol.* 8, 401–413.
- Liebermeister, W., Noor, E., Flamholz, A., Davidi, D., Bernhardt, J., and Milo, R. (2014). Visual account of protein investment in cellular functions. *Proc. Natl. Acad. Sci.* 111, 8488–8493.
- Lomonte, B., Tsai, W.-C., Ureña-Díaz, J.M., Sanz, L., Mora-Obando, D., Sánchez, E.E., Fry, B.G., Gutiérrez, J.M., Gibbs, H.L., Sović, M.G., et al. (2014). Venomics of New World pit vipers: Genus-wide comparisons of venom proteomes across Agkistrodon. *J. Proteomics* 96, 103–116.
- Lucero, N.E., Corazza, R., Almuzara, M.N., Reynes, E., Escobar, G.I., Boeri, E., and Ayala, S.M. (2010). Human *Brucella canis* outbreak linked to infection in dogs. *Epidemiol. Infect.* 138, 280–285.
- Malhotra, R., Thiel, S., Reid, K.B., and Sim, R.B. (1990). Human leukocyte C1q receptor binds other soluble proteins with collagen domains. *J. Exp. Med.* 172, 955–959.
- Manterola, L., Moriyon, I., Moreno, E., Sola-Landa, A., Weiss, D.S., Koch, M.H.J., Howe, J., Brandenburg, K., and Lopez-Goni, I. (2005). The lipopolysaccharide of *Brucella abortus* BvrS/BvrR mutants contains lipid modifications and has higher affinity for bactericidal cationic peptides. *J. Bacteriol.* 187, 5631–5639.
- Markiewski, M.M., Nilsson, B., Nilsson Ekdahl, K., Mollnes, T.E., and Lambris, J.D. (2007). Complement and coagulation: strangers or partners in crime? *Trends Immunol.* 28, 184–192.
- Martinez de Tejada, G., Pizarro-Cerdá, J., Moreno, E., and Moriyón, I. (1995). The outer membranes of *Brucella* spp. are resistant to bactericidal cationic peptides. *Infect. Immun.* 63, 3054–3061.
- Martín-Martin, A.I., Sancho, P., Tejedor, C., Fernández-Lago, L., and Vizcaino, N. (2011). Differences in the outer membrane-related properties of the six classical *Brucella* species. *Vet. J. Lond. Engl.* 1997 189, 103–105.
- Martirosyan, A., Moreno, E., and Gorvel, J.-P. (2011). An evolutionary strategy for a stealthy intracellular *Brucella* pathogen: *Brucella* pathogenesis. *Immunol. Rev.* 240, 211–234.
- Merle, N.S., Church, S.E., Fremeaux-Bacchi, V., and Roumenina, L.T. (2015). Complement system part I, molecular mechanisms of activation and regulation. *Front. Immunol.* 6, 262.
- Mogensen, T.H. (2009). Pathogen recognition and inflammatory signaling in innate immune defenses. *Clin. Microbiol. Rev.* 22, 240–273.



- Moore, D.H. (1945). Species difference in serum protein patterns. *J. Biol. Chem.* 161, 21–32.
- Moreno, E. (2014). Retrospective and prospective perspectives on zoonotic brucellosis. *Front. Microbiol.* 5, 213.
- Moreno, E., and Moriyón, I. (2006). The genus *Brucella*. In *The Prokaryotes*, M. Dworkin, S. Falkow, E. Rosenberg, K.-H. Schleifer, and E. Stackebrandt, eds. (New York, NY: Springer New York), pp. 315–456.
- Moreno, E., Berman, D.T., and Boettcher, L.A. (1981). Biological activities of *Brucella abortus* lipopolysaccharides. *Infect. Immun.* 31, 362–370.
- Nordstrom, T., Blom, A.M., Forsgren, A., and Riesbeck, K. (2004). The emerging pathogen *Moraxella catarrhalis* interacts with complement inhibitor C4b-binding protein through ubiquitous surface proteins A1 and A2. *J. Immunol.* 173, 4598–4606.
- Noris, M., and Remuzzi, G. (2013). Overview of complement activation and regulation. *Semin. Nephrol.* 33, 479–492.
- Palacios-Chaves, L., Conde-Álvarez, R., Gil-Ramírez, Y., Zúñiga-Ripa, A., Barquero-Calvo, E., Chacón-Díaz, C., Chaves-Olarte, E., Arce-Gorvel, V., Gorvel, J.-P., Moreno, E., et al. (2011). *Brucella abortus* Ornithine lipids are dispensable outer membrane components devoid of a marked pathogen-associated molecular pattern. *PLoS ONE* 6, e16030.
- Pizarro-Cerdá, J., Desjardins, M., Moreno, E., Akira, S., and Gorvel, J.P. (1999). Modulation of endocytosis in nuclear factor IL-6(-/-) macrophages is responsible for a high susceptibility to intracellular bacterial infection. *J. Immunol. Baltim. Md 1950* 162, 3519–3526.
- Raghavan, M., Wijeyesakere, S.J., Peters, L.R., and Del Cid, N. (2013). Calreticulin in the immune system: ins and outs. *Trends Immunol.* 34, 13–21.
- Rautemaa, R., and Meri, S. (1999). Complement-resistance mechanisms of bacteria. *Microbes Infect. Inst. Pasteur* 1, 785–794.
- Ruiz-Ranwez, V., Posadas, D.M., Estein, S.M., Abdian, P.L., Martin, F.A., and Zorreguieta, A. (2013). The BtaF trimeric autotransporter of *brucella suis* is involved in attachment to various surfaces, resistance to serum and virulence. *PLoS ONE* 8, e79770.
- Sangari, F.J., and Agüero, J. (1991). Mutagenesis of *Brucella abortus*: comparative efficiency of three transposon delivery systems. *Microb. Pathog.* 11, 443–446.
- Sato, E., Koyama, S., Nomura, H., Kubo, K., and Sekiguchi, M. (1996). Bradykinin stimulates alveolar macrophages to release neutrophil, monocyte, and eosinophil chemotactic activity. *J. Immunol. Baltim. Md 1950* 157, 3122–3129.
- Schmaier, A.H. (2016). The contact activation and kallikrein/kinin systems: pathophysiologic and physiologic activities. *J. Thromb. Haemost.* 14, 28–39.
- Schmidt, C.Q., Lambris, J.D., and Ricklin, D. (2016). Protection of host cells by complement regulators. *Immunol. Rev.* 274, 152–171.
- Scholz, H.C., Nockler, K., Gollner, C., Bahn, P., Vergnaud, G., Tomaso, H., Al Dahouk, S., Kampfer, P., Cloeckert, A., Maquart, M., Zygmunt, M.S., Whatmore, A.M., Pfeiffer, M., Huber, B., Busse, H.J., De,

- B.K. (2010). *Brucella inopinata* sp. nov., isolated from a breast implant infection. *Int. J. Syst. Evol. Microbiol.* 60, 801–808.
- Starr, T., Child, R., Wehrly, T.D., Hansen, B., Hwang, S., López-Otin, C., Virgin, H.W., and Celli, J. (2012). Selective subversion of autophagy complexes facilitates completion of the *Brucella* intracellular cycle. *Cell Host Microbe* 11, 33–45.
- Śliwa-Dominiak, J., Tokarz-Deptuła, B., Niedźwiedzka-Rystwej, P., and Deptuła, W. (2010). Conglutinin - an important element of natural immunity in ruminants (a Review). *Acta Vet. Brno* 79, 99–104.
- Sundsmo, J., and Fair, D. (1983). Relationships among the complement, kinin, coagulation, and fibrinolytic systems. *Springer Semin. Immunopathol.* 6–6.
- Vandivier, R.W., Ogden, C.A., Fadok, V.A., Hoffmann, P.R., Brown, K.K., Botto, M., Walport, M.J., Fisher, J.H., Henson, P.M., and Greene, K.E. (2002). Role of surfactant proteins A, D, and C1q in the clearance of apoptotic cells in vivo and in vitro: calreticulin and CD91 as a common collectin receptor complex. *J. Immunol. Baltim. Md 1950* 169, 3978–3986.
- Velasco, J., Moll, H., Knirel, Y.A., Sinnwell, V., Moriyón, I., and Zähringer, U. (1998). Structural studies on the lipopolysaccharide from a rough strain of *Ochrobactrum anthropi* containing a 2,3-diamino-2,3-dideoxy-d-glucose disaccharide lipid A backbone. *Carbohydr. Res.* 306, 283–290.
- Velasco, J., Bengoechea, J.A., Brandenburg, K., Lindner, B., Seydel, U., González, D., Zähringer, U., Moreno, E., and Moriyón, I. (2000). *Brucella abortus* and its closest phylogenetic relative, *Ochrobactrum* spp., differ in outer membrane permeability and cationic peptide resistance. *Infect. Immun.* 68, 3210–3218.
- Whatmore, A.M., Gopaul, K.K., Koylass, M., Lawrie, A., Muchowski, J., Dale, E., Perrett, L.L., Dawson, C., Stubberfield, E., and Jones, M. (2015). Isolation of *Brucella* from a white's tree frog (*Litoria caerulea*). *JMM Case Rep.* 2.
- Wilm, M. (2009). Quantitative proteomics in biological research. *Proteomics* 9, 4590–4605.
- Zhu, W., Smith, J.W., and Huang, C.-M. (2010). Mass spectrometry-based label-free quantitative proteomics. *J. Biomed. Biotechnol.* 2010, 1–6.
- Zipfel, P.F., and Skerka, C. (2009). Complement regulators and inhibitory proteins. *Nat. Rev. Immunol.* 9, 729–740.
- Zipfel, P.F., Hallström, T., and Riesbeck, K. (2013). Human complement control and complement evasion by pathogenic microbes: Tipping the balance. *Mol. Immunol.* 56, 152–160.

## 10. APPENDIXES

**10.1 Appendix 1.** Human serum approval by the “Comité ético Científico, Universidad de Costa Rica” (VI-4277-2016).

**10.2 Appendix 2.** Function description of serum proteins adsorbed by *Brucella* surface. Information taken from UNIPROT data base.

**10.3 Appendix 3.** Input data for construction of Proteomaps.

**10.4 Appendix 4.** *B. abortus/ B. melintesis* fold change statistics (Wald Test and FDR adjusted p-values) for the 96 adsorbed serum proteins.

**10.5 Appendix 5.** *B. abortus/ B. melintesis* fold change statistics (Wald Test and FDR adjusted p-values) for the 96 adsorbed serum proteins.

**10.6 Appendix 6.** *B. abortus/ B. melintesis* fold change statistics (Wald Test and FDR adjusted p-values) for the 96 adsorbed serum proteins.

**10.7 Appendix 7.** Coagulation and complement proteins identified from *Brucella* outer membrane surface eluates. Red boxes indicated proteins that were adsorbed by *Brucella*. *Homo sapiens* complement and coagulation cascade pathways from. Modified from ([www.kegg.jp/kegg-bin/show\\_pathway?hsa04610](http://www.kegg.jp/kegg-bin/show_pathway?hsa04610)).

**10.8 Appendix 8.** Academic participations in congress and publication during my Master training.

**10.8.1 González-Espinoza, G.,** Gutiérrez-Fernandez, R.; Lizano, E., Barquero-Calvo, E., Chaves-Olarte, E., Chacón-Díaz, C., Moriyón, I., Moreno, E (2016). III Symposium Instituto de Salud Tropical (ISTUN), Universidad de Navarra, Spain. *Poster presentation:* Interaction of complement system with *Brucella* spp surface.

**10.8.2 González-Espinoza, G.,** Gutiérrez-Fernandez, R, Conde-Alvarez, R., Moreno, E., Chacón-Díaz, C., Moriyón I (2015). II Workshop, Instituto de Salud Tropical (ISTUN), Universidad de Navarra, Spain. *Oral presentation:* Interaction of complement system with *Brucella* spp membrane. <https://www.unav.edu/documents/5716157/0/workshop2015.pdf>.

**10.8.3** Chacón-Díaz, C., Altamirano-Silva, P., **González-Espinoza, G.,** Medina, M.-C., Alfaro-Alarcón, A., Bouza-Mora, L., Jiménez-Rojas, C., Wong, M., Barquero-Calvo, E., Chaves-Olarte, E. (2015). *Brucella canis* Is an Intracellular Pathogen That Induces a Lower Proinflammatory Response than Smooth Zoonotic Counterparts. *Infection and Immunity*, 83(12), 4861–4870. <http://doi.org/10.1128/IAI.00995-15>.

## 10.1 Appendix I



**VI** Vicerrectoría de  
Investigación

17 de mayo de 2016  
VI-4277-2016

M.Sc. Carlos Chacón Díaz  
Investigador  
CIET

Estimado señor:

El Comité Ético Científico (CEC) en su sesión No.12, celebrada el 11 de mayo de 2016 sometió a consideración el Proyecto de Investigación "Papel de los neutrófilos y el complemento en la modulación de la inmunidad adaptativa durante la brucelosis: Un modelo para comprender la regulación de la respuesta inmune en infecciones crónicas"

Después del análisis respectivo, el CEC indica que el proyecto está claro y bien elaborado.

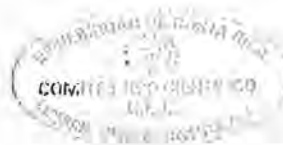
Por lo anteriormente expuesto, el CEC acuerda:

*Aprobar la ejecución del Proyecto de Investigación "Papel de los neutrófilos y el complemento en la modulación de la inmunidad adaptativa durante la brucelosis: Un modelo para comprender la regulación de la respuesta inmune en infecciones crónicas", del investigador Carlos Chacón Díaz. ACUERDO FIRME.*

Quedamos en la entera disposición de colaborar ante cualquier consulta ulterior.

Sin más por el momento, se suscribe cordialmente,

M.Sc. Alfonso Chacón Mata  
Presidente Comité Ético Científico



GCHZ

C.c. Ph.D. Esteban Chaves Olarte, Director, CIET.  
MPA, Darío Hernández C., Gestor de Proyectos VI.  
Archivo/consecutivo.

**10.2 Appendix 2.** Function description of serums proteins adsorbed by *Brucella* surface. Information taken from UNIPROT data base.

Identification	Protein Function (UNIPROT)
Mannose-binding protein	Calcium-dependent lectin involved in innate immune defense. Binds mannose, fucose and N-acetylglucosamine on different microorganisms and activates the lectin complement pathway. Binds to late apoptotic cells, as well as to apoptotic blebs and to necrotic cells, but not to early apoptotic cells, facilitating their uptake by macrophages
Conglutinin	Calcium-dependent lectin-like protein which binds to a yeast cell wall extract and immune complexes through the complement component (C3b). It is capable of binding non-reducing terminal N-acetylglucosamine, mannose, and fucose residues.
Complement C1q	C1q associates with the proenzymes C1r and C1s to yield C1, the first component of the complement system. The collagen-like regions of C1q interact with the Ca <sup>2+</sup> -dependent C1r2C1s2 proenzyme complex, and efficient activation of C1 takes place on interaction of the globular heads of C1q with the Fc regions of IgG or IgM antibody present in immune complexes.
Complement C2	Component C2 which is part of the classical pathway of the complement system is cleaved by activated factor C1 into two fragments: C2b and C2a. C2a, a serine protease, then combines with complement factor C4b to generate the C3 or C5 convertase
Complement C4	Non-enzymatic component of the C3 and C5 convertases and thus essential for the propagation of the classical complement pathway. Covalently binds to immunoglobulins and immune complexes and enhances the solubilization of immune aggregates and the clearance of IC through CR1 on erythrocytes. C4A isotype is responsible for effective binding to form amide bonds with immune aggregates or protein antigens, while C4B isotype catalyzes the transacylation of the thioester carbonyl group to form ester bonds with carbohydrate antigens.
Complement C3	C3 plays a central role in the activation of the complement system. Its processing by C3 convertase is the central reaction in both classical and alternative complement pathways. After activation C3b can bind covalently, via its reactive thioester, to cell surface carbohydrates or immune aggregates. Derived from proteolytic degradation of complement C3, C3a anaphylatoxin is a mediator of local inflammatory process. It induces the contraction of smooth muscle, increases vascular permeability and causes histamine release from mast cells and basophilic leukocytes. In chronic inflammation, acts as a chemoattractant for neutrophils.
Complement factor B	Factor B which is part of the alternate pathway of the complement system is cleaved by factor D into 2 fragments: Ba and Bb. Bb, a serine protease, then combines with complement factor 3b to generate the C3 or C5 convertase. It has also been implicated in proliferation and differentiation of preactivated B-lymphocytes, rapid spreading of peripheral blood monocytes, stimulation of lymphocyte blastogenesis and lysis of erythrocytes. Ba inhibits the proliferation of preactivated B-lymphocytes
Complement C5	Activation of C5 by a C5 convertase initiates the spontaneous assembly of the late complement components, C5-C9, into the membrane attack complex. C5b has a transient binding site for C6. The C5b-C6 complex is the

	foundation upon which the lytic complex is assembled. Derived from proteolytic degradation of complement C5, C5 anaphylatoxin is a mediator of local inflammatory process. C5a is a potent chemokine which stimulates the locomotion of polymorphonuclear leukocytes and directs their migration toward sites of inflammation.
<b>Complement component C6</b>	Constituent of the membrane attack complex (MAC) that plays a key role in the innate and adaptive immune response by forming pores in the plasma membrane of target cells
<b>Complement component C7</b>	Constituent of the membrane attack complex (MAC) that plays a key role in the innate and adaptive immune response by forming pores in the plasma membrane of target cells. C7 serves as a membrane anchor
<b>Complement component C8</b>	Constituent of the membrane attack complex (MAC) that plays a key role in the innate and adaptive immune response by forming pores in the plasma membrane of target cells. C8A inserts into the target membrane, but does not form pores by itself. C5-B8 binds C9 and acts as a catalyst in the polymerization of C9. The gamma subunit seems to be able to bind retinol.
<b>Complement component C9</b>	Constituent of the membrane attack complex (MAC) that plays a key role in the innate and adaptive immune response by forming pores in the plasma membrane of target cells.
<b>Complement Factor H</b>	Factor H functions as a cofactor in the inactivation of C3b by factor I and increases the rate of dissociation of the C3bBb complex (C3 convertase) and the (C3b) NBB complex (C5 convertase) in the alternative complement pathway.
<b>C4b-binding protein</b>	Controls the classical pathway of complement activation. It binds as a cofactor to C3b/C4b inactivator (C3bINA), which then hydrolyzes the complement fragment C4b. It also accelerates the degradation of the C4bC2a complex (C3 convertase) by dissociating the complement fragment C2a. Alpha chain binds C4b. It interacts also with serum amyloid P component.
<b>Vitronectin</b>	Vitronectin is a cell adhesion and spreading factor found in serum and tissues. Vitronectin interact with glycosaminoglycans and proteoglycans. Is recognized by certain members of the integrin family and serves as a cell-to-substrate adhesion molecule. Inhibitor of the membrane-damaging effect of the terminal cytolytic complement pathway.
<b>Clusterin</b>	Functions as extracellular chaperone that prevents aggregation of nonnative proteins. Prevents stress-induced aggregation of blood plasma proteins. Binding to cell surface receptors triggers internalization of the chaperone-client complex and subsequent lysosomal or proteasomal degradation. When secreted, protects cells against apoptosis and against cytolysis by complement. Intracellular forms interact with ubiquitin and SCF (SKP1-CUL1-F-box protein) E3 ubiquitin-protein ligase complexes and promote the ubiquitination and subsequent proteasomal degradation of target proteins. Promotes proteasomal degradation of COMMD1 and IKBKB. Modulates NF-kappa-B transcriptional activity. Promotes apoptosis when in the nucleus. Inhibits apoptosis when associated with the mitochondrial membrane by interference with BAX-dependent release of cytochrome c into the cytoplasm. Plays a role in the regulation of cell proliferation
<b>Coagulation factor VIII</b>	Factor VIII, along with calcium and phospholipid, acts as a cofactor for F9/factor IXa when it converts F10/factor X to the activated form, factor Xa.
<b>Coagulation factor V</b>	Central regulator of hemostasis. It serves as a critical cofactor for the prothrombinase activity of factor Xa that results in the activation of prothrombin to thrombin.

<b>Prothrombin</b>	Thrombin, which cleaves bonds after Arg and Lys, converts fibrinogen to fibrin and activates factors V, VII, VIII, XIII, and, in complex with thrombomodulin, protein C. Functions in blood homeostasis, inflammation and wound healing
<b>Thrombospondin-1</b>	Adhesive glycoprotein that mediates cell-to-cell and cell-to-matrix interactions. Can bind to fibrinogen, fibronectin, laminin and type V collagen.
<b>Factor XIIa inhibitor</b>	Factor XII is a serum glycoprotein that participates in the initiation of blood coagulation, fibrinolysis, and the generation of bradykinin and angiotensin. Prekallikrein is cleaved by factor XII to form kallikrein, which then cleaves factor XII first to alpha-factor XIIa and then trypsin cleaves it to beta-factor XIIa. Alpha-factor XIIa activates factor XI to factor XIa.
<b>Plasminogen (Fragment)</b>	Plasmin dissolves the fibrin of blood clots and acts as a proteolytic factor in a variety of other processes including embryonic development, tissue remodeling, tumor invasion, and inflammation. In ovulation, weakens the walls of the Graafian follicle. It activates the urokinase-type plasminogen activator, collagenases and several complement zymogens, such as C1 and C5. Cleavage of fibronectin and laminin leads to cell detachment and apoptosis. Also cleaves fibrin, thrombospondin and von Willebrand factor. Its role in tissue remodeling and tumor invasion may be modulated by CSPG4. Binds to cells
<b>Platelet factor 4</b>	Released during platelet aggregation. Neutralizes the anticoagulant effect of heparin because it binds more strongly to heparin than to the chondroitin-4-sulfate chains of the carrier molecule. Chemotactic for neutrophils and monocytes. Inhibits endothelial cell proliferation, the short form is a more potent inhibitor than the longer form
<b>Antithrombin-III</b>	Most important serine protease inhibitor in plasma that regulates the blood coagulation cascade. AT-III inhibits thrombin, matrix metalloproteinase-3 (MMP-3), as well as factors IXa, Xa and XIa. Its inhibitory activity is greatly enhanced in the presence of heparin
<b>Beta-2-glycoprotein 1</b>	Binds to various kinds of negatively charged substances such as heparin, phospholipids, and dextran sulfate. May prevent activation of the intrinsic blood coagulation cascade by binding to phospholipids on the surface of damaged cells.
<b>Fibronectin</b>	Fibronectins bind cell surfaces and various compounds including collagen, fibrin, heparin, DNA, and actin. Fibronectins are involved in cell adhesion, cell motility, opsonization, wound healing, and maintenance of cell shape. Involved in osteoblast compaction through the fibronectin fibrillogenesis cell-mediated matrix assembly process, essential for osteoblast mineralization. Participates in the regulation of type I collagen deposition by osteoblasts. Anastellin binds fibronectin and induces fibril formation. This fibronectin polymer, named superfibronectin, exhibits enhanced adhesive properties. Both anastellin and superfibronectin inhibit tumor growth, angiogenesis and metastasis. Anastellin activates p38 MAPK and inhibits lysophospholipid signaling.
<b>Hemoglobin subunit alpha-1/2</b>	Involved in oxygen transport from the lung to the various peripheral tissues.
<b>Ceruloplasmin</b>	Ceruloplasmin is a blue, copper-binding (6-7 atoms per molecule) glycoprotein. It has ferroxidase activity oxidizing Fe <sup>2+</sup> to Fe <sup>3+</sup> without releasing radical oxygen species. It is involved in iron transport across the cell membrane

Haptoglobin	Haptoglobin captures, and combines with free plasma hemoglobin to allow hepatic recycling of heme iron and to prevent kidney damage. Haptoglobin also acts as an antioxidant, has antibacterial activity and plays a role in modulating many aspects of the acute phase response. Hemoglobin/haptoglobin complexes are rapidly cleared by the macrophage CD163 scavenger receptor expressed on the surface of liver Kupfer cells through an endocytic lysosomal degradation pathway
Hemoglobin subunit beta	Involved in oxygen transport from the lung to the various peripheral tissues.
Hemopexin	Binds heme and transports it to the liver for breakdown and iron recovery, after which the free hemopexin returns to the circulation.
Lactotransferrin	Lactotransferrins are iron binding transport proteins which can bind two Fe <sup>3+</sup> ions in association with the binding of an anion, usually bicarbonate. Lactotransferrin is a major iron-binding and multifunctional protein found in exocrine fluids such as breast milk and mucosal secretions. Has antimicrobial activity. Antimicrobial properties may include bacteriostasis, which is related to its ability to sequester free iron and thus inhibit microbial growth, as well as direct bactericidal properties leading to the release of lipopolysaccharides from the bacterial outer membrane. The most effective inhibitory activity is seen against <i>E.coli</i> and <i>P.aeruginosa</i> . Has anabolic, differentiating and anti-apoptotic effects on osteoblasts and can also inhibit osteoclastogenesis, possibly playing a role in the regulation of bone growth. Interferes with the lipopolysaccharide (LPS)-stimulated TLR4 signaling, but cannot directly stimulate the TLR4 signaling pathway and subsequent NF-kappa-B activation.
Apolipoprotein A-1	Participates in the reverse transport of cholesterol from tissues to the liver for excretion by promoting cholesterol efflux from tissues and by acting as a cofactor for the lecithin cholesterol acyltransferase (LCAT). As part of the SPAP complex, activates spermatozoa motility.
Apolipoprotein A-IV	May have a role in chylomicrons and VLDL secretion and catabolism. Required for efficient activation of lipoprotein lipase by ApoC-II; potent activator of LCAT. ApoA-IV is a major component of HDL and chylomicrons
Apolipoprotein D	APOD occurs in the macromolecular complex with lecithin-transport and binding of bilin. Appears to be able to transport a variety of ligands in a number of different contexts
Apolipoprotein E	Mediates the binding, internalization, and catabolism of lipoprotein particles. It can serve as a ligand for the LDL (apo B/E) receptor and for the specific apo-E receptor (chylomicron remnant) of hepatic tissues.
Alpha-1-antitrypsin	Inhibits human leukocyte elastase, pig pancreatic elastase and bovine trypsin on a 1:1 molar basis.
Alpha-1B-glycoprotein	Involved in platelet and neutrophil degranulation
Alpha-2-HS-glycoprotein	Acute phase response. Involved in positive regulation of phagocytosis. Negative regulation of bone mineralization.
Alpha-2-macroglobulin	This protein has a peptide stretch, called the 'bait region' which contains specific cleavage sites for different proteinases. When a proteinase cleaves the bait region, a conformational change is induced in the protein which traps the proteinase. The entrapped enzyme remains active against low molecular weight substrates (activity against high molecular weight substrates is greatly reduced). Following cleavage in the bait region a thioester bond is hydrolyzed and mediates the covalent binding of the protein to the proteinase. Negative regulation of complement activation. Stem cell differentiation.



Inter-alpha-trypsin inhibitor	Type II acute-phase protein (APP) involved in inflammatory responses to trauma. May also play a role in liver development or regeneration.
Metalloproteinase inhibitor 3	Complexes with metalloproteinases (such as collagenases) and irreversibly inactivates them by binding to their catalytic zinc cofactor. May form part of a tissue-specific acute response to remodeling stimuli. Known to act on MMP-1, MMP-2, MMP-3, MMP-7, MMP-9, MMP-13, MMP-14 and MMP-15.
Plasma kallikrein	The enzyme cleaves Lys-Arg and Arg-Ser bonds. It activates, in a reciprocal reaction, factor XII after its binding to a negatively charged surface. It also releases bradykinin from HMW kininogen and may also play a role in the renin-angiotensin system by converting prorenin into renin
Plasma serine protease inhibitor	Heparin-dependent serine protease inhibitor acting in body fluids and secretions. Inactivates serine proteases by binding irreversibly to their serine activation site. Involved in the regulation of intravascular and extravascular proteolytic activities. Plays hemostatic roles in the blood plasma. Acts as a procoagulant and proinflammatory factor by inhibiting the anticoagulant activated protein C factor as well as the generation of activated protein C factor by the thrombin/thrombomodulin complex. Acts as an anticoagulant factor by inhibiting blood coagulation factors like prothrombin, factor XI, factor Xa, plasma kallikrein and fibrinolytic enzymes such as tissue- and urinary-type plasminogen activators. In seminal plasma, inactivates several serine proteases implicated in the reproductive system. In urine, inhibits urinary-type plasminogen activator and kallikrein activities. Inactivates membrane-anchored serine proteases activities such as MPRSS7 and TMPRSS11E. Inhibits urinary-type plasminogen activator-dependent tumor cell invasion and metastasis. May also play a non-inhibitory role in seminal plasma and urine as a hydrophobic hormone carrier by its binding to retinoic acid
Pregnancy zone protein	Is able to inhibit all four classes of proteinases by a unique 'trapping' mechanism. This protein has a peptide stretch, called the 'bait region' which contains specific cleavage sites for different proteinases. When a proteinase cleaves the bait region, a conformational change is induced in the protein which traps the proteinase. The entrapped enzyme remains active against low molecular weight substrates (activity against high molecular weight substrates is greatly reduced). Following cleavage in the bait region a thioester bond is hydrolyzed and mediates the covalent binding of the protein to the proteinase.
Serpin A3-2	Serine protease inhibitor.
Trypsin	Digestive protease specialized for the degradation of trypsin inhibitors. In the ileum, may be involved in defensin processing, including DEFA5
Catalase	Occurs in almost all aerobically respiring organisms and serves to protect cells from the toxic effects of hydrogen peroxide. Promotes growth of cells.
Protein S100-A8	S100A8 is a calcium- and zinc-binding protein which plays a prominent role in the regulation of inflammatory processes and immune response. It can induce neutrophil chemotaxis and adhesion. Predominantly found as calprotectin (S100A8/A9) which has a wide plethora of intra- and extracellular functions. The extracellular functions involve proinflammatory, antimicrobial, oxidant-scavenging and apoptosis-inducing activities. Its proinflammatory activity includes recruitment of leukocytes, promotion of cytokine and chemokine production, and regulation of leukocyte adhesion and migration. Acts as an alarmin or a danger associated molecular pattern (DAMP) molecule and stimulates innate immune cells via binding to pattern recognition receptors such as Toll-

	<p>like receptor 4 (TLR4) and receptor for advanced glycation endproducts (AGER). Binding to TLR4 and AGER activates the MAP-kinase and NF-kappa-B signaling pathways resulting in the amplification of the proinflammatory cascade. Has antimicrobial activity towards bacteria and fungi and exerts its antimicrobial activity probably via chelation of Zn<sup>2+</sup> which is essential for microbial growth. Can induce cell death via autophagy and apoptosis and this occurs through the cross-talk of mitochondria and lysosomes via reactive oxygen species (ROS) and the process involves BNIP3. Can regulate neutrophil number and apoptosis by an anti-apoptotic effect; regulates cell survival via ITGAM/ITGB and TLR4 and a signaling mechanism involving MEK-ERK. Its role as an oxidant scavenger has a protective role in preventing exaggerated tissue damage by scavenging oxidants. Can act as a potent amplifier of inflammation in autoimmunity as well as in cancer development and tumor spread.</p>
Cathelicidin-2	<p>Binds to the lipid A moiety of bacterial lipopolysaccharides (LPS), a glycolipid present in the outer membrane of all Gram-negative bacteria. Shows a potent antimicrobial activity against the Gram-negative bacteria <i>E.coli</i>, <i>S.typhimurium</i> and <i>P.aeruginosa</i>. Less active against the Gram-positive bacteria <i>S.aureus</i>, <i>L.monocytogenes</i> and <i>B.subtilis</i>.</p>
Cathelicidin-6	<p>Exerts a potent antimicrobial activity against Gram-negative and Gram-positive bacteria, including methicillin-resistant <i>Staphylococcus aureus</i>, and fungi.</p>
Putative lysozyme C-2	<p>Lysozymes have primarily a bacteriolytic function; those in tissues and body fluids are associated with the monocyte-macrophage system and enhance the activity of immunoagents. In the intestine they may also have a digestive function.</p>
Myeloperoxidase	<p>Part of the host defense system of polymorphonuclear leukocytes. It is responsible for microbicidal activity against a wide range of organisms. In the stimulated PMN, MPO catalyzes the production of hypohalous acids, primarily hypochlorous acid in physiologic situations, and other toxic intermediates that greatly enhance PMN microbicidal activity.</p>
Ig gamma-1 chain C region	<p>Constant region of immunoglobulin heavy chains. Immunoglobulins, also known as antibodies, are membrane-bound or secreted glycoproteins produced by B lymphocytes. In the recognition phase of humoral immunity, the membrane-bound immunoglobulins serve as receptors which, upon binding of a specific antigen, trigger the clonal expansion and differentiation of B lymphocytes into immunoglobulins-secreting plasma cells. Secreted immunoglobulins mediate the effector phase of humoral immunity, which results in the elimination of bound antigens. The antigen binding site is formed by the variable domain of one heavy chain, together with that of its associated light chain. Thus, each immunoglobulin has two antigen binding sites with remarkable affinity for a particular antigen.</p>
Ig kappa chain V-III region NG9 (Fragment)	<p>V region of the variable domain of immunoglobulin light chains that participates in the antigen recognition. Immunoglobulins, also known as antibodies, are membrane-bound or secreted glycoproteins produced by B lymphocytes. In the recognition phase of humoral immunity, the membrane-bound immunoglobulins serve as receptors which, upon binding of a specific antigen, trigger the clonal expansion and differentiation of B lymphocytes into immunoglobulins-secreting plasma cells. Secreted immunoglobulins mediate the effector phase of humoral immunity, which results in the elimination of bound antigens. The antigen binding site is formed by</p>

		the variable domain of one heavy chain, together with that of its associated light chain. Thus, each immunoglobulin has two antigen binding sites with remarkable affinity for a particular antigen.
<b>Ig lambda chain V-I region EPS</b>		Interacting selectively and non-covalently with an antigen, any substance which is capable of inducing a specific immune response and of reacting with the products of that response, the specific antibody or specifically sensitized T-lymphocytes, or both. Binding may counteract the biological activity of the antigen
<b>Ig lambda chain V-III region LOI</b>		Interacting selectively and non-covalently with an antigen, any substance which is capable of inducing a specific immune response and of reacting with the products of that response, the specific antibody or specifically sensitized T-lymphocytes, or both. Binding may counteract the biological activity of the antigen
<b>Ig mu chain C region</b>		Antigen binding
<b>Immunoglobulin J chain</b>		Serves to link two monomer units of either IgM or IgA. In the case of IgM, the J chain-joined dimer is a nucleating unit for the IgM pentamer, and in the case of IgA it induces larger polymers. It also helps to bind these immunoglobulins to secretory component.
<b>Immunoglobulin lambda-like polypeptide 5</b>		Located within the immunoglobulin lambda locus, but does not require somatic rearrangement for expression.
<b>Polymeric immunoglobulin receptor</b>		This receptor binds polymeric IgA and IgM at the basolateral surface of epithelial cells. The complex is then transported across the cell to be secreted at the apical surface. During this process a cleavage occurs that separates the extracellular (known as the secretory component) from the transmembrane segment.
<b>Lipopolysaccharide-binding protein</b>		Plays a role in the innate immune response. Binds to the lipid A moiety of bacterial lipopolysaccharides (LPS), a glycolipid present in the outer membrane of all Gram-negative bacteria. Acts as an affinity enhancer for CD14, facilitating its association with LPS. Promotes the release of cytokines in response to bacterial lipopolysaccharide.
<b>Peptidoglycan recognition protein 1</b>		Pattern receptor that binds to murein peptidoglycans (PGN) of Gram-positive bacteria. Has bactericidal activity towards Gram-positive bacteria. May kill Gram-positive bacteria by interfering with peptidoglycan biosynthesis. Binds also to Gram-negative bacteria. Involved in innate immunity. Is microbicidal for Gram-positive and Gram-negative bacteria and yeast.
<b>Serum albumin</b>		Serum albumin, the main protein of plasma, has a good binding capacity for water, Ca <sup>2+</sup> , Na <sup>+</sup> , K <sup>+</sup> , fatty acids, hormones, bilirubin and drugs. Its main function is the regulation of the colloidal osmotic pressure of blood. Major zinc transporter in plasma, typically binds about 80% of all plasma zinc.
<b>Beta-casein</b>		Important role in determination of the surface properties of the casein micelles.
<b>Filaggrin-2</b>		Stabilishment of skin barrier. Neutrophil degranulation
<b>Hornerin</b>		Component of the epidermal cornified cell envelopes.
<b>Ankyrin-1</b>		Attaches integral membrane proteins to cytoskeletal elements; binds to the erythrocyte membrane protein band 4.2, to Na-K ATPase, to the lymphocyte membrane protein GP85, and to the cytoskeletal proteins fodrin, tubulin, vimentin and desmin. Erythrocyte ankyrins also link spectrin (beta chain) to the cytoplasmic domain of the erythrocytes anion exchange protein; they retain most or all of these binding functions. Publication Isoform Mu17 together with obscurin in skeletal muscle may provide a molecular link between the sarcoplasmic reticulum and myofibrils.

<b>Beta-adducin</b>	Membrane-cytoskeleton-associated protein that promotes the assembly of the spectrin-actin network. Binds to the erythrocyte membrane receptor SLC2A1/GLUT1 and may therefore provide a link between the spectrin cytoskeleton to the plasma membrane. Binds to calmodulin. Calmodulin binds preferentially to the beta subunit (By similarity).
<b>Coiled-coil domain-containing protein 125</b>	May be involved in the regulation of cell migration.
<b>Connective tissue growth factor</b>	Major connective tissue mitogen secreted by vascular endothelial cells. Promotes proliferation and differentiation of chondrocytes (By similarity). Mediates heparin- and divalent cation-dependent cell adhesion in many cell types including fibroblasts, myofibroblasts, endothelial and epithelial cells (By similarity). Enhances fibroblast growth factor-induced DNA synthesis.
<b>Desmoglein-1</b>	Component of intercellular desmosome junctions. Involved in the interaction of plaque proteins and intermediate filaments mediating cell-cell adhesion.
<b>Desmoplakin</b>	Major high molecular weight protein of desmosomes. Involved in the organization of the desmosomal cadherin-plakoglobin complexes into discrete plasma membrane domains and in the anchoring of intermediate filaments to the desmosomes.
<b>Erythrocyte band 7 integral membrane protein</b>	Regulates ion channel activity and transmembrane ion transport. Regulates ASIC2 and ASIC3 channel activity.
<b>Junction plakoglobin</b>	Common junctional plaque protein. The membrane-associated plaques are architectural elements in an important strategic position to influence the arrangement and function of both the cytoskeleton and the cells within the tissue. The presence of plakoglobin in both the desmosomes and in the intermediate junctions suggests that it plays a central role in the structure and function of submembranous plaques. Acts as a substrate for VE-PTP and is required by it to stimulate VE-cadherin function in endothelial cells. Can replace beta-catenin in E-cadherin/catenin adhesion complexes which are proposed to couple cadherins to the actin cytoskeleton.
<b>Protein 4.1</b>	Protein 4.1 is a major structural element of the erythrocyte membrane skeleton. It plays a key role in regulating membrane physical properties of mechanical stability and deformability by stabilizing spectrin-actin interaction. Recruits DLG1 to membranes. Required for dynein-dynactin complex and NUMA1 recruitment at the mitotic cell cortex during anaphase.
<b>Protein KIAA1199 homolog</b>	Mediates depolymerization of hyaluronic acid (HA) via the cell membrane-associated clathrin-coated pit endocytic pathway. Binds to hyaluronic acid. Hydrolyzes high molecular weight hyaluronic acid to produce an intermediate-sized product, a process that may occur through rapid vesicle endocytosis and recycling without intracytoplasmic accumulation or digestion in lysosomes. Involved in hyaluronan catabolism in the dermis of the skin and arthritic synovium. Positively regulates epithelial-mesenchymal transition (EMT), and hence tumor cell growth, invasion and cancer dissemination. In collaboration with HSPA5/BIP, promotes cancer cell migration in a calcium and PKC-dependent manner. May be involved in hearing.
<b>Putative annexin A2-like protein</b>	Calcium-regulated membrane-binding protein whose affinity for calcium is greatly enhanced by anionic phospholipids. It binds two calcium ions with high affinity. May be involved in heat-stress response (By

	similarity). Inhibits PCSK9-enhanced LDLR degradation, probably reduces PCSK9 protein levels via a translational mechanism but also competes with LDLR for binding with PCSK9
<b>Spectrin alpha chain, erythrocytic 1</b>	Spectrin is the major constituent of the cytoskeletal network underlying the erythrocyte plasma membrane. It associates with band 4.1 and actin to form the cytoskeletal superstructure of the erythrocyte plasma membrane.
<b>Spondin-1</b>	Activator of the canonical Wnt signaling pathway by acting as a ligand for LGR4-6 receptors. Upon binding to LGR4-6 (LGR4, LGR5 or LGR6), LGR4-6 associate with phosphorylated LRP6 and frizzled receptors that are activated by extracellular Wnt receptors, triggering the canonical Wnt signaling pathway to increase expression of target genes. Also regulates the canonical Wnt/beta-catenin-dependent pathway and non-canonical Wnt signaling by acting as an inhibitor of ZNRF3, an important regulator of the Wnt signaling pathway. Acts as a ligand for frizzled FZD8 and LRP6. May negatively regulate the TGF-beta pathway. Has a essential roles in ovary determination. Regulates Wnt signaling by antagonizing DKK1/KREM1-mediated internalization of LRP6 through an interaction with KREM1
<b>Tubulin</b>	Tubulin is the major constituent of microtubules. It binds two moles of GTP, one at an exchangeable site on the beta chain and one at a non-exchangeable site on the alpha chain.
<b>Wiskott-Aldrich protein homolog 1</b>	Has a role in regulating actin assembly, so regulating polarized growth.
<b>Adiponectin</b>	Important adipokine involved in the control of fat metabolism and insulin sensitivity, with direct anti-diabetic, anti-atherogenic and anti-inflammatory activities. Stimulates AMPK phosphorylation and activation in the liver and the skeletal muscle, enhancing glucose utilization and fatty-acid combustion. Antagonizes TNF-alpha by negatively regulating its expression in various tissues such as liver and macrophages, and also by counteracting its effects. Inhibits endothelial NF-kappa-B signaling through a cAMP-dependent pathway. May play a role in cell growth, angiogenesis and tissue remodeling by binding and sequestering various growth factors with distinct binding affinities, depending on the type of complex, LMW, MMW or HMW (By similarity).
<b>Alpha-enolase</b>	Multifunctional enzyme that, as well as its role in glycolysis, plays a part in various processes such as growth control, hypoxia tolerance and allergic responses. May also function in the intravascular and pericellular fibrinolytic system due to its ability to serve as a receptor and activator of plasminogen on the cell surface of several cell-types such as leukocytes and neurons. Stimulates immunoglobulin production. MBP1 binds to the myc promoter and acts as a transcriptional repressor. May be a tumor suppressor.
<b>Carbonic anhydrase 2</b>	Reversible hydration of carbon dioxide.
<b>Glyceraldehyde-3-phosphate dehydrogenase</b>	Has both glyceraldehyde-3-phosphate dehydrogenase and nitrosylase activities, thereby playing a role in glycolysis and nuclear functions, respectively. Glyceraldehyde-3-phosphate dehydrogenase is a key enzyme in glycolysis that catalyzes the first step of the pathway by converting D-glyceraldehyde 3-phosphate (G3P) into 3-phospho-D-glyceroyl phosphate. Modulates the organization and assembly of the cytoskeleton. Facilitates the CHP1-dependent microtubule and membrane associations through its ability to stimulate the binding of CHP1 to microtubules. Also participates in nuclear events including transcription, RNA transport, DNA replication and apoptosis. Nuclear functions are probably due to the nitrosylase activity that mediates cysteine S-nitrosylation of nuclear target proteins such as SIRT1, HDAC2 and PRKDC. Component of the GAIT (gamma interferon-

	activated inhibitor of translation) complex which mediates interferon-gamma-induced transcript-selective translation inhibition in inflammation processes. Upon interferon-gamma treatment assembles into the GAIT complex which binds to stem loop-containing GAIT elements in the 3'-UTR of diverse inflammatory mRNAs (such as ceruplasmin) and suppresses their translation (By similarity).
Heat shock protein HSP 90-alpha	Molecular chaperone that promotes the maturation, structural maintenance and proper regulation of specific target proteins involved for instance in cell cycle control and signal transduction. Undergoes a functional cycle that is linked to its ATPase activity which is essential for its chaperone activity. This cycle probably induces conformational changes in the client proteins, thereby causing their activation. Interacts dynamically with various co-chaperones that modulate its substrate recognition, ATPase cycle and chaperone function. Engages with a range of client protein classes via its interaction with various co-chaperone proteins or complexes, that act as adapters, simultaneously able to interact with the specific client and the central chaperone itself. Recruitment of ATP and co-chaperone followed by client protein forms a functional chaperone. After the completion of the chaperoning process, properly folded client protein and co-chaperone leave HSP90 in an ADP-bound partially open conformation and finally, ADP is released from Hsp90 which acquires an open conformation for the next cycle.
Hepatocyte growth factor activator	Activates hepatocyte growth factor (HGF) by converting it from a single chain to a heterodimeric form.
Histone H1.3	Core component of nucleosome. Nucleosomes wrap and compact DNA into chromatin, limiting DNA accessibility to the cellular machineries which require DNA as a template. Histones thereby play a central role in transcription regulation, DNA repair, DNA replication and chromosomal stability. DNA accessibility is regulated via a complex set of post-translational modifications of histones, also called histone code, and nucleosome remodeling.
Peptidyl-glycine alpha-amidating monooxygenase	Bifunctional enzyme that catalyzes 2 sequential steps in C-terminal alpha-amidation of peptides. The monooxygenase part produces an unstable peptidyl(2-hydroxyglycine) intermediate that is dismutated to glyoxylate and the corresponding desglycine peptide amide by the lyase part. C-terminal amidation of peptides such as neuropeptides is essential for full biological activity.
Peroxiredoxin-2	Involved in redox regulation of the cell. Reduces peroxides with reducing equivalents provided through the thioredoxin system. It is not able to receive electrons from glutaredoxin. May play an important role in eliminating peroxides generated during metabolism. Might participate in the signaling cascades of growth factors and tumor necrosis factor-alpha by regulating the intracellular concentrations of H2O2.
Phosphatidylinositol-glycan-specific phospholipase D Primary amine oxidase, liver isozyme	This protein hydrolyzes the inositol phosphate linkage in proteins anchored by phosphatidylinositol glycans (GPI-anchor) thus releasing these proteins from the membrane. Inhibited by amiloride in a competitive manner.
Proteasome subunit beta type-I	Component of the 20S core proteasome complex involved in the proteolytic degradation of most intracellular proteins. This complex plays numerous essential roles within the cell by associating with different regulatory particles. Associated with two 19S regulatory particles, forms the 26S proteasome and thus participates in the

	ATP-dependent degradation of ubiquitinated proteins. The 26S proteasome plays a key role in the maintenance of protein homeostasis by removing misfolded or damaged proteins that could impair cellular functions, and by removing proteins whose functions are no longer required. Associated with the PA200 or PA28, the 20S proteasome mediates ubiquitin-independent protein degradation. This type of proteolysis is required in several pathways including spermatogenesis (20S-PA200 complex) or generation of a subset of MHC class I-presented antigenic peptides (20S-PA28 complex). Within the 20S core complex, PSMB6 displays a peptidylglutanyl-hydrolyzing activity also termed postacidic or caspase-like activity, meaning that the peptides bond hydrolysis occurs directly after acidic residues.
<b>Protein disulfide-isomerase</b>	This multifunctional protein catalyzes the formation, breakage and rearrangement of disulfide bonds. At the cell surface, seems to act as a reductase that cleaves disulfide bonds of proteins attached to the cell. May therefore cause structural modifications of exofacial proteins. Inside the cell, seems to form/rearrange disulfide bonds of nascent proteins. At high concentrations, functions as a chaperone that inhibits aggregation of misfolded proteins. At low concentrations, facilitates aggregation (anti-chaperone activity). May be involved with other chaperones in the structural modification of the TG precursor in hormone biogenesis. Also acts a structural subunit of various enzymes such as prolyl 4-hydroxylase and microsomal triacylglycerol transfer protein MTTP. Receptor for LGALS9; the interaction retains P4HB at the cell surface of Th2 T helper cells, increasing disulfide reductase activity at the plasma membrane, altering the plasma membrane redox state and enhancing cell migration.
<b>Protein eyes shut homolog</b>	Required to maintain the integrity of photoreceptor cells.
Putative trypsin-6	May regulate cell migration.
<b>Pyruvate kinase isozymes M1/M2</b>	Glycolytic enzyme that catalyzes the transfer of a phosphoryl group from phosphoenolpyruvate (PEP) to ADP, generating ATP. Stimulates POU5F1-mediated transcriptional activation.
Ribonuclease 4	This RNase has marked specificity towards the 3' side of uridine nucleotides.
<b>Transforming growth factor-beta-induced protein ig-h3</b>	Plays a role in cell adhesion. May play a role in cell-collagen interactions
Transthyretin	Thyroid hormone-binding protein. Probably transports thyroxine from the bloodstream to the brain (By similarity).
<b>Leukocyte cell-derived chemotaxin-2</b>	Has a neutrophil chemotactic activity. Also, a positive regulator of chondrocyte proliferation.
<b>Neural cell adhesion molecule 1-A</b>	This protein is a cell adhesion molecule involved in neuron-neuron adhesion, neurite fasciculation, outgrowth of neurites, etc.
<b>Protein AMBP</b>	Inter-alpha-trypsin inhibitor inhibits trypsin, plasmin, and lysosomal granulocytic elastase. Inhibits calcium oxalate crystallization. Trypstatin is a trypsin inhibitor. By similarity. May diffuse into follicular fluid after an ovulatory stimulus to act as a structural linker that ensures normal cumulus expansion, through stabilization of the cumulus extracellular matrix, thus supporting the process of ovulation.

### 10.3 Appendix 3. Input data for construction of Proteomaps.

Abbreviation	Description Level 4	KEGG Classification,(Category)			Average normalized abundance			
		Level 1	Level 2	Level 3	<i>B.melitensis</i> 16M	<i>B.abortus</i>	<i>B.melitensis</i> 16M $\Delta$ wadC	<i>B.melitensis</i> 16M $\Delta$ per
ADIPO	Adiponectin	Environmental Information Processing	Signal transduction	AMPK signaling pathway	2772.051525	1892.170933	3403.61849	4995.18273
Alpha-1-AP	Alpha-1-antitrypsin	Organismal Systems	Immune system	Complement and coagulation cascades	9908.14344	8431.892503	23490.3075	20944.1062
Alpha-1-BG	Alpha-1B-glycoprotein	Not mapped	Not mapped	Not mapped	16770.36887	3733.393846	2020.04204	1160.1863
Alpha-2HS-G	Alpha-2-HS-glycoprotein	Not mapped	Not mapped	Not mapped	161324.6934	168311.4985	170960.353	101717.207
Alpha-2-M	Alpha-2-macroglobulin	Organismal Systems	Immune system	Complement and coagulation cascades	2056.786244	397.253092	501.829027	201.158298
AMBP	Protein AMBP	Not mapped	Not mapped	Not mapped	161.8712523	126.9906569	483.901833	18.264621
ANK-1	Ankyrin-1	Organismal Systems	Immune system	Toll and Imd signaling pathway	905.5211046	1026.559439	673.212062	3273.70098
Annexin A2	Putative annexin A2-like protein	Exosome	Exosomal proteins	Proteins found in most exosomes	16766.7125	9912.955251	11361.8207	3955.53962
Apo-A1	Apolipoprotein A-I	Organismal Systems	Endocrine system	PPAR signaling pathway	5657.334471	2897.911727	2887.43599	2851.78986
Apo-D	Apolipoprotein D	Exosome	Exosomal proteins	Exosomal proteins of other cancer cells	3044.241073	2881.125822	672.305351	4056.03258
Apo-E	Apolipoprotein E	Exosome	Exosomal proteins	Exosomal proteins of other cancer cells	62615.80012	40250.07568	56669.5281	209141.338
ATIII	Antithrombin-III	Organismal Systems	Immune system	Complement and coagulation cascades	1189.420177	402.9759347	2093.40038	586.450646
Beta(2)GPI	Beta-2-glycoprotein 1	Exosome	Exosomal proteins	Exosomal proteins of other cancer cells	36211.11587	21031.0261	29829.4462	53302.1661
Beta-Adducin	Beta-adducin	Eukaryotic cytoskeleton proteins	Intermediate filaments	Intermediate filament-binding proteins	755.684828	356.9456576	2038.39083	726.175548
Beta-Casein	Beta-casein	Organismal Systems	Endocrine system	Prolactin signaling pathway	59520.86434	23661.33155	17031.6688	1439.33371



BSA	Serum albumin	Organismal Systems	Endocrine system	Thyroid hormone synthesis	7290.013176	12654.81166	45608.5547	12903.4787
C1q	Complement C1q	Organismal Systems	Immune system	Complement and coagulation cascades	655.5420413	894.0570817	4423.25061	40446.9269
C2	Complement C2	Organismal Systems	Immune system	Complement and coagulation cascades	6144.322771	6443.068742	1587.09852	30.4423342
C3	Complement C3	Organismal Systems	Immune system	Complement and coagulation cascades	933688.1388	640253.3908	1333306.48	825389.967
C4	Complement C4	Organismal Systems	Immune system	Complement and coagulation cascades	14051.85905	11436.25417	6322.0653	42083.748
C4BP	C4b-binding protein	Organismal Systems	Immune system	Complement and coagulation cascades	1840.157134	1451.980335	504.163826	105.24384
C5	Complement C5	Organismal Systems	Immune system	Complement and coagulation cascades	517387.6796	288803.4967	146260.038	37694.3845
C6	Complement component C6	Organismal Systems	Immune system	Complement and coagulation cascades	189543.9281	123402.6811	42383.9648	19860.3984
C7	Complement component C7	Organismal Systems	Immune system	Complement and coagulation cascades	494517.59	289644.1637	108680.603	39916.6164
C8	Complement component C8	Organismal Systems	Immune system	Complement and coagulation cascades	341801.9362	400622.0049	296404.982	52986.4957
C9	Complement component C9	Organismal Systems	Immune system	Complement and coagulation cascades	409710.4941	222643.1867	112925.048	75511.9647
CA-I	Carbonic anhydrase 2	Metabolism	Overview	Nitrogen metabolism	713.0724445	423.4333935	505.735531	1401.81684
CAT	Catalase	Metabolism	Overview	Carbon metabolism	1378.102908	3901.526809	7573.63948	3232.50276
CCDCP-125	Coiled-coil domain-containing protein 125	Not mapped	Not mapped	Not mapped	12711.70607	6915.866213	41556.5251	2774.96766
CFB	Complement factor B	Organismal Systems	Immune system	Complement and coagulation cascades	470710.9341	271953.4496	125693.939	244966.964
CFH	Complement Factor H	Organismal Systems	Immune system	Complement and coagulation cascades	25471.60921	20616.04118	2961.49271	48469.2659
CGN	Conglutinin	Cellular Processes	Transport and catabolism	Phagosome	4791.941509	2327.907254	604.611955	12.5949609
CLU	Clusterin	Organismal Systems	Immune system	Complement and coagulation cascades	11556.13428	9278.98792	3255.72716	880.257512

CP	Ceruloplasmin	Metabolism	Metabolism of cofactors and vitamins	Porphyrin and chlorophyll metabolism	11836.02167	18324.38568	71185.3737	29493.798
CTGF	Connective tissue growth factor	Environmental Information Processing	Signal transduction	Hippo signaling pathway	26771.28391	13892.58857	66590.1309	56917.8772
CTHL	Cathelicidin	Organismal Systems	Immune system	NOD-like receptor signaling pathway	5757.038758	5441.0057	2401.94354	963.18196
DP	Desmoplakin	Eukaryotic cytoskeleton proteins	Intermediate filaments	Intermediate filament-binding proteins	4622.207762	598.9202792	788.492095	2355.75165
DSG1	Desmoglein-1	Human Diseases	Infectious diseases	Staphylococcus aureus infection	441.4638504	597.738496	857.9342	25541.0064
ENO-A	Alpha-enolase	Metabolism	Overview	Carbon metabolism	1645.109019	637.532653	4965.4556	2857.39909
EPB72	Erythrocyte band 7 integral membrane protein	Exosome	Exosomal proteins	Exosomal proteins of breast milk	6169.354166	3075.218475	1898.48027	34657.8544
EYS	Protein eyes shut homolog	Not mapped	Not mapped	Not mapped	159.4492739	74.19537171	30.4528297	146.256937
FLG-2	Filaggrin-2	Eukaryotic cytoskeleton proteins	Intermediate filaments	Intermediate filament-binding proteins	450.6096903	104.3551089	50.5786363	22.8776155
FN	Fibronectin	Environmental Information Processing	Signal transduction	PI3K-Akt signaling pathway	2922.435228	5341.972316	2518.26132	1770.21457
FV	Coagulation factor V	Organismal Systems	Immune system	Complement and coagulation cascades	18819.38494	17156.2094	24656.408	178241.088
FVIII	Coagulation factor VIII	Organismal Systems	Immune system	Complement and coagulation cascades	21052.99642	20278.29976	18334.2487	10193.8334
GADPH	Glyceraldehyde-3-phosphate dehydrogenase	Metabolism	Overview	Carbon metabolism	9816.786371	15391.06174	5156.03734	5188.90675
HBA	Hemoglobin	Exosome	Exosomal proteins	Exosomal proteins of hepatic cells	2022.925502	2216.834027	5443.48764	7749.27152
HGFA	Hepatocyte growth factor activator	Enzymes	Hydrolases	Acting on peptide bonds Serine endopeptidases	17343.88579	12926.18211	9526.53159	62381.0253
H3H3.3	Histone H3.3	Chromosome	Eukaryotic Type	Nucleosome assembly factors Histones	1621.697791	1388.553539	6049.88546	2320.91198
HMPX	Hemopexin	Enzymes	Hydrolases	Glycosylases	376.170358	303.7972478	2080.35708	3230.20068

HORN	Hornerin	Not mapped	Not mapped	Not mapped	14838.08261	28633.03212	54326.8015	12564.6466
HPT	Haptoglobin	Peptidases	Serine Peptidases	Family S1; chymotrypsin family	7475.121709	9812.636676	1834.74344	672.077678
HSP90A	Heat shock protein HSP 90-alpha	Genetic Information Processing	Folding, sorting and degradation	Protein processing in endoplasmic reticulum	509.8351343	204.597504	1412.0483	9358.67884
I-ATI	Inter-alpha-trypsin inhibitor	Glycosaminoglycan binding proteins	Hyaluronan	Extracellular matrix or blood plasma proteins	2525.962377	1795.971984	2827.57	305335.93
Ig	Immunoglobulin	Environmental Information Processing	Signal transduction	NF-kappa B signaling pathway	14525.24143	9729.184997	13613.155	28257.9186
JUP	Junction plakoglobin	Exosome	Exosomal proteins	Exosomal proteins of other body fluids (saliva and urine)	611.5507142	3936.697255	1799.18317	3198.07211
KLK1	Plasma kallikrein	Organismal Systems	Immune system	Complement and coagulation cascades	17.47430903	206.3924981	1190.05837	9965.70662
Lactoferrin	Lactotransferrin	Enzymes	Hydrolases	Acting on peptide bonds (peptidases)	1830.963665	1188.300757	864.988107	18248.3125
LBP	Lipopolysaccharide-binding protein	Environmental Information Processing	Signal transduction	NF-kappa B signaling pathway	82364.66525	75792.76578	81075.8141	69156.747
LECT-2	Leukocyte cell-derived chemotaxin-2	Not mapped	Not mapped	Not mapped	69635.37481	51390.76168	106339.586	212466.717
LYZ	Lysozyme C, tracheal isozyme	Organismal Systems	Digestive system	Salivary secretion	41.72241654	14.01098837	44.5623502	65.190818
LYZ-C2	Putative lysozyme C-2	Organismal Systems	Digestive system	Salivary secretion	252.7438885	228.999747	1166.83737	288.557994
MBP-C	Mannose-binding protein C	Organismal Systems	Immune system	Complement and coagulation cascades	3748.58628	6351.870421	8.43192957	17.8013819
MPO	Myeloperoxidase	Cellular Processes	Transport and catabolism	Phagosome	2633.84201	2199.46921	4857.47926	2081.97378
NCAM-1-A	Neural cell adhesion molecule 1-A	Environmental Information Processing	Signaling molecules and interaction	Cell adhesion molecules (CAMs)	839.7798912	1950.101368	4030.29909	12171.3702
P4.1	Protein 4.1	Eukaryotic cytoskeleton proteins	Actin filaments / Microfilaments	Actin-binding proteins	156.2381736	9.658327765	437.673733	30.2296632
PAM	Peptidyl-glycine alpha-amidating monoxygenase	Enzymes	Lyases	Carbon-nitrogen lyases Amidine-lyases peptidylamidoglycolate lyase	76.51586291	1569.145444	2445.34744	1518.13686

PAO	Primary amine oxidase, liver isozyme	Metabolism	Amino acid metabolism	Glycine, serine and threonine metabolism	3869.678104	2214.314012	439.106428	597.801371
PCI	Plasma serine protease inhibitor	Organismal Systems	Immune system	Complement and coagulation cascades	76.96480344	206.9832687	22.1748348	211.834491
PDI	Protein disulfide-isomerase	Enzymes	Isomerases	Intramolecular oxidoreductases Intramolecular oxidoreductases protein disulfide-isomerase	203.4098908	144.51631	314.742703	16.1052012
PGRP-1	Peptidoglycan recognition protein 1	Not mapped	Not mapped	Not mapped	2163.524106	1099.504121	2298.98429	611.166433
PI-G PLD	Phosphatidylinositol-glycan-specific phospholipase D	Not mapped	Not mapped	Not mapped	94680.21485	43193.77902	2222.76473	961.080751
PiGR	Polymeric immunoglobulin receptor	Organismal Systems	Immune system	Intestinal immune network for IgA production	192.5189434	1402.596376	5039.42768	0.1
PKIAA1199	Protein KIAA1199 homolog	Glycosaminoglycan binding proteins	Hyaluronan	Cell surface receptors	95.63504024	1374.208475	3097.34903	85.5980465
PKM	Pyruvate kinase isozymes M1/M2	Metabolism	Overview	Carbon metabolism	161469.307	108420.3494	129961.48	26317.0793
PLF4	Platelet factor 4	Organismal Systems	Immune system	Complement and coagulation cascades	4592.239521	2297.215904	1020.09362	333.935883
PLG	Plasminogen	Organismal Systems	Immune system	Complement and coagulation cascades	8374.742025	2257.876471	1012.5321	5093.65126
PRDX-2	Peroxiredoxin-2	Cellular Processes	Cell growth and death	Apoptosis	506.0988433	826.4555543	305.193161	6608.01626
PRSS3P2	Putative trypsin-6	Not mapped	Not mapped	Not mapped	878.334314	240.8086868	260.774891	1319.98624
PSMII6	Proteasome subunit beta type-1	Genetic Information Processing	Folding, sorting and degradation	Proteasome	1735.15746	1902.113749	1003.81979	2066.45908
PTI-FII	Prothrombin	Organismal Systems	Immune system	Complement and coagulation cascades	5957.073557	4705.282358	7297.89281	15167.8666
PZP	Pregnancy zone protein	Not mapped	Not mapped	Not mapped	21582.51526	14707.58654	60198.4736	56705.4536
RNase-4	Ribonuclease-4	Enzymes	Hydrolases	Acting on ester bonds	198240.3467	115378.2679	96671.1096	17167.9407
S100-A8	Protein S100-A8	Organismal Systems	Immune system	IL-17 signaling pathway	20154.2276	19791.58325	9036.29919	6808.31834

SPA-32	Serpin A3-2	Not mapped	Not mapped	Not mapped	7410.121315	4570.668716	2534.98629	534.730457
SPO-1	Spondin-1	Not mapped	Not mapped	Not mapped	114841.7081	22839.82143	20682.8921	16007.4538
SPTA-1	Spectrin	Eukaryotic cytoskeleton proteins	Actin filaments Microfilaments	Actin-binding proteins Cross-linking proteins	5972.977494	8576.413091	6510.78269	42742.9961
TGFB1	Transforming growth factor-beta-induced protein ig-h3	Cell adhesion molecules and their ligands	Integrin Family	Beta integrins	9356.557692	3979.24075	7604.39712	10456.6701
THBS	Thrombospondin-1	Environmental Information Processing	Signal transduction	PI3K-Akt signaling pathway	2457.923375	2593.05124	1458.44562	736.694071
TIMP-3	Metalloproteinase inhibitor 3	Human Diseases	Cancers	MicroRNAs in cancer	4.895809145	11.35053356	20.1999364	13273.3334
TRYP	Trypsin	Not mapped	Not mapped	Not mapped	4857.80724	118.4895725	308.096478	102.301416
TTR	Transthyretin	Organismal Systems	Endocrine system	Thyroid hormone synthesis	588.8721958	567.7119528	1043.44348	2696.99053
TUB	Tubulin	Cellular Processes	Transport and catabolism	Phagosome	3822.995669	1932.750179	2215.36366	1629.36441
VTN	Vitronectin	Organismal Systems	Immune system	Complement and coagulation cascades	2973.268673	2654.716643	4844.52911	9125.40759
WASP	Wiskott-Aldrich syndrome protein homolog 1	Not mapped	Not mapped	Not mapped	0.950987307	0.551712349	2423.09695	0.1
XIIaINH	Factor XIIa inhibitor	Organismal Systems	Immune system	Complement and coagulation cascades	54993.7572	32455.53655	19300.3394	5934.72041

**10.4 Appendix 4** *B. abortus/B. melitensis* fold change statistics (Wald Test, and FDR adjusted p-values) for the 96 adsorbed serum proteins

#	Protein	FC <sup>A</sup>	S.E. <sup>B</sup>	Wald	p-value <sup>C</sup>	FDR adjusted (p-value) <sup>D</sup>
<b>1</b>	<b>Mannose-binding protein C<sup>1</sup></b>	<b>1,10074478</b>	<b>0,18861263</b>	<b>5,836007915</b>	<b>5,35E-09</b>	<b>7,26E-08</b>
2	Conglutinin	-0,68592018	0,27512502	-2,493121816	0,01266254	0,03894979
<b>3</b>	<b>Complement C1q</b>	<b>0,79214702</b>	<b>0,21297684</b>	<b>3,719404586</b>	<b>0,00019969</b>	<b>0,00145929</b>
4	Complement C2	0,44564133	0,24142397	1,845886854	0,06490864	0,1434028
5	Complement C4	0,08591731	0,23252882	0,369491001	0,71176178	0,79549846
6	Complement factor B	-0,42940582	0,1591596	-2,697957471	0,00697664	0,02454742
7	Complement C3	-0,17345002	0,15484946	-1,120120308	0,2626625	0,38988964
8	Complement C5	-0,46911077	0,24125921	-1,944426383	0,05184405	0,12012647
9	Complement component C6	-0,26620765	0,26076762	-1,020861602	0,30732001	0,42934414
10	Complement component C7	-0,40195907	0,16284083	-2,468416915	0,01357122	0,03906865
<b>11</b>	<b>Complement component C8</b>	<b>0,59464238</b>	<b>0,1872062</b>	<b>3,176403306</b>	<b>0,00149113</b>	<b>0,00708289</b>
12	Complement component C9	-0,47421848	0,23607987	-2,008720516	0,04456678	0,11141695
13	Complement Factor H	0,02188885	0,28576933	0,076596224	0,93894476	0,95913712
14	C4b-binding protein	0,0672003	0,34333552	0,195727779	0,84482324	0,89941839
15	Vitronectin	0,23913208	0,25266484	0,946439873	0,34392428	0,46681189
16	Clusterin	0,06047896	0,31293468	0,193263861	0,84675233	0,89941839
17	Coagulation factor VIII	0,26915968	0,23817221	1,130105302	0,25843186	0,38969883
18	Coagulation factor V	0,24144331	0,17376549	1,389477916	0,16468747	0,28446018
19	Prothrombin	0,04625127	0,24804338	0,186464424	0,85208058	0,89941839
20	Thrombospondin-1	0,46717784	0,30746331	1,519458832	0,12864704	0,23502825
21	Factor XIIa inhibitor	-0,33877908	0,32643257	-1,037822536	0,29935268	0,4244553
22	Plasminogen	-1,2989394	0,76086426	-1,707189392	0,08778686	0,18129894
23	Platelet factor 4	-0,580553	0,3685385	-1,575284523	0,11519078	0,22332907
<b>24</b>	<b>Antithrombin-III</b>	<b>-1,10727881</b>	<b>0,32526555</b>	<b>-3,404230224</b>	<b>0,00066351</b>	<b>0,00393958</b>

25	Beta-2-glycoprotein 1	-0,37064491	0,2839018	-1,305539125	0,19170933	0,31951556
26	Fibronectin	1,13969383	0,45920601	2,481879145	0,01306916	0,03894979
27	Hemoglobin	0,52681195	0,24062134	2,189381606	0,02856912	0,07754474
28	Ceruloplasmin	1,02331851	0,2485589	4,117006053	3,84E-05	0,00030386
29	Haptoglobin	0,74755898	0,17053137	4,383703531	1,17E-05	0,00011084
30	Hemopexin	0,06866415	0,35014603	0,196101459	0,84453075	0,89941839
31	Lactotransferrin	-0,21467811	0,30877271	-0,695262576	0,48689076	0,6167283
32	Apolipoprotein A-I	-0,57348391	0,44275907	-1,295250502	0,19523383	0,31977955
33	Apolipoprotein D	0,31895496	0,25009246	1,275348173	0,20218603	0,32412097
34	Apolipoprotein E	-0,25313228	0,16480969	-1,535906539	0,1245613	0,23202596
35	Alpha-1-antiproteinase	0,02932938	0,46375183	0,063243689	0,94957246	0,95967429
36	Alpha-1B-glycoprotein	-1,67607257	0,45880084	-3,653159335	0,00025903	0,00175773
37	Alpha-2-HS-glycoprotein	0,41826239	0,22909681	1,825701545	0,06789523	0,14659197
38	Alpha-2-macroglobulin	-1,81225249	0,65730827	-2,757081535	0,00583198	0,02130916
39	Inter-alpha-trypsin inhibitor	-0,10085076	0,26042785	-0,387250293	0,69857092	0,79416042
40	Metalloproteinase inhibitor 3	0,79048808	0,96598561	0,818322834	0,41317287	0,53042463
41	Plasma kallikrein	2,69627911	0,87332126	3,087385177	0,00201926	0,00841532
42	Plasma serine protease inhibitor	1,62409012	0,47020931	3,453972703	0,00055239	0,00349849
43	Pregnancy zone protein	-0,20506552	0,18469137	-1,110314578	0,26686349	0,39003126
44	Serpin A3-2	-0,34715161	0,70872934	-0,489822554	0,62425947	0,74307511
45	Trypsin	-4,89764872	0,25716206	-19,04498924	7,23E-81	6,87E-79
46	Catalase	1,81899013	0,21914875	8,300253281	1,04E-16	1,97E-15
47	Protein S100-A8	0,36224282	0,28908095	1,253084389	0,210175	0,32412097
48	Cathelicidin	0,28830381	0,23076027	1,249365065	0,21153158	0,32412097
49	Putative lysozyme C-2	0,25006366	0,41377745	0,604343377	0,54561537	0,66453154
50	Lysozyme C, tracheal isozyme	-0,79283302	0,83777393	-0,946356756	0,34396665	0,46681189
51	Myeloperoxidase	0,14494219	0,29718258	0,487721016	0,62574746	0,74307511
52	Immunoglobulin	-0,21117672	0,20245652	-1,043071949	0,29691497	0,4244553

53	<b>Polymeric immunoglobulin receptor</b>	<b>2,50119311</b>	<b>0,77303137</b>	<b>3,235564815</b>	<b>0,00121402</b>	<b>0,00607012</b>
54	Lipopolysaccharide-binding protein	0.2549571	0,55712193	0,457632503	0,64721649	0,75908107
55	<b>Peptidoglycan recognition protein 1</b>	<b>-0,62227646</b>	<b>0,24197913</b>	<b>-2,571612138</b>	<b>0,01012262</b>	<b>0,03316032</b>
56	<b>Scrum albumin</b>	<b>1,18853097</b>	<b>0,38529539</b>	<b>3,084726663</b>	<b>0,00203739</b>	<b>0,00841532</b>
57	Beta-casein	-0.95997858	0,56212296	-1,707773279	0,08767842	0,18129894
58	Filaggrin-2	-1.46726746	0,62697	-2,340251457	0,01927076	0,05384477
59	<b>Hornerin</b>	<b>1,33899937</b>	<b>0,39770933</b>	<b>3,366778876</b>	<b>0,00076052</b>	<b>0,00424994</b>
60	Ankyrin-1	0,54983392	0,32809684	1,67582814	0,09377186	0,18953887
61	Beta-adducin	-0,61554512	0,39614049	-1,553855616	0,12021886	0,22841584
62	Coiled-coil domain-containing protein 125	-0,55839043	0,35308233	-1,581473726	0,11376976	0,22332907
63	Connective tissue growth factor	-0,58679704	0,39981541	-1,467669878	0,14219392	0,25487589
64	Desmoglein-1	0,8349879	0,42118148	1,982489571	0,04742447	0,11263312
65	<b>Desmoplakin</b>	<b>-2,49691511</b>	<b>0,26280214</b>	<b>-9,501121666</b>	<b>2,08E-21</b>	<b>4,93E-20</b>
66	<b>Erythrocyte band 7 integral membrane protein</b>	<b>-0,62240478</b>	<b>0,19810696</b>	<b>-3,141761313</b>	<b>0,00167935</b>	<b>0,00759705</b>
67	<b>Junction plakoglobin</b>	<b>3,04241926</b>	<b>0,22633501</b>	<b>13,44210646</b>	<b>3,43E-41</b>	<b>1,63E-39</b>
68	Protein 4.1	-3,23695884	0,59949882	-5,399441568	6,68E-08	7,94E-07
69	<b>Protein KIAA1199 homolog</b>	<b>4,00589991</b>	<b>0,36042088</b>	<b>11,1145056</b>	<b>1,07E-28</b>	<b>3,38E-27</b>
70	Putative annexin A2-like protein	-0,43840975	0,32181266	-1,362313549	0,17309895	0,29365001
71	Spectrin	0,82226258	0,33149103	2,480497226	0,01311993	0,03894979
72	Spondin-1	-1,74886861	0,52496043	-3,331429366	0,00086401	0,00456006
73	Tubulin	-0,59405217	0,27734804	-2,141901447	0,03220141	0,08497595
74	Wiskott-Aldrich syndrome protein homolog 1	-0,09763239	0,74963772	-0,130239433	0,896377	0,93577818
75	Adiponectin	-0,19897956	0,21463814	-0,927046608	0,35390234	0,46695447
76	Alpha-enolase	-0,84755613	0,82347618	-1,029241836	NA	NA
77	Carbonic anhydrase 2	-0,36817341	0,58592659	-0,628360985	0,52976749	0,65360924
78	<b>Glyceraldehyde-3-phosphate dehydrogenase</b>	<b>0,98722829</b>	<b>0,20049799</b>	<b>4,923881277</b>	<b>8,48E-07</b>	<b>8,96E-06</b>



79	Heat shock protein HSP 90-alpha	-0,89806673	0,71140401	-1,26238637	0,20680979	0,32412097
80	Hepatocyte growth factor activator	0,01396771	0,33299749	0,041945401	0,96654222	0,96654222
<b>81</b>	<b>Histone H1.3</b>	<b>0,12802427</b>	<b>0,31349953</b>	<b>0,408371479</b>	<b>0,68300097</b>	<b>0,79128161</b>
82	Peptidyl-glycine alpha-amidating monooxygenase	4,11231358	0,61504491	6,6862005	2,29E-11	3,63E-10
<b>83</b>	<b>Peroxiredoxin-2</b>	<b>0,93292919</b>	<b>0,49804687</b>	<b>1,873175495</b>	<b>0,06104415</b>	<b>0,13807606</b>
84	Phosphatidylinositol-glycan-specific phospholipase D	-0,77978401	0,18087462	-4,311185295	1,62E-05	0,00014024
<b>85</b>	<b>Primary amine oxidase, liver isozyme</b>	<b>-0,46608711</b>	<b>0,50011548</b>	<b>-0,931958965</b>	<b>0,35135773</b>	<b>0,46695447</b>
86	Proteasome subunit beta type-1	0,50542121	0,18873778	2,677901639	0,0074085	0,02513597
<b>87</b>	<b>Protein disulfide-isomerase</b>	<b>-0,18344837</b>	<b>0,4797972</b>	<b>-0,382345641</b>	<b>0,70220501</b>	<b>0,79416042</b>
88	Protein eyes shut homolog	-0,68683081	0,81873008	-0,838897734	0,4015267	0,52253475
<b>89</b>	<b>Putative trypsin-6</b>	<b>-0,86619167</b>	<b>0,30775505</b>	<b>-2,814548986</b>	<b>0,00488457</b>	<b>0,01856138</b>
90	Pyruvate kinase isozymes M1/M2	-0,17413665	0,27471473	-0,633881731	0,52615801	0,65360924
<b>91</b>	<b>Ribonuclease 4</b>	<b>-0,39099045</b>	<b>0,19644934</b>	<b>-1,99028638</b>	<b>0,0465594</b>	<b>0,11263312</b>
92	Transforming growth factor-beta-induced protein ig-h3	-0,88015203	0,43248243	-2,035116261	0,04183918	0,10742491
<b>93</b>	<b>Transthyretin</b>	<b>0,31292924</b>	<b>0,22165585</b>	<b>1,411779774</b>	<b>0,15801482</b>	<b>0,27798903</b>
<b>94</b>	<b>Leukocyte cell-derived chemotaxin-2</b>	<b>-0,06509933</b>	<b>0,18350209</b>	<b>-0,354760698</b>	<b>0,72276887</b>	<b>0,79840748</b>
<b>95</b>	<b>Neural cell adhesion molecule 1-A</b>	<b>1,39575312</b>	<b>0,46086168</b>	<b>3,02857277</b>	<b>0,00245712</b>	<b>0,0097261</b>
96	Protein AMBP	0,03509512	0,44402379	0,079038823	0,93700174	0,95913712

<sup>A</sup> The logarithm (to basis 2) of the fold change

<sup>B</sup> Standard error estimate for the log<sub>2</sub> fold change

<sup>C</sup> p value for the statistical significance for the log<sub>2</sub> fold change

<sup>D</sup> p value adjusted for false discovery rate (FDR)

<sup>E</sup> Proteins in bold letters have a statistical significance for the log<sub>2</sub> fold change p>0.01

**9.5 Appendix 5. *B. melitensis* Δ*wadC*/*B. melitensis* fold change statistics (Wald Test, and FDR adjusted p-values) for the 96 adsorbed serum proteins.**

#	Protein	FC <sup>A</sup>	S.E. <sup>B</sup>	Wald	p-value <sup>C</sup>	FDR adjusted (p-value) <sup>D</sup>
1	Mannose-binding protein C <sup>E</sup>	-7,61866007	0,83989367	-9,07098169	1,18E-19	2,80E-18
2	<b>Conglutinin</b>	<b>-2,61055881</b>	<b>0,58959565</b>	<b>-4,42771044</b>	<b>9,52E-06</b>	<b>9,05E-05</b>
3	Complement C1q	3,32596183	0,76068637	4,37231686	1,23E-05	0,00010237
4	Complement C2	-1,57636113	0,98994159	-1,59237792	0,11129981	0,18549969
5	Complement C4	-0,3712911	0,76955727	-0,48247365	0,62946952	0,71190005
6	<b>Complement factor B</b>	<b>-1,41209211</b>	<b>0,27269414</b>	<b>-5,17830022</b>	<b>2,24E-07</b>	<b>2,66E-06</b>
7	Complement C3	1,1079331	0,5079313	2,18126565	0,02916377	0,0675746
8	<b>Complement C5</b>	<b>-1,46133911</b>	<b>0,45214927</b>	<b>-3,23198378</b>	<b>0,00122934</b>	<b>0,00449182</b>
9	Complement component C6	-1,72715088	0,32821885	-5,26219283	1,42E-07	1,93E-06
10	<b>Complement component C7</b>	<b>-1,59995159</b>	<b>0,42207297</b>	<b>-3,79069899</b>	<b>0,00015022</b>	<b>0,00075112</b>
11	Complement component C8	0,37780533	0,46723125	0,80860457	0,41874263	0,50355127
12	Complement component C9	-1,49063994	0,60134026	-2,47886271	0,0131802	0,03912873
13	<b>Complement Factor II</b>	<b>-2,43341963</b>	<b>0,58071653</b>	<b>-4,19037433</b>	<b>2,78E-05</b>	<b>0,00020352</b>
14	<b>C4b-binding protein</b>	<b>-1,32153361</b>	<b>0,37170611</b>	<b>-3,55531854</b>	<b>0,00037752</b>	<b>0,00149436</b>
15	Vitronectin	1,38039584	0,68507946	2,01494267	0,04391066	0,09270028
16	Clusterin	-1,50758239	0,83756644	-1,79995559	0,07186765	0,13387111
17	Coagulation factor VIII	0,34220951	0,40113756	0,85309765	0,39360515	0,47939089
18	<b>Coagulation factor V</b>	<b>0,9339549</b>	<b>0,39938112</b>	<b>2,33862247</b>	<b>0,01935498</b>	<b>0,05107564</b>
19	Prothrombin	0,77382832	0,26285931	2,94388778	0,00324117	0,01140413
20	Thrombospondin-1	-0,16995315	0,49149145	-0,34579066	0,72950005	0,78332541
21	Factor XIIa inhibitor	-1,13158384	1,10850018	-1,02082423	0,30733772	0,40355987
22	<b>Plasminogen</b>	<b>-2,55740784</b>	<b>1,0473088</b>	<b>-2,44188518</b>	<b>0,01461079</b>	<b>0,04200375</b>
23	Platelet factor 4	-1,75670637	1,01513422	-1,73051636	0,08353806	0,15236533
24	<b>Antithrombin-III</b>	<b>1,5195953</b>	<b>0,75381851</b>	<b>2,0158636</b>	<b>0,04381424</b>	<b>0,09270028</b>
25	Beta-2-glycoprotein 1	0,02159391	0,73781173	0,02926751	0,97665124	0,97665124
26	<b>Fibronectin</b>	<b>0,25345219</b>	<b>0,71655249</b>	<b>0,35371058</b>	<b>0,7235558</b>	<b>0,78332541</b>

27	<b>Hemoglobin</b>	<b>1,96912573</b>	<b>0,60612223</b>	<b>3,24872711</b>	<b>0,00115923</b>	<b>0,00440506</b>
28	<b>Ceruloplasmin</b>	<b>3,21430922</b>	<b>0,78889768</b>	<b>4,07443105</b>	<b>4,61E-05</b>	<b>0,00029214</b>
29	Haptoglobin	-1,56270759	1,28391687	-1,21714079	0,22355065	0,32177745
30	<b>Hemopexin</b>	<b>3,10826325</b>	<b>0,80114243</b>	<b>3,87978857</b>	<b>0,00010455</b>	<b>0,00058423</b>
31	Lactotransferrin	-0,77235437	0,70683737	-1,09269036	0,27452978	0,37797578
32	Apolipoprotein A-I	-0,65005457	0,57930933	-1,12211997	0,26181143	0,36576597
33	Apolipoprotein D	-1,76992881	0,40582887	-4,3612689	1,29E-05	0,00010237
34	Apolipoprotein E	0,09335486	0,92043889	0,10142429	0,91921365	0,93138776
35	Alpha-1-antiproteinase	1,43182066	0,63185712	2,26605133	0,02344824	0,0586206
36	Alpha-1B-glycoprotein	-2,57576856	1,12949948	-2,2804513	0,02258094	0,05797808
37	Alpha-2-HS-glycoprotein	0,52205883	0,3031062	1,7223628	0,08500382	0,15236533
38	Alpha-2-macroglobulin	-1,26747222	0,97191888	-1,3040926	0,19220201	0,28573853
39	Inter-alpha-trypsin inhibitor	0,70127807	0,43018227	1,63018823	0,10306172	0,17483685
40	Metalloproteinase inhibitor 3	2,15045634	1,27275188	1,6896116	0,09110229	0,16027254
41	Plasma kallikrein	5,33520547	1,42098965	3,75457025	0,00017364	0,00082479
42	Plasma serine protease inhibitor	-0,99426741	0,95483202	-1,04130087	0,29773593	0,40355987
43	Pregnancy zone protein	1,68430261	0,71287919	2,3626761	0,01814352	0,0492467
44	Serpin A3-2	-0,97605994	0,96163158	-1,01500404	0,3101039	0,40355987
45	Trypsin	-3,02051389	0,84867044	-3,55911287	0,00037211	0,00149436
46	<b>Catalase</b>	<b>2,96825657</b>	<b>0,40625153</b>	<b>7,30645013</b>	<b>2,74E-13</b>	<b>5,21E-12</b>
47	Protein S100-A8	-0,78746183	0,57261893	-1,37519349	0,16907146	0,26769649
48	<b>Cathelicidin</b>	<b>-0,85566896</b>	<b>0,46844328</b>	<b>-1,82662233</b>	<b>0,06775657</b>	<b>0,13136479</b>
49	Putative lysozyme C-2	2,8947204	1,00542883	2,8790903	NA	NA
50	<b>Lysozyme C, tracheal isozyme</b>	<b>0,67329626</b>	<b>0,93929468</b>	<b>0,71681047</b>	<b>0,47349105</b>	<b>0,56227062</b>
51	Myeloperoxidase	1,09217117	0,83077663	1,31463877	0,18863133	0,28573853
52	Immunoglobulin	0,25336696	0,42944075	0,58999282	0,55519546	0,64321425
53	<b>Polymeric immunoglobulin receptor</b>	<b>5,19308901</b>	<b>0,45492465</b>	<b>11,4152729</b>	<b>3,51E-30</b>	<b>1,11E-28</b>
54	Lipopolysaccharide-binding protein	0,28074208	0,90395853	0,31056965	0,75612781	0,79322663

55	Peptidoglycan recognition protein 1	0,84676532	0,86748702	0,97611296	0,32900849	0,41674408
56	<b>Serum albumin</b>	<b>3,16271062</b>	<b>0,55542714</b>	<b>5,69419534</b>	<b>1,24E-08</b>	<b>1,96E-07</b>
57	Beta-casein	-1,47426049	1,13123911	-1,30322623	0,19249754	0,28573853
58	<b>Filaggrin-2</b>	<b>-2,59548446</b>	<b>1,1884857</b>	<b>-2,18385839</b>	<b>0,02897266</b>	<b>0,0675746</b>
59	<b>Hornerin</b>	<b>2,22997605</b>	<b>0,55596672</b>	<b>4,01098838</b>	<b>6,05E-05</b>	<b>0,00035901</b>
60	<b>Ankyrin-1</b>	<b>0,15082962</b>	<b>0,4933794</b>	<b>0,30570717</b>	<b>0,75982761</b>	<b>0,79322663</b>
61	Beta-adducin	2,17208229	1,02264348	2,12398781	0,03367116	0,07616096
62	Coiled-coil domain-containing protein 125	1,63100014	1,3239019	1,2319645	0,21796235	0,31856035
63	<b>Connective tissue growth factor</b>	<b>1,78482197</b>	<b>0,48882393</b>	<b>3,65125735</b>	<b>0,00026096</b>	<b>0,00118053</b>
64	<b>Desmoglein-1</b>	<b>1,61519591</b>	<b>0,72436047</b>	<b>2,22982336</b>	<b>0,02575917</b>	<b>0,0627467</b>
65	Desmoplakin	<b>-2,17626603</b>	<b>0,76660605</b>	<b>-2,83883233</b>	<b>0,00452789</b>	<b>0,0153625</b>
66	Erythrocyte band 7 integral membrane protein	-1,13157411	0,43630447	-2,59354234	0,00949928	0,02911071
67	Junction plakoglobin	1,65139993	1,0496228	1,57332704	0,11564311	0,18941544
68	<b>Protein 4.1</b>	<b>2,14437657</b>	<b>1,10931219</b>	<b>1,93306861</b>	<b>0,05322775</b>	<b>0,10534658</b>
69	<b>Protein KIAA1199 homolog</b>	<b>4,61458018</b>	<b>1,20090167</b>	<b>3,84259618</b>	<b>0,00012174</b>	<b>0,00064251</b>
70	<b>Putative annexin A2-like protein</b>	<b>-0,29201401</b>	<b>0,69043948</b>	<b>-0,42293933</b>	<b>0,67233953</b>	<b>0,74270064</b>
71	Spectrin	0,84886528	0,82295828	1,03148033	0,30231563	0,40355987
72	<b>Spondin-1</b>	<b>-1,88376079</b>	<b>0,52179416</b>	<b>-3,61016076</b>	<b>0,00030601</b>	<b>0,0013214</b>
73	Tubulin	-0,39302565	0,39448588	-0,9962984	0,31910518	0,40966206
74	<b>Wiskott-Aldrich syndrome protein homolog 1</b>	<b>11,435648</b>	<b>0,90645082</b>	<b>12,6158505</b>	<b>1,73E-36</b>	<b>1,64E-34</b>
75	Adiponectin	0,82923492	0,4100444	2,02230518	0,04314483	0,09270028
76	<b>Alpha-enolase</b>	<b>1,97316773</b>	<b>1,19605742</b>	<b>1,64972658</b>	<b>0,09899887</b>	<b>0,17099805</b>
77	Carbonic anhydrase 2	-0,19271722	0,78511112	-0,2454649	0,80609649	<b>0,83238224</b>
78	<b>Glyceraldehyde-3-phosphate dehydrogenase</b>	<b>-0,37852073</b>	<b>0,4036966</b>	<b>-0,93763666</b>	<b>0,34843116</b>	<b>0,43553896</b>
79	Heat shock protein HSP 90-alpha	1,77345494		1,94891758	0,05130527	0,10370214

80	Hepatocyte growth factor activator	-0,35076027	<b>0,39039474</b>	-0,89847591	0,36893188	0,4551757
81	Histone H1.3	1,86684969	1,24987495	1,49362917	0,13527257	<b>0,21781177</b>
82	<b>Peptidyl-glycine alpha-amidating monooxygenase</b>	<b>5,34040354</b>	<b>1,12109582</b>	<b>4,76355674</b>	<b>1,90E-06</b>	<b>2,01E-05</b>
83	Peroxiredoxin-2	-0,22189826	0,65263098	-0,34000571	0,73385223	0,78332541
84	<b>Phosphatidylinositol-glycan-specific phospholipase D</b>	<b>-4,82467913</b>	<b>0,39886319</b>	<b>-12,0960751</b>	<b>1,11E-33</b>	<b>5,26E-32</b>
85	<b>Primary amine oxidase, liver isozyme</b>	<b>-2,64064747</b>	0,63308469	<b>-4,17108094</b>	<b>3,03E-05</b>	<b>0,00020571</b>
86	Proteasome subunit beta type-1	<b>-0,48204074</b>	<b>0,76505476</b>	-0,63007351	0,52864649	<b>0,62001749</b>
87	Protein disulfide-isomerase	1,18351155	0,48672432	2,431585	0,01503292	0,04200375
88	Protein eyes shut homolog	<b>-1,79468044</b>	<b>0,98754286</b>	-1,81731904	0,06916828	0,13141973
89	Putative trypsin-6	-0,5782074	0,43755694	-1,32144492	0,18635306	0,28573853
90	Pyruvate kinase isozymes M1/M2	0,2615701	<b>0,49454245</b>	0,52891333	<b>0,59686557</b>	<b>0,68315939</b>
91	Ribonuclease 4	-0,46713318	0,41289462	-1,13136174	0,25790287	0,36568317
92	<b>Transforming growth factor-beta-induced protein ig-h3</b>	<b>-0,11334282</b>	<b>1,15140109</b>	-0,09843904	0,92158368	<b>0,93138776</b>
93	Transthyretin	1,5187061	0,76473893	1,98591447	0,04704282	0,09715365
94	<b>Leukocyte cell-derived chemotaxin-2</b>	0,68345457	<b>1,46838381</b>	<b>0,46544682</b>	<b>0,64161151</b>	<b>0,71709522</b>
95	Neural cell adhesion molecule 1- $\Lambda$	2,8908326	1,02413442	2,82270817	0,00476199	0,01559962
96	<b>Protein AMBP</b>	<b>2,26083363</b>	<b>0,82530909</b>	<b>2,7393781</b>	<b>0,00615555</b>	<b>0,01949259</b>

<sup>A</sup> The logarithm (to basis 2) of the fold change

<sup>B</sup> Standard error estimate for the  $\log_2$  fold change

<sup>C</sup> p value for the statistical significance for the  $\log_2$  fold change

<sup>D</sup> p value adjusted for false discovery rate (FDR)

<sup>E</sup> Proteins in bold letters have a statistical significance for the  $\log_2$  fold change  $p > 0.01$

**10.6 Appendix 6. *B. melitensis* Δper/*B. melitensis* fold change statistics (Wald Test, and FDR adjusted p-values) for the 96 adsorbed serum proteins**

#	Protein	FC <sup>A</sup>	S.E. <sup>B</sup>	Wald	p-value <sup>C</sup>	FDR adjusted (p-value) <sup>D</sup>
1	Mannose-binding protein C <sup>E</sup>	-6,57558866	<b>1,04582725</b>	<b>-6,28745204</b>	<b>3,23E-10</b>	<b>1,78E-09</b>
2	<b>Conglutinin</b>	<b>-7,3562303</b>	<b>1,04302624</b>	<b>-7,05277586</b>	<b>1,75E-12</b>	<b>1,50E-11</b>
3	Complement C1q	6,53455344	0,83510648	7,82481463	5,08E-15	5,97E-14
4	<b>Complement C2</b>	<b>-6,90927864</b>	<b>0,44995133</b>	<b>-15,3556134</b>	<b>3,25E-53</b>	<b>3,05E-51</b>
5	Complement C4	2,30572565	0,57646294	3,9997812	6,34E-05	0,00020551
6	Complement factor B	-0,3298312	0,64827853	-0,50878007	0,61090639	0,6755906
7	Complement C3	0,43597283	0,3426093	1,2725073	0,20319293	0,27681356
8	<b>Complement C5</b>	<b>-3,15853291</b>	<b>0,37654157</b>	<b>-8,3882714</b>	<b>4,93E-17</b>	<b>7,73E-16</b>
9	Complement component C6	-2,59387807	0,35103192	-7,38929408	1,48E-13	1,54E-12
10	<b>Complement component C7</b>	<b>-2,95874724</b>	<b>0,30823179</b>	<b>-9,5990983</b>	<b>8,06E-22</b>	<b>1,90E-20</b>
11	Complement component C8	-1,99667933	0,55369571	-3,60609502	0,00031084	0,00091309
12	<b>Complement component C9</b>	<b>-3,32685785</b>	<b>0,47643235</b>	<b>-6,98285462</b>	<b>2,89E-12</b>	<b>2,27E-11</b>
13	Complement Factor H	1,49265592	<b>0,47870064</b>	3,11814061	0,00181996	<b>0,00438657</b>
14	<b>C4b-binding protein</b>	<b>-3,30332345</b>	<b>0,75951787</b>	<b>-4,34923732</b>	<b>1,37E-05</b>	<b>5,14E-05</b>
15	Vitronectin	2,33215657	0,65409591	3,56546577	0,00036321	0,00100417
16	<b>Clusterin</b>	<b>-3,11024569</b>	<b>0,47226746</b>	<b>-6,58577172</b>	<b>4,53E-11</b>	<b>3,27E-10</b>
17	Coagulation factor VIII	-0,35229517	0,37752631	<b>-0,93316721</b>	0,35073364	0,44552652
18	<b>Coagulation factor V</b>	<b>3,90341733</b>	<b>0,39818092</b>	<b>9,80312512</b>	<b>1,09E-22</b>	<b>3,42E-21</b>
19	Prothrombin	2,06643317	0,59128803	3,49479958	0,00047442	0,00127415
20	Thrombospondin-1	-1,22317775	0,81907863	-1,49335814	0,13534346	0,19878571
21	Factor XIIa inhibitor	-2,57794773	1,20849516	-2,1331883	<b>0,03290928</b>	0,05624496
22	Plasminogen	0,02618617	1,3393361	0,01955161	<b>0,98440107</b>	0,98440107
23	Platelet factor 4	-2,99004477	0,64014883	-4,67085878	3,00E-06	1,23E-05
24	Antithrombin-III	-0,30318346	<b>0,56759418</b>	<b>-0,53415533</b>	<b>0,59323407</b>	<b>0,67185545</b>
25	Beta-2-glycoprotein 1	1,2366803	0,75670688	1,63429239	0,10219747	0,15748463

26	<b>Fibronectin</b>	0,1091153	1,33815331	0,08154171	0,93501116	0,94506504
27	Hemoglobin	2,41512604	0,64293942	3,75638196	0,00017239	0,00052272
28	<b>Ceruloplasmin</b>	2,03794056	0,91173547	2,2352323	0,0254021	0,0457851
29	<b>Haptoglobin</b>	-2,6970125	0,91561379	-2,94557873	0,00322351	0,00704674
30	<b>Hemopexin</b>	3,57245904	0,7727248	4,62319706	3,78E-06	1,48E-05
31	Lactotransferrin	3,74064172	1,4328715	2,6105912	NA	NA
32	<b>Apolipoprotein A-I</b>	-0,47637691	0,85893977	-0,55461038	0,57916119	0,66391648
33	Apolipoprotein D	1,12344189	0,80086853	1,40277943	0,16068262	0,23098095
34	<b>Apolipoprotein E</b>	2,41031032	0,43274592	5,56980489	2,55E-08	1,33E-07
35	Alpha-1-antiproteinase	1,4715454	0,92694459	1,58752251	0,11239435	0,16928262
36	<b>Alpha-1B-glycoprotein</b>	-3,20496987	0,49022308	-6,53777838	6,24E-11	4,19E-10
37	Alpha-2-III-glycoprotein	0,05166204	0,56172166	0,09197089	0,92672116	0,94506504
38	<b>Alpha-2-macroglobulin</b>	-2,63071082	0,8667306	-3,03521165	0,00240367	0,00537964
39	Inter-alpha-trypsin inhibitor	7,3943713	1,40503779	5,26275616	NA	NA
40	<b>Metalloproteinase inhibitor 3</b>	10,59676	1,62881584	6,50580605	7,73E-11	4,84E-10
41	Plasma kallikrein	9,54632332	0,82161651	11,6189526	3,30E-31	1,55E-29
42	<b>Plasma serine protease inhibitor</b>	2,16249943	0,52240106	4,13953877	3,48E-05	0,00011683
43	Pregnancy zone protein	1,81100343	0,81247951	2,22898351	0,025815	0,0457851
44	<b>Serpin A3-2</b>	-3,0175842	0,98062647	-3,07720043	0,00208955	0,00490232
45	<b>Trypsin</b>	-4,94421553	0,59984753	-8,2424538	1,69E-16	2,27E-15
46	<b>Catalase</b>	1,91450885	0,53221793	3,59722728	0,00032163	0,00091615
47	Protein S100-A8	-1,08567296	1,05055795	-1,0334251	0,301405	0,39350098
48	<b>Cathelicidin</b>	-1,87415308	0,38433092	-4,87640467	1,08E-06	4,84E-06
49	Putative lysozyme C-2	0,89881873	1,18631276	0,75765747	0,44865606	0,53876046
50	<b>Lysozyme C, tracheal isozyme</b>	1,38240797	0,98900011	1,39778343	0,16217811	0,23098095
51	Myeloperoxidase	0,31084275	0,93250389	0,33334204	0,73887611	0,78038601
52	<b>Immunoglobulin</b>	1,51950981	0,67605089	2,24762639	0,02460002	0,04534122
53	<b>Polymeric immunoglobulin receptor</b>	-9,27399752	1,73626192	-5,34135858	9,23E-08	4,34E-07

54	Lipopolysaccharide-binding protein	0,33404254	1,17850294	0,2834465	0,77683459	0,81136057
55	Peptidoglycan recognition protein 1	-1,00538787	0,96414572	-1,04277585	0,29705212	0,39328027
56	Serum albumin	1,40244758	0,61144541	2,29365952	0,02181006	0,04148457
57	Beta-casein	-4,69521276	1,18533365	-3,96108956	7,46E-05	0,00023377
58	Filaggrin-2	-3,17214501	1,28755852	-2,46368997	0,0137515	0,02810089
59	Hornerin	0,41660683	0,58763459	0,70895559	0,47835204	0,56206364
60	Ankyrin-1	2,39401549	0,95488177	2,5071329	0,01217149	0,0254249
61	Beta-adducin	0,57693539	0,68321404	0,84444311	0,39842184	0,49278491
62	Coiled-coil domain-containing protein 125	-1,4711604	0,71160889	-2,06737216	0,0386991	0,06271923
63	Connective tissue growth factor	1,50042886	1,08798267	1,37909261	0,1678662	0,23551377
64	Desmoglein-1	6,17269532	1,26968794	4,8615846	1,16E-06	4,98E-06
65	Desmoplakin	-0,42760473	1,11441237	-0,38370422	0,70119768	0,75761589
66	Erythrocyte band 7 integral membrane protein	3,1491075	1,00952278	3,11940212	0,00181218	0,00438657
67	Junction plakoglobin	2,91623837	0,68917741	4,23147701	2,32E-05	8,39E-05
68	Protein 4.1	-1,65348464	0,62374125	-2,65091436	0,00802742	0,01714949
69	Protein KIAA1199 homolog	0,51046202	1,45649776	0,35047223	0,72598433	0,77548326
70	Putative annexin A2-like protein	-1,39993338	0,43845438	-3,19288263	0,0014086	0,00357861
71	Spectrin	3,39747444	0,53690648	6,32787007	2,49E-10	1,46E-09
72	Spondin-1	-1,94478522	0,94596579	-2,05587267	0,03979479	0,06340187
73	Tubulin	-0,4779721	0,52993658	-0,90194209	0,36708763	0,46008317
74	Wiskott-Aldrich syndrome protein homolog 1	-1,93689179	2,4928235	-0,77698714	0,43716636	0,53368361
75	Adiponectin	1,24907247	1,66371067	0,75077506	0,45278804	0,53876046
76	Alpha-enolase	1,51658364	1,32171655	1,14743485	0,25120194	0,33732832
77	Carbonic anhydrase 2	1,6334866	0,71203538	2,29410874	0,02178425	0,04148457
78	Glyceraldehyde-3-phosphate dehydrogenase	-0,15221608	1,27668248	-0,11922783	0,90509486	0,93493315



79	<b>Heat shock protein HSP 90-alpha</b>	<b>4.44511096</b>	<b>1.44776469</b>	<b>3.07032697</b>	<b>0.00213825</b>	<b>0.00490232</b>
80	Hepatocyte growth factor activator	2.55367583	1.06313194	2.40203095	0.01630433	0.03260866
81	Histone H1.3	0.80133032	1.5314625	0.52324514	0.60080367	0.67232792
82	<b>Peptidyl-glycine alpha-amidating monooxygenase</b>	<b>4.83202609</b>	<b>1.1603725</b>	<b>4.16420253</b>	<b>3.12E-05</b>	<b>0.00010878</b>
83	Peroxiredoxin-2	3.60223334	1.57355992	2.28922541	0.02206626	0.04148457
84	<b>Phosphatidylinositol-glycan-specific phospholipase D</b>	<b>-5.75793443</b>	<b>0.63985416</b>	<b>-8.99882313</b>	<b>2.28E-19</b>	<b>4.29E-18</b>
85	Primary amine oxidase, liver isozyme	-1.97705251	1.13076962	-1.74841318	0.08039251	0.12594826
86	Proteasome subunit beta type-1	0.76493311	0.76396217	1.00127093	0.31669584	0.40780013
87	Protein disulfide-isomerase	-2.65776241	1.23778695	-2.14718891	0.03177825	0.05531769
88	Protein eyes shut homolog	0.49149041	0.99135547	0.49577616	0.62005235	0.67773163
89	Putative trypsin-6	1.87962653	0.90256942	2.08252849	0.03729422	0.06150275
90	Pyruvate kinase isozymes M1/M2	-1.81055048	1.42054284	-1.27454832	0.20246916	0.27681356
91	Ribonuclease 4	-2.91993068	0.54365109	-5.37096443	7.83E-08	3.87E-07
92	Transforming growth factor-beta-induced protein ig-l3	0.6263368	0.98927625	0.63312628	0.52665118	0.61117544
93	Transthyretin	2.84107646	0.8173394	3.47600575	0.00050894	0.0013289
94	Leukocyte cell-derived chemotaxin-2	2.02758013	1.28096694	1.58285126	0.11345537	0.16928262
95	Neural cell adhesion molecule 1-A	4.45067655	0.60976379	7.29901745	2.90E-13	2.72E-12
96	Protein AMBP	-2.46263014	1.1802305	-2.08656711	0.03692728	0.06150275

<sup>A</sup> The logarithm (to basis 2) of the fold change

<sup>B</sup> Standard error estimate for the log<sub>2</sub> fold change

<sup>C</sup> p value for the statistical significance for the log<sub>2</sub> fold change

<sup>D</sup> p value adjusted for false discovery rate (FDR)

<sup>E</sup> Proteins in bold letters have a statistical significance for the log<sub>2</sub> fold change p>0.01



# *Brucella canis* Is an Intracellular Pathogen That Induces a Lower Proinflammatory Response than Smooth Zoonotic Counterparts

Carlos Chacón-Díaz,<sup>a</sup> Pamela Altamirano-Silva,<sup>a</sup> Gabriela González-Espinoza,<sup>a</sup> María-Concepción Medina,<sup>b</sup> Alejandro Alfaro-Alarcón,<sup>c</sup> Laura Bouza-Mora,<sup>d</sup> César Jiménez-Rojas,<sup>b</sup> Melissa Wong,<sup>a</sup> Elías Barquero-Calvo,<sup>a,b</sup> Norman Rojas,<sup>a</sup> Caterina Guzmán-Verri,<sup>a,b</sup> Edgardo Moreno,<sup>b,\*</sup> Esteban Chaves-Olarte<sup>a,b</sup>

Centro de Investigación en Enfermedades Tropicales, Facultad de Microbiología, Universidad de Costa Rica, San José, Costa Rica<sup>a</sup>; Programa de Investigación en Enfermedades Tropicales, Escuela de Medicina Veterinaria, Universidad Nacional, Heredia, Costa Rica<sup>b</sup>; Departamento de Patología, Escuela de Medicina Veterinaria, Universidad Nacional, Heredia, Costa Rica<sup>c</sup>; Laboratorio de Análisis Clínicos, Escuela de Medicina Veterinaria, Universidad Nacional, Heredia, Costa Rica<sup>d</sup>; Instituto Clodomiro Picado, Facultad de Microbiología, Universidad de Costa Rica, San José, Costa Rica<sup>e</sup>

Canine brucellosis caused by *Brucella canis* is a disease of dogs and a zoonotic risk. *B. canis* harbors most of the virulence determinants defined for the genus, but its pathogenic strategy remains unclear since it has not been demonstrated that this natural rough bacterium is an intracellular pathogen. Studies of *B. canis* outbreaks in kennel facilities indicated that infected dogs displaying clinical signs did not present hematological alterations. A virulent *B. canis* strain isolated from those outbreaks readily replicated in different organs of mice for a protracted period. However, the levels of tumor necrosis factor alpha, interleukin-6 (IL-6), and IL-12 in serum were close to background levels. Furthermore, *B. canis* induced lower levels of gamma interferon, less inflammation of the spleen, and a reduced number of granulomas in the liver in mice than did *B. abortus*. When the interaction of *B. canis* with cells was studied *ex vivo*, two patterns were observed, a predominant scattered cell-associated pattern of nonviable bacteria and an infrequent intracellular replicative pattern of viable bacteria in a perinuclear location. The second pattern, responsible for the increase in intracellular multiplication, was dependent on the type IV secretion system VirB and was seen only if the inoculum used for cell infections was in early exponential phase. Intracellular replicative *B. canis* followed an intracellular trafficking route undistinguishable from that of *B. abortus*. Although *B. canis* induces a lower proinflammatory response and has a stealthier replication cycle, it still displays the pathogenic properties of the genus and the ability to persist in infected organs based on the ability to multiply intracellularly.

**B**rucellosis is a disease of animals and humans caused by members of the genus *Brucella*. Zoonotic species such as *Brucella melitensis*, *Brucella abortus*, and *Brucella suis* are facultative extracellular-intracellular stealthy pathogens that are able to overcome innate immunity at early times of infection (1–3) and at specific stages of adaptive immunity (4, 5). In addition to influencing the immune response, these *Brucella* species are able to circumvent the killing action of professional and nonprofessional phagocytes, transit within phagocytic vacuoles, and replicate extensively within the endoplasmic reticulum of cells (6). These properties allow the bacterium to spread throughout the reticuloendothelial system and promote chronic infection (3).

There are other *Brucella* species that are also relevant pathogens; however, their infective strategies remain unclear and are not in tune with the solid results accepted for the previously mentioned zoonotic brucellae. Among these are *Brucella canis*, the etiological agent of brucellosis in dogs and a zoonotic pathogen (7). This pathogen induces a subclinical infection that may remain undiagnosed for protracted periods (8–10). *B. canis* invades the conjunctiva or the oronasal system or penetrates through the venereal route. Then it is distributed to different organs of the reticuloendothelial system (11). The main clinical consequence of canine brucellosis is abortion in females and epididymitis and prostatitis in male dogs (12, 13). In stud males and bitches, the disease also causes sterility, a factor that causes significant economic losses in commercial kennels. *B. canis* is transmitted through contaminated aborted fetuses, milk, urine, vaginal secretions, and semen.

*B. canis* is highly specific to dogs and has not been observed in

other animals. Nevertheless, the bacterium has the ability to infect humans. Because of the low number of reported human cases, it has been proposed that the bacteria are less infective for humans than are the classical species *B. melitensis*, *B. abortus*, and *B. suis* (3). However, this may be a misconception. In the last decade, there has been a rise in the detection of human infections due to *B. canis* (8, 9). This is due to awareness of the disease in areas where it is endemic and improved diagnoses, as well as increased prevalence of the bacterium in kennel facilities and roaming dogs (10, 14, 15). Therefore, it may be that *B. canis* displays an infectivity similar to that of the other zoonotic brucellae but has the potential to produce no symptoms for prolonged periods (16, 17) by using a stealth strategy.

Histological examination of a dog's infected placenta has sug-

Received 11 August 2015. Returned for modification 2 September 2015.

Accepted 29 September 2015.

Accepted manuscript posted online 5 October 2015.

Citation Chacón-Díaz C, Altamirano-Silva P, González-Espinoza G, Medina M-C, Alfaro-Alarcón A, Bouza-Mora L, Jiménez-Rojas C, Wong M, Barquero-Calvo E, Rojas N, Guzmán-Verri C, Moreno E, Chaves-Olarte E. 2015. *Brucella canis* is an intracellular pathogen that induces a lower proinflammatory response than smooth zoonotic counterparts. *Infect Immun* 83:4861–4870. doi:10.1128/IAI.00995-15.

Editor: C. R. Roy

Address correspondence to Edgardo Moreno, emoreno@racsa.co.cr, or Esteban Chaves-Olarte, esteban.chaves@ucr.ac.cr.

Copyright © 2015, American Society for Microbiology. All Rights Reserved.

gested that *B. canis* replicates intracellularly (18). In addition, large numbers of *B. canis* bacteria attach to the cell surface; however, studies of cells have failed to demonstrate unambiguously that this bacterium actually replicates intracellularly (19–25). This is significant, since *B. canis* harbors most of the virulence determinants defined for the genus, and the genome of this bacterium is 98 to 99% identical to the genomes of other virulent *Brucella* species. Noticeable differences in relation to other zoonotic *Brucella* species are the structure and biological characteristics of the *B. canis* cell envelope (21–29), features that may influence its virulent behavior.

On the basis of clinical features of natural canine infections, as well as murine experimental brucellosis and *ex vivo* culture models, we propose that *B. canis* uses a stealthier infective strategy than other virulent brucellae. This investigation contributes to the dissection of the pathogenic strategies used by the species of the genus *Brucella* and the understanding of their relative virulence and host specificity.

## MATERIALS AND METHODS

**Ethics statement.** Dogs were voluntarily taken by their owners to the Veterinary Hospital of the Veterinary School of the National University of Costa Rica for diagnosis. The owners of the dogs signed a written consent form and were carefully informed regarding all of the medical and diagnostic procedures and informed of the results. Protocols for the use of samples were revised and approved by the Comité Institucional para el Cuido y Uso de los Animales of the Universidad Nacional de Costa Rica (approval SIA 0434-14) and were in agreement with the corresponding law, Ley de Bienestar de los Animales, of Costa Rica (law 7451 on animal welfare).

Protocols for experimentation with mice were revised and approved by the Comité Institucional para el Cuido y Uso de los Animales of the Universidad de Costa Rica (CICUA-47-12) and were in agreement with the corresponding law, Ley de Bienestar de los Animales, of Costa Rica (law 7451 on animal welfare). Mice were housed in the animal building of the Veterinary School, Universidad Nacional, Costa Rica. All of the animals were kept in cages with water and food *ad libitum* under biosafety containment conditions previous to and during the experiment.

**Hematological, serological, and clinical chemistry analyses of blood samples.** Several cases of epididymitis and abortions were detected in a small number of commercial kennels of golden/Labrador retriever and Pomeranian dogs in Heredia, Costa Rica, between October 2009 and February 2013. Blood and serum samples were recovered from the affected dogs. Hematological, serological, and clinical chemistry tests were performed as described elsewhere (30).

**Bacterial strains and constructs.** Seventeen isolates of Gram-negative bacteria compatible with *B. canis* were isolated from seminal fluid of stud males, from vaginal swabs of bitches, or from aborted fetuses between 2009 and 2013. The bacterial strains were characterized as *B. canis* by bacteriological analysis (3), molecular Bruce-ladder multiplex PCR assay, and multiplex single nucleotide polymorphism (SNP) detection as reported previously (31, 32). One representative *B. canis* strain named beanCR12 (here *B. canis*) isolated from a vaginal swab of a Pomeranian bitch after abortion was chosen for biological studies. The results of bacteriological analysis (33), Bruce-ladder multiplex PCR assay (31), multiplex SNP detection (32), and multilocus variable-number tandem-repeat analysis based on 16 loci (MLVA16) (34) were consistent with the *B. canis* genotype.

*Brucella* strains were grown and maintained as described previously (1). Strains were stored at  $-80^{\circ}\text{C}$  in 20% glycerol brain heart infusion. Bacteria were routinely grown in standard tryptic soy broth (TSB) either plain or supplemented with 100  $\mu\text{g}/\text{ml}$  ampicillin or 50  $\mu\text{g}/\text{ml}$  kanamycin (Km).

Plasmid and chromosomal DNA samples were extracted with the

QIAprep spin Miniprep and DNeasy blood and tissue kit (Qiagen GmbH, Hilden, Germany). DNA was purified from agarose gels with the QIAquick gel extraction kit (Qiagen GmbH, Hilden, Germany). Primers were synthesized by Life Technologies Inc. DNA sequencing of fragments was done by Macrogen Inc. (Seoul, Republic of Korea).

A *B. canis virB10* mutant ( $\Delta virB10$ ) was constructed as reported elsewhere (35). Briefly, an in-frame deletion was generated by PCR overlap with genomic DNA of *B. canis* as the template. Primers were designed by using the available sequence corresponding to reference strain *B. canis* ATCC 23365. The primers used to generate fragment 1 were virB10-F1 (5'-GACAAGTCGGAAAGCATCGT-3') and virB10-R2 (5'-TGAAGCC CACGACAAAGAGAAA-3'). Those used to generate fragment 2 were virB10-F3 (5'-TTTCTCTTTGTCGTGGGCTTCAGCTATGCAACCCGAAGGTC-3') and virB10-R4 (5'-CTCGCTCGCAGAACACTTC-3'). Both fragments were ligated by PCR overlap with nucleotides virB10-F1 and virB10-R4. The resulting deletion allele was cloned into plasmid pCR2.1 (Life Technologies) and subcloned into the BamHI-XbaI site of suicide plasmid pJQKm. Plasmid pJQKm, containing the deletion allele, was introduced into *B. canis* by conjugation. Colonies corresponding to the integration of the suicide vector into the chromosome were selected with polymyxin B (PxB) and Km resistance; excision of the suicide plasmid led to the construction of the mutant by allelic exchange, and bacteria were selected by PxB and sucrose resistance and Km sensitivity. The resulting colonies were screened with primers virB10-F1 and virB10-R4. Mutant colonies generated a 694-bp fragment, and the parental strain generated a 1,522-bp fragment. The mutation generated resulted in the loss of 71% of the *virB10* open reading frame.

*B. canis* harboring plasmid pBBR-2-GFP with resistance to Kan and constitutively expressing green fluorescent protein (GFP) (*B. canis*-GFP) was constructed and selected as reported before (36). The expression of GFP was evaluated in bacterial cultures under UV illumination and by fluorescence microscopy as described previously (36). *B. canis* containing a plasmid coding for GFP under the control of the tetracycline-inducible *tetA* promoter (*B. canis*-iGFP) was constructed through conjugation of plasmid pJc45 as described elsewhere (37). With the exception of green fluorescence, the *B. canis*-GFP and *B. canis*-iGFP strains kept the same *in vitro* and *ex vivo* growth and bacteriological characteristics as the parental strain (data not shown).

**Virulence assays with mice.** Female BALB/c mice (18 to 24 g) were intraperitoneally (i.p.) inoculated with the indicated inoculum of either *B. canis* beanCR12 or the *B. canis* beanCR12  $\Delta virB10$  mutant, and bacterial counts in the spleen, inguinal lymph nodes, liver, and bone marrow were determined at various times as described elsewhere (38, 39). In some experiments, mice were i.p. infected with the indicated inoculum of *B. abortus* 2308. Levels of infection were expressed as mean values and standard deviations (SDs) ( $n = 5$ ) of the log number of CFU per organ at each time point selected. For histopathological studies, organs from *Brucella*-infected mice were fixed in 10% neutral buffered formalin, processed, and stained with hematoxylin and eosin as described elsewhere (40).

**Gentamicin protection assay.** Cell infections for estimation of bacterial invasion and replication were performed as described previously (41). Briefly, HeLa cells or Raw 264.7 macrophages were grown to subconfluence in 24-well tissue culture plates. The *B. canis* strains used for cell infections were grown in 20 ml of TSB in glass flasks at 200 rpm as described elsewhere. Flasks were inoculated with  $5 \times 10^9$  bacteria (42). At different time points on the growth curve, aliquots were used for cell infection. Bacterial inocula taken out at 5, 8, and 12 h correspond to exponential-phase conditions (a, b, and c, respectively), while inocula taken out at 24 and 30 h correspond to stationary-phase conditions (d and e, respectively) (see Fig. 5A). Alternatively, to induce low-aeration conditions, *B. canis* strains were grown in 10 ml of TSB in 50-ml conical plastic tubes at 120 rpm. The multiplicity of infection (MOI) used was adjusted by diluting the bacteria in Eagle's minimal essential medium. Cells were infected with an MOI of either 100 CFU/Raw 264.7 macrophage or 500 CFU/HeLa cell. All of the inocula used to infect cells were serially diluted

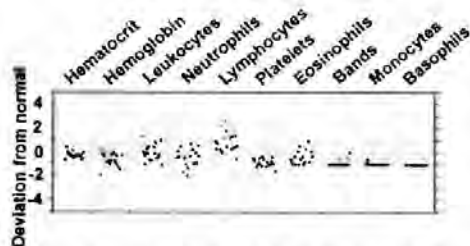


FIG 1 Hematological profiles of infected dogs. The blood cell counts of 17 *B. canis*-infected dogs in a canine brucellosis outbreak in Costa Rica are shown. The gray area demarcates the normal value range of each cell type. The dogs are represented by circles numbered 1 to 17, with number 1 being the farthest to the left in each panel.

and plated in parallel in tryptic soy agar (TSA) to confirm that they contained the same amount of viable bacteria. Plates containing the infected cells were centrifuged at 1,600 rpm at 4°C, incubated for 45 min at 37°C under 5% CO<sub>2</sub>, and washed with phosphate-buffered saline. Extracellular bacteria were eliminated by treatment with gentamicin at 100 µg/ml for 1 h, and cells were incubated for the times indicated in the presence of gentamicin at 5 µg/ml. After incubation, cells were lysed by treatment with 0.1% Triton X-100 for 10 min. Aliquots were serially diluted and plated in TSA (Oxoid) and incubated at 37°C for 3 days for determination of CFU counts.

**Immunological assays.** Cytokine quantitation in the plasma of *Brucella*-infected mice was performed by enzyme-linked immunosorbent assay (eBioscience) according to the manufacturer's instructions. For epifluorescence and confocal microscopy, cells ( $5 \times 10^5$ ) were grown on 12-mm glass slides and inoculated with *B. canis* strains as described above. GFP expression in *B. canis* iGFP was induced by the addition of 200 nM anhydrotetracycline (ATc; Sigma-Aldrich) prior to immunofluorescence staining as previously described (37). The antibodies used to localize different intracellular compartments were LAMP1 mouse monoclonal antibody H4A3 (Abcam) and rabbit anti-calnexin polyclonal antibody ab75801 (Abcam). Mouse polyclonal antibodies to *B. canis* were used to detect extracellular *Brucella* as reported elsewhere (43). An Alexa Fluor 488-conjugated goat anti-mouse antibody and an Alexa Fluor 594-conjugated anti-mouse antibody (Life Technologies) were used as developing antibodies. Confocal analysis was performed with an Olympus U-TB190 (100×) under oil immersion. Confocal images of 1,024 by 1,024 pixels were acquired with the FV10-AV ver.03.01 software (Olympus) and assembled with Adobe Photoshop CS3 (Adobe Systems, San Jose, CA).

## RESULTS

***B. canis*-infected dogs fail to show signs of sepsis or clinical or hematological alterations.** In the course of our clinical studies of infected dogs from which *B. canis* was isolated, we did not detect proinflammatory signs that are characteristic of other bacterial sepsis. Although significant quantities of antibodies against *Brucella* proteins were detected in the sera of 17 infected dogs, the biochemical parameters, including protein concentration, coagulation time, C-reactive protein, and liver and renal functions were within the normal ranges in all of the dogs. Likewise, the blood profiles of the 17 dogs from which *B. canis* strains were isolated were mostly normal, with a few exceptions (Fig. 1). One dog showed mild leukocytosis, while three dogs demonstrated mild neutropenia, probably as a result of lymphocytosis (dogs 7, 11, and 12); 8 of the 17 dogs showed mild lymphocytosis. At the time of sampling, none of the animals had signs of fatigue, displayed an abnormal temperature, or lost weight. These results are consistent with the stealth strategy used by *Brucella* organisms to evade the

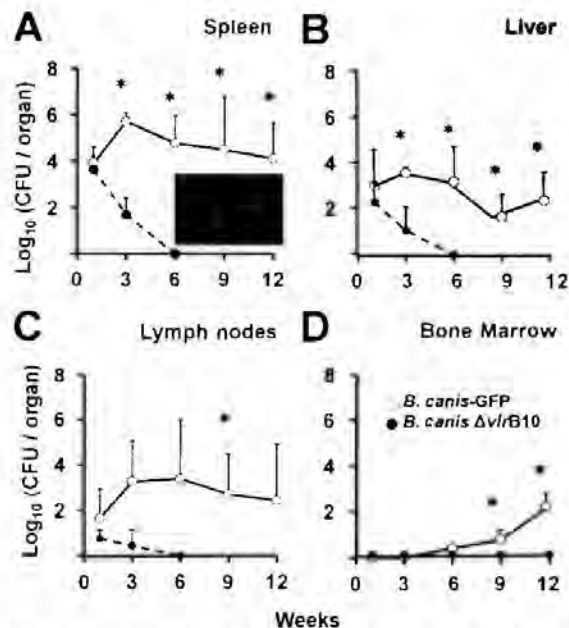
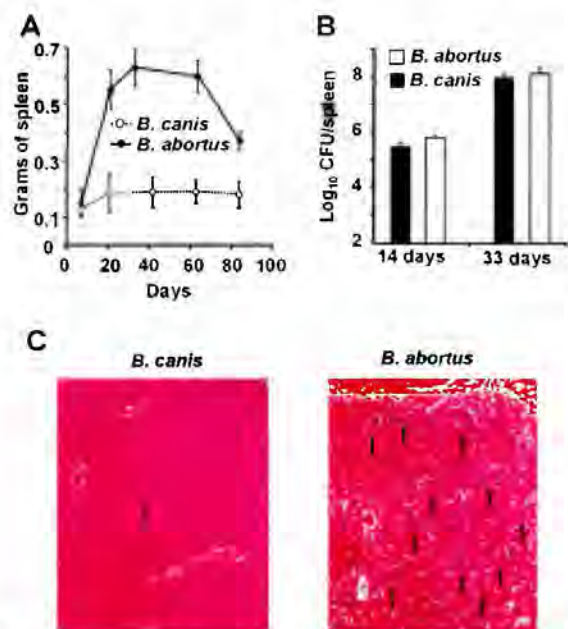


FIG 2 *B. canis* persists and replicates within cells of the reticuloendothelial system. Groups of 30 mice were inoculated i.p. with  $10^7$  CFU of *B. canis*-GFP or *B. canis*  $\Delta$ virB10-GFP. Groups of five mice were killed at the times indicated to determine the CFU counts in the spleen (A), liver (B), lymph nodes (C), and bone marrow (D). Cells from a spleen infected with *B. canis*-GFP for 21 days were visualized by epifluorescence (inset in panel A). Note the large amounts of *B. canis*-GFP within phagocytic cells.  $\Delta$ virB10-GFP was not observed within resident cells of the spleen. Error bars represent SDs. Data are representative of at least three independent experiments. Statistical significance was calculated by Student *t* test. \*,  $P < 0.01$ .

innate immune response and in agreement with the absence of endotoxemia symptoms in *Brucella* infections (1). Following this, we decided to explore the outcome of *B. canis* infection in the mouse model and in cells.

***B. canis* persists and replicates in the reticuloendothelial system of mice, inducing low proinflammatory responses.** First, we determined the virulence of the *B. canis* strain in groups of five mice inoculated i.p. with  $10^7$  CFU of *B. canis*-GFP. As expected, the spleen replication curve profile achieved by *B. canis*-GFP was consistent with previous reports (44) (Fig. 2A). Since very little is known regarding organ colonization by *B. canis*, we decided to study the presence of this bacterium in the liver, lymph nodes, and bone marrow (Fig. 2B to D). The replication of *B. canis* in the target organs was somewhat lower than that attained by smooth brucellae and followed a different time course, with a maximal load reached at 3 weeks instead of 1 week (45). However, bacterial loads were maintained and persisted for a protracted period of time in all of the organs tested (Fig. 2). Moreover, the *B. canis* CFU counts in bone marrow increased steadily, coinciding with the persistence and chronicity of the infection (Fig. 2D). Examination of spleen cells from infected mice by immunofluorescence revealed the presence of *B. canis* inside phagocytes, demonstrating the intracellular replication of this bacterium *in vivo* (Fig. 2A, inset). In agreement with a previous report (44), the *B. canis* *virB10* mutant was already rapidly eliminated from all organs at 6 weeks postinfection (p.i.) and was not recovered from bone marrow or observed inside phagocytic cells (Fig. 2).

Although *B. canis* readily replicates inside phagocytic cells of



**FIG 3** *B. canis* induces a lower proinflammatory response than *B. abortus*. Groups of 30 mice were inoculated i.p. with  $10^7$  CFU of *B. canis*-GFP or  $10^6$  CFU of *B. abortus* 2308. Groups of five mice were killed at various times to determine the spleen weight during 12 weeks of infection (A) and bacterial loads at 14 and 33 days p.i. (B). (C) Histological examination of the liver at 2 weeks p.i. with *B. canis* or *B. abortus*. Note that although the *B. canis* and *B. abortus* loads are similar (not statistically significantly different) at 2 weeks p.i., the granulomas (indicated by arrows) are more prominent in the *B. abortus*-infected liver than in the *B. canis*-infected liver. Error bars represent SDs. Data are representative of at least three independent experiments. In panel A, all of the values after 20 days are statistically significantly different ( $P < 0.001$ ).

the spleen, the bacterium barely induced swelling of this organ (Fig. 3A), in contrast to the splenomegaly induced by the same bacterial load of *B. abortus* (Fig. 3B). Histological examination of the liver demonstrated that the number of granulomas induced by *B. canis* infection was considerably lower than that observed in mice infected with *B. abortus* (Fig. 3C). Likewise, histological examination of the spleens of *B. canis*-infected mice also revealed a general milder cellular inflammation than that induced by virulent *B. abortus* (data not shown). In general, the tumor necrosis factor alpha (TNF- $\alpha$ ), interleukin-6 (IL-6), and IL-12 cytokine levels of mice infected with *B. canis* after 2 and 3 weeks were low and resembled those induced by *B. abortus* (Fig. 4). An important difference was the level of gamma interferon (IFN- $\gamma$ ), which was rather low in *B. canis* infections, mainly at 2 weeks p.i. (Fig. 4). This is relevant since IFN- $\gamma$  has been described as the central cytokine during establishment of the adaptive immune response in brucellosis (46). These results demonstrate that *B. canis* induces a lower proinflammatory response in mice than other zoonotic brucellae do (45).

**Growth phase state determines the ability of *B. canis* to achieve intracellular replication.** Previous works have failed to demonstrate *B. canis* replication *ex vivo* in a variety of cell lines (19–25). We hypothesized that the physiological state of the inoculum would have an impact on the ability of *B. canis* to achieve intracellular replication. To test this hypothesis, we grew the bacteria for 22 h under two different conditions, (i) in 125-ml Erlenmeyer flasks containing 20 ml of TSB at 200 rpm (high aeration)

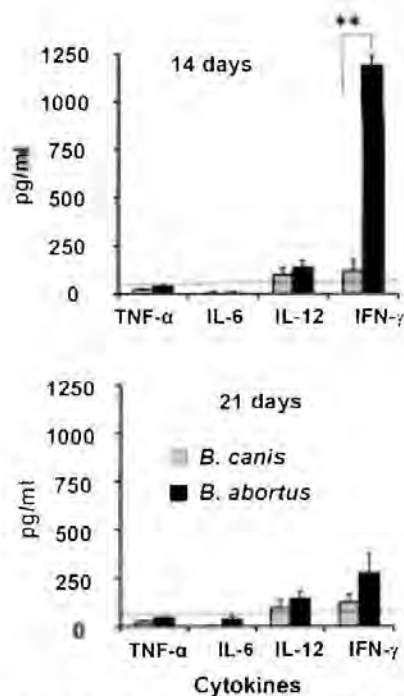


**FIG 4** *B. canis* induces a lower cytokine response than *B. abortus*. Groups of 10 mice were inoculated i.p. with  $10^7$  CFU of *B. canis*-GFP or  $10^6$  CFU of *B. abortus* 2308. Groups of five mice were killed and bled after 2 and 3 weeks, respectively, to determine serum cytokine levels. Note the small amount of IFN- $\gamma$  induced after 2 weeks by *B. canis* infection in comparison to that induced by *B. abortus* infection. The dashed lines represent the average background value (SD, <10%). Error bars represent SDs. Data are representative of at least three independent experiments. Statistical significance was calculated by Student *t* test. \*\*,  $P < 0.001$ .

and (ii) in 50-ml conical tubes containing 10 ml of TSB at 120 rpm (low aeration). The inoculum grown under the high-aeration conditions achieved a high bacterial density and was in late exponential phase at the time of cell infection, whereas the inoculum grown under low-aeration conditions achieved a low bacterial density and was in early exponential phase (Fig. 5A). Both inocula were used at the same MOI to infect cells, and their ability to multiply intracellularly was monitored by a gentamicin protection assay. The inoculum prepared under high-aeration conditions was rapidly cleared from cells, with no CFU being recoverable at 48 h (Fig. 5B). On the contrary, the inoculum prepared under low-aeration conditions displayed a curve compatible with intracellular multiplication, with a 10-fold increase from 24 to 48 h (Fig. 5B). These results indicate that the bacterial state on the growth curve influences the ability of *B. canis* to achieve intracellular replication.

To further investigate the permissive replicating conditions of the bacteria, we prepared cell infection inocula taken at different points on the growth curve (Fig. 6A) and then evaluated their intracellular replication competence. In Raw 264.7 macrophages, unambiguous intracellular replication was achieved when the *B. canis* inoculum was at some point of the exponential phase (a, b, c), whereas rapid intracellular clearance was detected when the inoculum was in the stationary phase (Fig. 6B). In epithelial HeLa cells, intracellular replication was achieved only when early-exponential-phase inocula (a, b) were used. Bacteria in the mid-expo-

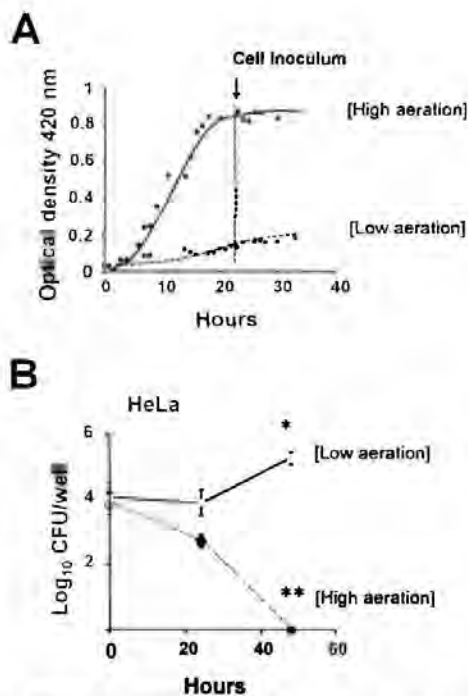


**FIG 5** Modulation of the aeration conditions in the bacterial inoculum allows intracellular replication of *B. canis*. (A) *B. canis* cells ( $5 \times 10^9$  CFU) were inoculated and grown for 30 h under high-aeration conditions (20 ml of TSB in 125-ml glass Erlenmeyer flasks, 37°C, 200 rpm) and low-aeration conditions (10 ml of TSB in 50-ml plastic tubes, 37°C, 120 rpm). Aliquots were taken at different times, and the optical densities at 420 nm were measured to determine the growth curves. (B) *B. canis* grown under the conditions indicated in panel A (dashed line) for 22 h was used to prepare the bacterial inoculum. HeLa cells were infected at an MOI of 500 in a gentamicin protection assay. After the incubation times indicated, CFU counts were determined. Error bars represent SDs. Data are representative of at least three independent experiments. Statistical significance was calculated by one-way analysis of variance. *P* values of  $<0.05$  (\*) and  $<0.01$  (\*\*) in relation to the corresponding  $T_0$  value of each bacterial condition are indicated.

nential and stationary phases did not multiply intracellularly (Fig. 6C). The *B. canis* *virB10* mutant was unable to achieve intracellular multiplication in either cell line under conditions that generate competent replicating *B. canis* (Fig. 7), strengthening the conclusion that we were indeed monitoring intracellular replication.

***B. canis* displays two different cell-associated bacterial patterns.** Once the culture conditions for generating infective *B. canis* were established, we explored the interaction of *B. canis*-GFP with epithelial cells. Two types of cell-associated patterns were observed; the first one corresponded to scattered cell-associated bacteria (Fig. 8A, a to c). This was the predominant pattern observed in the majority of the infected cells at 24 and 48 h p.i. The second pattern corresponded to a phenotype compatible with intracellular replicative bacteria and was characterized by a massive presence of *B. canis*-GFP at a perinuclear location (Fig. 8A, d to f). This pattern was observed in an extremely small proportion of the cells.

The extracellular or intracellular location of *B. canis*-GFP in each pattern was unambiguously determined by adding an anti-*B. canis* antibody to nonpermeabilized cells (Fig. 8B). As expected, the extracellular location of the first pattern was demonstrated since bacteria were accessible to the antibody. Concomitantly, the second pattern indeed corresponded to intracellular replicating bacteria since they were not accessible to the antibody.

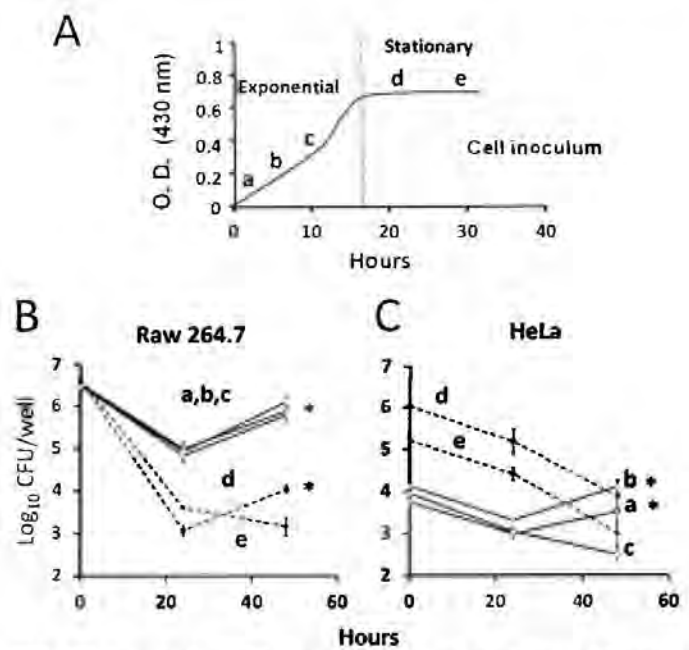


**FIG 6** The growth phase of the bacterial inoculum determines the ability of *B. canis* to replicate intracellularly. (A) *B. canis* cells ( $5 \times 10^9$  CFU) were inoculated into 20 ml of TSB in a 125-ml Erlenmeyer flask and incubated at 37°C and 200 rpm for 30 h. Aliquots were taken at 5, 8, and 12 h (a, b, c), representing exponential-phase conditions, and at 24 and 30 h (d and e), representing stationary-phase conditions. O. D., optical density. Bacteria collected under each condition (a to e) were used to inoculate Raw 264.7 macrophages (MOI, 100 CFU) (B) and HeLa cells (MOI, 500 CFU) (C) in a gentamicin protection assay. At the times indicated, the number of CFU per well was determined. Error bars represent SDs. Data are representative of at least three independent experiments. In panels B and C, statistically significant differences between the 24- and 48-h points for each condition were calculated by Student *t* test. \*, *P* < 0.01.

**Intracellular *B. canis* bacteria are viable and nontoxic.** The viability of the scattered cell-associated and intracellular replicative bacteria was determined in HeLa cells infected with *B. canis* expressing GFP under the control of an ATc-inducible promoter. At 48 h p.i., GFP was induced by the addition of ATc and the samples were examined for fluorescence (Fig. 9A). Scattered cell-associated bacteria did not express GFP upon ATc induction, indicating that they were dead bacteria probably killed by gentamicin. In contrast, intracellular replicative bacteria showed robust expression of GFP after the addition of ATc, demonstrating that they are transcriptionally active and thus were viable organisms. As demonstrated for *B. abortus* (1, 41), intracellular replication of *B. canis* was nontoxic, since mitotic cells with a high number of intracellular *B. canis* bacteria were observed (Fig. 9B). This behavior is in clear opposition to mutant rough brucellae, which are highly toxic to cells (47).

The percentage of cells showing intracellular replicative bacteria at 48 h p.i. was determined in monolayers infected with *B. canis* at different points on the growth curve. This percentage was significantly higher in both cell lines when the inoculum was in early phases of the growth curve than when the inoculum was in the late exponential or stationary phase (Fig. 10), showing a strict correlation with the result obtained with the intracellular growth curves (Fig. 6).

***B. canis* replicates within the endoplasmic reticulum and exits through LAMP1-positive vacuoles.** *B. abortus* replicates inside

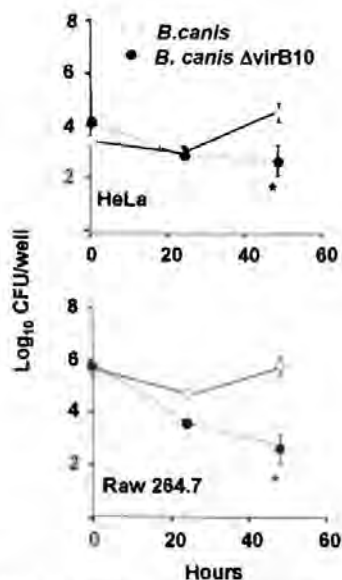


**FIG 7** The *B. canis* virB10 mutant is unable to replicate in HeLa cells and Raw 264.7 macrophages. Early-exponential-phase (5 h) *B. canis* or *B. canis* ΔvirB10 was used to infect HeLa cells (MOI, 500 CFU) or Raw 264.7 macrophages (MOI, 100 CFU) in a gentamicin protection assay. At the times indicated, the number of CFU per well was determined. Error bars represent SDs. Data are representative of at least three independent experiments. Statistically significant differences between the counts achieved by both strains at 48 h were calculated by Student *t* test. \*,  $P < 0.01$ .

the endoplasmic reticulum of its host cell and completes its intracellular cycle by reaching compartments displaying autophagocytic characteristics that allow exodus of the bacterium from the cell (37). We analyzed whether *B. canis* uses the same intracellular pathway. HeLa cells were infected with *B. canis*-GFP grown under conditions that allow intracellular replication. After 48 h of infection, intracellular replicative *B. canis* mostly colocalized with the endoplasmic reticulum marker calnexin, though a small proportion of bacteria was found in LAMP1-positive compartments (Fig. 11A, left side). Despite the low number of cells displaying intracellular replicative bacteria after 72 h of infection, some of them harbored large bacterial clumps inside vacuoles (Fig. 11B) resembling those previously described for *B. abortus* (37). These bacterial clumps were located within large vacuoles devoid of calnexin but surrounded by the LAMP1 marker (Fig. 11A, right side). These LAMP1-positive vacuoles containing bacterial clumps were absent from cells infected with the *B. canis* virB10 mutant or *B. canis* beanCR12 grown under stationary-phase conditions (data not shown).

## DISCUSSION

Similar to rough *B. abortus*, *B. melitensis*, and *B. suis* mutants lacking the O-polysaccharide chain of lipopolysaccharide (LPS), *B. canis* displays an exposed oligosaccharide that cross-reacts with core determinants (29). This "rough-like" phenotype also correlates with higher surface hydrophobicity, greater mucousness, and broader adherence to surfaces and cell membranes than those of smooth virulent brucellae (21, 28). Since the rough mutants are attenuated (48), it may be assumed that the slower-replication profile of *B. canis* in the murine model could be due to the absence of the O chain. Nevertheless and *sensu stricto*, *B. canis* is not a

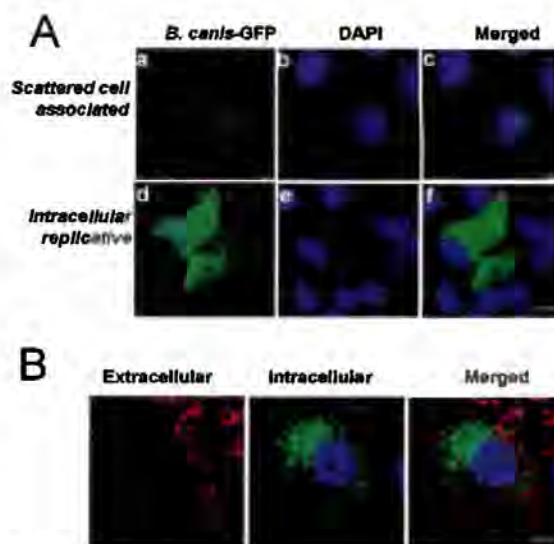


**FIG 8** *B. canis* displays two different patterns of interaction with epithelial cells. (A) HeLa cells were infected at an MOI of 500 CFU with an early-exponential-phase inoculum of *B. canis*-GFP grown under low-aeration conditions as indicated in Fig. 5A. After 48 h of incubation, cells were fixed and their nuclei were stained with 4',6-diamidino-2-phenylindole (DAPI; blue) and visualized by fluorescence microscopy. (A) Two interacting patterns are shown: HeLa cells displaying scattered cell-associated bacteria (a to c) and intracellular replicative bacteria (d and e). (B) At 48 h p.i., living nonpermeabilized HeLa cells were incubated with an antibody to *B. canis* for 30 min at 4°C, followed by an anti-mouse antibody conjugated with Alexa Fluor 594 (Life Technologies). Cells were then fixed, permeabilized, and processed for an immunofluorescence assay. Intracellularly located bacteria are exclusively green (GFP signal), whereas extracellular bacteria are red (anti-*B. canis* signal). Images were contrasted and saturated with the Hue tool to obtain suitable color separation. Scale bars, 5 μm.

rough bacterium and displays significant differences from rough mutants derived from virulent smooth strains. First, it persists in mouse organs, including bone marrow, for a protracted period of time, revealing its ability to maintain a chronic state. Second, *B. canis* is highly infective and virulent for dogs, inducing pathological signs corresponding to brucellosis. Third, *B. canis* is much more resistant than smooth *Brucella* and rough mutants to low pH, complement, hydrogen peroxide, and bactericidal cationic peptides (27), all properties associated with virulence (49, 50). Fourth, *B. canis* induces a lower proinflammatory response than rough *Brucella* mutants in animal models (25), a characteristic linked to its furtive strategy. Fifth, while intracellular *B. canis* is nontoxic to cells, rough *Brucella* mutants induce cell death (47), a trait associated with its intracellular life style. Finally, in contrast to rough mutants but similar to smooth brucellae, *B. canis* penetrates macrophages through lipid rafts (25). Other properties such as iron acquisition and growth metabolic requirements have also been pointed out as relevant differences between *B. canis* and other *Brucella* species (20, 51).

In addition to being highly pathogenic for dogs, *B. canis* is also able to infect humans and eventually cause severe disease (8, 52, 53). Despite this, the bacterium does not induce obvious clinical signs at the onset of infection. The incubation period may last a long time and cause no symptoms before abortion or epididymitis is manifested in dogs. Likewise, experimental infections of monkeys (54) or natural active infections of humans generally last a



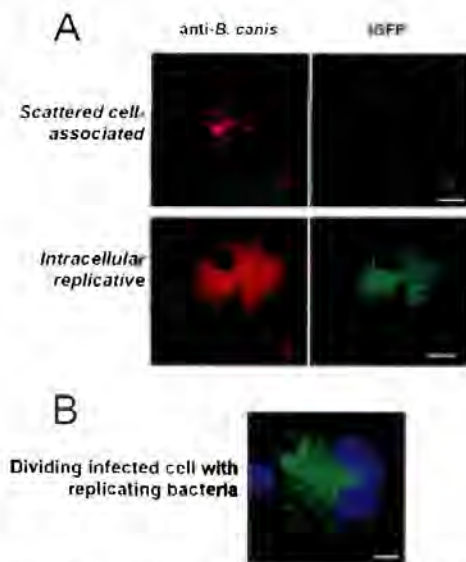


**FIG 9** Intracellular *B. canis* bacteria are viable replicating bacteria. (A) HeLa cells were infected at an MOI of 500 with an early-exponential-phase inoculum of *B. canis*-iGFP grown under low-aeration conditions as indicated in Fig. 5A. This strain harbors ATc-inducible GFP. At 48 h p.i., GFP was induced by ATc addition. The cells were then fixed and visualized by fluorescence microscopy. Note that scattered cell-associated bacteria do not display green fluorescence, indicating that they are dead, while the intracellular type of bacterial cells show green fluorescence, indicating active metabolism. (B) Intracellular *B. canis* (green) is shown replicating in dividing cells. Images were contrasted and saturated with the Hue tool to obtain suitable color separation. Scale bars, 10  $\mu$ m.

long time without any pyogenic signs (16, 17) until the disease is finally manifested. In experimental murine brucellosis, persistence is clearly demonstrated by bone marrow infection at later times, with low cytokine production.

It is therefore evident that *B. canis*, like other virulent brucellae (1, 2), follows a stealth strategy to evade the immune response of its host, mainly during the first stages of infection. However, *B. canis* seems to display even stealthier behavior, since it promotes a lower and slower proinflammatory response than that induced by the classical zoonotic smooth *Brucella* species. Despite inducing significant pathology in dogs, *B. canis* barely promotes altered hematological profiles or signs of endotoxicity. The milder inflammation of the target organs and the smaller amounts of IFN- $\gamma$  induced during *B. canis* infections of mice are in agreement with this proposal. This claim is also endorsed by works demonstrating rather low cytokine induction, even with heat-killed *B. canis* or *B. canis*  $\Delta$ *virB* mutant bacteria (44, 55), absence of macrophage activation (25), and the lower reactive oxygen species response in *B. canis*-infected humans than in those infected with smooth *Brucella* species (56–58)

As in other brucellae, the stealth strategy followed by *B. canis* seems to be linked to the absence of recognition of putative pathogen-associated molecular patterns (PAMPs) as a result of significant changes in the cell envelope components that also allow the bacterium to persist for a longer time (21, 25–29). Moreover, a large proportion of the *B. canis* infecting bacteria that remain extracellularly located are killed, exposing putative intracellular PAMPs; still, the cytokine levels remain low. This phenomenon is reminiscent of the absence of cytokine production after the administration of killed *B. abortus* to mice (1)

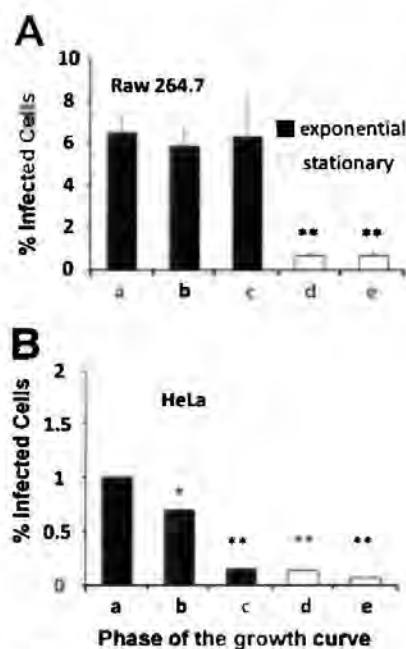


**FIG 10** The growth phase of the bacterial inoculum relates to the ability to detect *B. canis* replicating intracellularly. (A) *B. canis* bacterial cells were grown for 30 h in 20 ml of TSB in a glass Erlenmeyer flask at 200 rpm. Aliquots were taken out at 5, 8, and 12 h (a, b, and c, respectively), representing exponential-phase conditions, and at 24 and 30 h (d and e, respectively), representing stationary-phase conditions, as indicated in the legend to Fig. 6A. Bacteria from each condition (a to e) were used to inoculate cells. The proportions of Raw 264.7 macrophages (B) and HeLa epithelial cells (C) displaying intracellular replicative *B. canis* at 48 h p.i. are shown. Error bars represent SDs. Data are representative of at least three independent experiments. The statistical significance of differences was calculated by Student *t* test. \*,  $P < 0.01$ ; \*\*,  $P < 0.001$  (in relation to inoculum a [early exponential phase]).

In addition to the low proinflammatory response behavior of *B. canis*, the extremely low percentage of individual bacterial cells able to achieve productive intracellular replication, even under optimal *in vitro* growth conditions, seems to be a crucial part of the strategy used by *B. canis*. This low rate of intracellular replication, which still takes place in the same compartments described for smooth brucellae, might contribute to the avoidance of strong activation of the immune response and allow *B. canis* to slowly colonize various organs before effective adaptive immunity develops.

The relevance of the *virB* operon for *B. canis* virulence has been demonstrated before in the mouse model (44), but its participation in the intracellular lifestyle of this species has not. As is the case with other *Brucella* species, this system is an essential component of the achievement of successful intracellular replication of *B. canis* within the endoplasmic reticulum of host cells. We demonstrated that in order to achieve intracellular survival competence, the bacterium requires restricted culture conditions and needs to be in early stages of the growth curve. These conditions may allow the regulation of this injection machinery, as well as other systems important for virulence that impact the expression of the *virB* operon, such as the transcriptional regulator VjBR and the two-component system BvRR/BvRS, before cell infection (59, 60). Alternatively, *B. canis* in late stages of the growth curve may secrete metabolites that would inhibit intracellular replication. Even

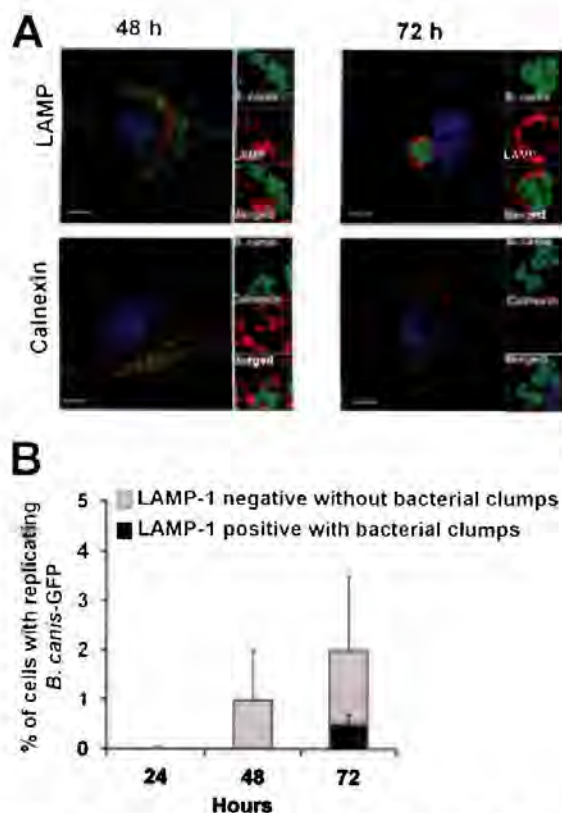


**FIG 11** *B. canis* transits through the endoplasmic reticulum and reaches autophagosome-like vacuoles at late times postinfection. (A) HeLa cells were infected at an MOI of 500 with an early-exponential-phase inoculum of *B. canis*-GFP grown under low-aeration conditions as indicated in Fig 5A. At the times indicated, cells were processed for an immunofluorescence assay with antibodies to LAMP1 (red, top) or calnexin (red, bottom). Cells were visualized by confocal microscopy. Scale bars, 5  $\mu$ m. (B) Percentages of cells displaying intracellular replicative *B. canis* (gray bars) and clumps of bacteria surrounded by LAMP1 (black bars). Images were contrasted and saturated with the Hue tool to obtain suitable color separation. Error bars represent SDs. Data are representative of at least three independent experiments.

though our purpose was not to dissect in molecular and cellular detail the process by which *B. canis* becomes prone to achieve replication in cultured cells, the protocols designed allow further investigation of this relevant mechanism of control of intracellular replication.

The host constraint and cell envelope properties of *B. canis* are partially shared with *Brucella ovis*, an intracellular pathogenic species restricted to sheep that is also devoid of *N*-formylperosamine polysaccharides (61). However, *B. canis* departs from *B. ovis* in many respects, including the antigenicity of its LPS, its host preference, and its zoonotic potential (3, 29). In addition, genetic analysis has indicated that *B. canis* and *B. ovis* emerged as two independent *Brucella* lineages (62). Indeed, the absence of the O-polysaccharide chain linked to the rough LPS corresponds to convergent evolution rather than a common origin of these two species, since *B. ovis* carries a frameshift in *wbkF* (63) and a GI-2 deletion (64) while *B. canis* conserves GI-2 but carries a deletion overlapping *wbkD* and *wbkF* (63).

There is a long history of the coexistence of dogs and humans (65). Still, the reported number of human cases of *B. canis* brucellosis is low. From a practical perspective, it should be noted that

the stealthier strategy and the long incubation period in the absence of obvious clinical signs make it difficult to detect *B. canis* infection. As has been pointed out before, this is aggravated by deficiencies in testing, mainly because of a lack of available diagnostic capabilities that leads to underestimation of the disease (9). As a consequence, a great many infections may go undiagnosed. In addition, the low socioeconomic conditions under which many canine infections have been detected may hamper the diagnosis of the disease, as previously proposed (52).

In conclusion, there are several reports of *Brucella* organisms not replicating intracellularly in *ex vivo* assays (21, 22, 66, 67). In light of the results presented here, the absence of intracellular replication of *Brucella* bacteria in cultured cells should be taken cautiously. There is also an urgent need for the standardization of infection protocols in order to decipher and compare the vast number of published results in brucellosis research.

#### ACKNOWLEDGMENTS

We thank Daphne Garita (Universidad Nacional, Heredia, Costa Rica) for her help in the serological diagnosis of *B. canis* infections. We also thank Nazareth Ruiz-Villalobos (Universidad Nacional, Heredia, Costa Rica) for helping in the MLVA16 characterization of the *B. canis* isolates. We also thank Jean Celli (University of Washington) for providing the GFP-inducible plasmid.

This work was funded by Fondos de Recursos del Sistema FEES/CONARE projects 803-B4-654 and 803-B5-653 ([www.conare.ac.cr](http://www.conare.ac.cr)), Red Temática de Brucelosis, Vice-Presidency for Research, University of Costa Rica, project 803-B3-761 ([www.vinv.ucr.ac.cr](http://www.vinv.ucr.ac.cr)), The National Council of Science and Technology of Costa Rica through FORINVES grant FV-0004-13 ([www.conicit.go.cr](http://www.conicit.go.cr)), and The International Center for Genomic Engineering and Biotechnology, contract CRP/12/007 ([www.icgeb.trieste.it](http://www.icgeb.trieste.it)) Fellowship support for María Concepción Medina from the Teasdale-Corti Project, Honduras-Canada, and fellowship support for Carlos Chacón Díaz from SEP-CONARE are gratefully acknowledged. The funders had no role in study design, data collection and analysis, the decision to publish, or preparation of the manuscript.

#### REFERENCES

- Barquero-Calvo E, Chaves-Olarte E, Weiss DS, Guzmán-Verri C, Chacón-Díaz C, Rucavado A, Moriyón I, Moreno E. 2007. *Brucella abortus* uses a stealthy strategy to avoid activation of the innate immune system during the onset of the infection. *PLoS One* 2:e631. <http://dx.doi.org/10.1371/journal.pone.0000631>.
- Martirosyan A, Moreno E, Gorvel JP. 2011. An evolutionary strategy for a stealthy intracellular *Brucella* pathogen. *Immunol Rev* 240:211–234. <http://dx.doi.org/10.1111/j.1600-065X.2010.00982.x>.
- Moreno E, Moriyón I. 2006. The genus *Brucella*, p 315–456. In Dworkin M, Falkow S, Rosenberg E, Schleifer K-H, Stackebrandt E (ed), *The prokaryotes*, vol 5. Springer Verlag, New York, NY.
- Martirosyan A, Gorvel JP. 2013. *Brucella* evasion of adaptive immunity. *Future Microbiol* 8:147–154. <http://dx.doi.org/10.2217/fmb.12.140>.
- Xavier MJ, Winter MG, Spees AM, Nguyen K, Atluri VL, Silva TM, Bäumlér AJ, Müller W, Santos RL, Tsois RM. 2013. CD4<sup>+</sup> T cell-derived IL-10 promotes *Brucella abortus* persistence via modulation of macrophage function. *PLoS Pathog* 9:e1003454. <http://dx.doi.org/10.1371/journal.ppat.1003454>.
- von Barga K, Gorvel JP, Salcedo S. 2012. Internal affairs: investigating the *Brucella* intracellular lifestyle. *FEMS Microbiol Rev* 36:533–562. <http://dx.doi.org/10.1111/j.1574-6976.2012.00334.x>.
- Swenson RM, Carmichael LE, Cundy KR. 1972. Human infection with *Brucella canis*. *Ann Intern Med* 76:435–438. <http://dx.doi.org/10.7326/0003-4819-76-3-435>.
- Lucero NE, Jacob NO, Ayala SM, Escobar GI, Tuccillo P, Jacques I. 2005. Unusual clinical presentation of brucellosis caused by *Brucella canis*. *J Med Microbiol* 54:505–508. <http://dx.doi.org/10.1099/jmm.0.45928-0>.
- Lucero NE, Corazza R, Almuzara MN, Reynes E, Escobar GI, Boeri

- E, Ayala SM. 2010. Human *Brucella canis* outbreak linked to infection in dogs. *Epidemiol Infect* 138:280–285. <http://dx.doi.org/10.1017/S0950268809990525>.
10. Lucero NE, Escobar GI, Ayala SM, Jacob N. 2005. Diagnosis of human brucellosis caused by *Brucella canis*. *J Med Microbiol* 54:457–461. <http://dx.doi.org/10.1099/jmm.0.45927-0>.
  11. Carmichael LE, Joubert JC. 1988. Transmission of *Brucella canis* by contact exposure. *Cornell Vet* 78:63–73.
  12. Carmichael LE, Kenney RM. 1968. Canine abortion caused by *Brucella canis*. *J Am Vet Med Assoc* 152:605–616.
  13. Moore JA, Kakuk TJ. 1969. Male dogs naturally infected with *Brucella canis*. *J Am Vet Med Assoc* 155:1352–1358.
  14. Ayala SM, Hasan DB, Celestino CA, Escobar GI, Zhao DM, Lucero NE. 2014. Validation of a simple universal IELISA for the diagnosis of human brucellosis. *Eur J Clin Microbiol Infect Dis* 33:1239–1246. <http://dx.doi.org/10.1007/s10096-014-2066-2>.
  15. Di D, Cui B, Wang H, Zhao H, Piao D, Tian L, Tian G, Kang J, Mao X, Zhang X, Du P, Zhu L, Zhao Z, Mao L, Yao W, Guan P, Fan W, Jiang H. 2014. Genetic polymorphism characteristics of *Brucella canis* isolated in China. *PLoS One* 9:e84862. <http://dx.doi.org/10.1371/journal.pone.0084862>.
  16. Olivera M, Di-Lorenzo C. 2009. Aislamiento de *Brucella canis* en un humano conviviente con caninos infectados. Informe de un caso. *Colomb Med* 40:218–220.
  17. Polt SS, Dismukes WE, Flint A, Schaefer J. 1982. Human brucellosis caused by *Brucella canis*: clinical features and immune response. *Ann Intern Med* 97:717–719. <http://dx.doi.org/10.7326/0003-4819-97-5-717>.
  18. Gyurancz M, Szeredi L, Rónai Z, Dénes B, Dencso L, Dán Á, Pálmai N, Hauser Z, Lami E, Makrai L, Erdélyi K, Jánosi S. 2011. Detection of *Brucella canis*-induced reproductive diseases in a kennel. *J Vet Diagn Invest* 23:143–147. <http://dx.doi.org/10.1177/104063871102300127>.
  19. Caron E, Liautard JP, Köhler S. 1994. Differentiated U937 cells exhibit increased bactericidal activity upon LPS activation and discriminate between virulent and avirulent *Listeria* and *Brucella* species. *J Leukoc Biol* 56:174–181.
  20. Eskra L, Covert J, Glasner J, Splitter G. 2012. Differential expression of iron acquisition genes by *Brucella melitensis* and *Brucella canis* during macrophage infection. *PLoS One* 7:e31747. <http://dx.doi.org/10.1371/journal.pone.0031747>.
  21. Detilleux PG, Deyoe BL, Chevillat NF. 1990. Entry and intracellular location of *Brucella* spp. in Vero cells: fluorescence and electron microscopy. *Vet Pathol* 27:317–328.
  22. Rittig MJ, Kauffmann A, Robins A, Shaw B, Sprenger H, Gemsa D, Foulongne V, Rouot B, Dornand J. 2003. Smooth and rough lipopolysaccharide types of *Brucella* induce different intracellular trafficking and cytokine/chemokine release in human monocytes. *J Leukoc Biol* 74:1045–1055. <http://dx.doi.org/10.1189/jlb.0103015>.
  23. Delpino MV, Fossati CA, Baldi PC. 2009. Proinflammatory response of human osteoblastic cell lines and osteoblast-macrophage interaction upon infection with *Brucella* spp. *Infect Immun* 77:984–995. <http://dx.doi.org/10.1128/IAI.01259-08>.
  24. Ferrero MC, Fossati CA, Baldi PC. 2009. Smooth *Brucella* strains invade and replicate in human lung epithelial cells without inducing cell death. *Microbes Infect* 11:476–483. <http://dx.doi.org/10.1016/j.micinf.2009.01.010>.
  25. Martín-Martín AI, Vizcaíno N, Fernández-Lago L. 2010. Cholesterol, ganglioside GM1 and class A scavenger receptor contribute to infection by *Brucella ovis* and *Brucella canis* in murine macrophages. *Microbes Infect* 12:246–251. <http://dx.doi.org/10.1016/j.micinf.2009.12.008>.
  26. Dees SB, Hollis DG, Weaver RE, Moss CW. 1981. Cellular fatty acids of *Brucella canis* and *Brucella suis*. *J Clin Microbiol* 14:111–112.
  27. Martín-Martín AI, Sancho P, Tejedor C, Fernández-Lago L, Vizcaíno N. 2011. Differences in the outer membrane-related properties of the six classical *Brucella* species. *Vet J* 189:103–105. <http://dx.doi.org/10.1016/j.tvjl.2010.05.021>.
  28. Martínez de Tejada G, Moriyón I. 1993. The outer membranes of *Brucella* spp. are not barriers to hydrophobic permeants. *J Bacteriol* 175:5273–5275.
  29. Moreno E, Jones LM, Berman DT. 1984. Immunochemical characterization of rough *Brucella* lipopolysaccharides. *Infect Immun* 43:779–782.
  30. Lumsden JH, Mullen K, McSherry BJ. 1979. Canine hematology and biochemistry reference values. *Can J Comp Med* 43:125–131.
  31. López-Goñi I, García-Yoldi D, Marín CM, de Miguel MJ, Barquero-Calvo E, Guzmán-Verri Albert D, Garin-Bastuji B. 2011. New Brucella ladder multiplex PCR assay for the biovar typing of *Brucella suis* and the discrimination of *Brucella suis* and *Brucella canis*. *Vet Microbiol* 154:152–155. <http://dx.doi.org/10.1016/j.vetmic.2011.06.035>.
  32. Scott J, Koylass MS, Stubberfield MR, Whatmore A. 2007. Multiplex assay based on single-nucleotide polymorphism for rapid identification of *Brucella* isolates at the species level. *Appl Environ Microbiol* 73:7331–7337. <http://dx.doi.org/10.1128/AEM.00976-07>.
  33. Alton GG, Jones L, Verger A. 1988. Techniques for the brucellosis laboratory. Institut National de la Recherche Agronomique, Paris, France.
  34. Le Flèche P, Jacques I, Grayon M, Al Dahouk S, Bouchon P, Denoëud F, Nockler K, Neubauer H, Guilloteau L, Vergnaud G. 2006. Evaluation and selection of tandem repeat loci for a *Brucella* MLVA typing assay. *BMC Microbiol* 6:9. <http://dx.doi.org/10.1186/1471-2180-6-9>.
  35. Conde-Álvarez R, Grilló MJ, Salcedo de Miguel S, Fugier MJ, Gorvel E, Moriyón JP, Iriarte I, M. 2006. Synthesis of phosphatidylcholine, a typical eukaryotic phospholipid, is necessary for full virulence of the intracellular bacterial parasite *Brucella abortus*. *Cell Microbiol* 8:1322–1335. <http://dx.doi.org/10.1111/j.1462-5822.2006.00712.x>.
  36. Chacón-Díaz C, Muñoz-Rodríguez M, Barquero-Calvo E, Guzmán-Verri C, Chaves-Olarte E, Grilló MJ, Moreno E. 2011. The use of green fluorescent protein as a marker for *Brucella* vaccines. *Vaccine* 29:577–582. <http://dx.doi.org/10.1016/j.vaccine.2010.09.109>.
  37. Starr T, Child R, Wehrly TD, Hansen B, Hwang S, López-Otin C, Virgin HW, Celli J. 2012. Selective subversion of autophagy complexes facilitates completion of the intracellular cycle. *Cell Host Microbe* 11:33–45. <http://dx.doi.org/10.1016/j.chom.2011.12.002>.
  38. Barquero-Calvo E, Chacón-Díaz C, Chaves-Olarte E, Moreno E. 2013. Bacterial counts in spleen. *Bio Protoc* 3:e954. <http://www.bio-protocol.org/e954>.
  39. Grilló MJ, Manterola L, de Miguel MJ, Muñoz P, Blasco JM, Moriyón I, López-Goñi. 2006. Increases of efficacy as vaccine against *Brucella abortus* infection in mice by simultaneous inoculation with avirulent smooth bvrS/bvrR and rough wbkA mutants. *Vaccine* 24:2910–2916. <http://dx.doi.org/10.1016/j.vaccine.2005.12.038>.
  40. Aughey E, Frye FL. 2001. Comparative veterinary histology: with clinical correlates. Manson Publishing, London, England.
  41. Chaves-Olarte E, Guzmán-Verri C, Méresse S, Desjardins M, Pizarro-Cerdá J, Badilla J, Gorvel JP, Moreno E. 2002. Activation of Rho and Rab GTPases dissociates *Brucella abortus* internalization from intracellular trafficking. *Cell Microbiol* 4:663–676. <http://dx.doi.org/10.1046/j.1462-5822.2002.00221.x>.
  42. Martínez-Núñez C, Altamirano-Silva P, Alvarado-Guillén F, Moreno E, Guzmán-Verri C, Chaves-Olarte E. 2010. The two-component system BvrR/BvrS regulates the expression of the type IV secretion system VirB in *Brucella abortus*. *J Bacteriol* 192:5603–5608. <http://dx.doi.org/10.1128/JB.00567-10>.
  43. Pizarro-Cerdá J, Moreno E, Sanguedolce V, Mege JL, Gorvel JP. 1998. Virulent *Brucella abortus* prevents lysosome fusion and is distributed within autophagosome-like compartments. *Infect Immun* 66:2387–2392.
  44. Palomares-Resendiz E, Arellano-Reynoso B, Hernández-Castro R, Tenorio-Gutiérrez V, Salas-Téllez E, Suárez-Güemes F, Díaz-Aparicio E. 2012. Immunogenic response of *Brucella canis* virB10 and virB11 mutants in a murine model. *Front Cell Infect Microbiol* 2:35. <http://dx.doi.org/10.3389/fcimb.2012.00035>.
  45. Grilló MJ, Blasco JM, Gorvel JP, Moriyón I, Moreno E. 2012. What have we learned from brucellosis in the mouse model? *Vet Res* 43:29. <http://dx.doi.org/10.1186/1297-9716-43-29>.
  46. Baldwin CL, Goenka R. 2006. Host immune responses to the intracellular bacteria *Brucella*: does the bacteria instruct the host to facilitate chronic infection? *Crit Rev Immunol* 26:407–442. <http://dx.doi.org/10.1615/CritRevImmunol.v26.i5.30>.
  47. Pei J, Turse JE, Wu Q, Ficht TA. 2006. *Brucella abortus* rough mutants induce macrophage oncosis that requires bacterial protein synthesis and direct interaction with the macrophage. *Infect Immun* 74:2667–2675. <http://dx.doi.org/10.1128/IAI.74.5.2667-2675.2006>.
  48. González D, Grilló MJ, de Miguel MJ, Ali T, Arce-Gorvel V, Delrue RM, Conde-Álvarez R, Muñoz P, López-Goñi I, Iriarte M, Marín CM, Weintraub A, Widmalm G, Zygmunt M, Letesson JJ, Gorvel JP, Blasco JM, Moriyón I. 2008. Brucellosis vaccines: assessment of *Brucella melitensis* lipopolysaccharide rough mutants defective in core and O-polysaccharide synthesis and export. *PLoS One* 3:e2760. <http://dx.doi.org/10.1371/journal.pone.0002760>.

49. Martínez de Tejada G, Pizarro-Cerdá J, Moreno E, Moriyón I. 1995. The outer membranes of *Brucella* spp. are resistant to bactericidal cationic peptides. *Infect Immun* 63:3054–3061.
50. Freer E, Moreno E, Moriyón I, Pizarro-Cerdá J, Weintraub A, Gorvel JP. 1996. *Brucella-Salmonella* lipopolysaccharide chimeras are less permeable to hydrophobic probes and more sensitive to cationic peptides and EDTA than are their native *Brucella* sp. counterparts. *J Bacteriol* 178:5867–5876.
51. Jenner DC, Dassa E, Whatmore AM, Atkins HS. 2009. ATP-binding cassette systems of *Brucella*. *Comp Funct Genomics* 2009:354649. <http://dx.doi.org/10.1155/2009/354649>.
52. Krueger WS, Lucero NE, Brower A, Heil GL, Gray GC. 2014. Evidence for unapparent *Brucella canis* infections among adults with occupational exposure to dogs. *Zoonoses Public Health* 61:509–518. <http://dx.doi.org/10.1111/zph.12102>.
53. Marzetti S, Carranza C, Roncallo M, Escobar GI, Lucero NE. 2013. Recent trends in human *Brucella canis* infection. *Comp Immunol Microbiol Infect Dis* 36:55–61. <http://dx.doi.org/10.1016/j.cimid.2012.09.002>.
54. Percy D, Egwu HI, Jonas AM. 1972. Experimental *Brucella canis* infection in the monkey (*Macaca arctoides*). *Can J Comp Med* 36:221–225.
55. Clausse M, Díaz AG, Ghersi G, Zylberman V, Cassataro J, Giambartolomei GH, Goldbaum FA, Estein SM. 2013. The vaccine candidate BLSOmp31 protects mice against *Brucella canis* infection. *Vaccine* 31:6129–6135. <http://dx.doi.org/10.1016/j.vaccine.2013.07.041>.
56. Karsen H, Karahocagil MK, Akdeniz H, Ceylan MR, Binici I, Selek S, Celik H. 2011. Serum paraoxonase and arylesterase activities and oxidant status in patients with brucellosis. *Afr J Microbiol Res* 5:1701–1706. <http://dx.doi.org/10.5897/AJMR11.438>.
57. Serefhanoglu K, Taskin A, Turan H, Timurkaynak FE, Arslan H, Erel O. 2009. Evaluation of oxidative status in patients with brucellosis. *Braz J Infect Dis* 13:249–251. <http://dx.doi.org/10.1590/S1413-86702009000400001>.
58. Ustaa M, Arasb Z, Tasc A. 2012. Oxidant and antioxidant parameters in patients with *Brucella canis*. *Clin Biochem* 45:366–367. <http://dx.doi.org/10.1016/j.clinbiochem.2011.12.028>.
59. Sola-Landa A, Pizarro-Cerdá J, Grilló MJ, Moreno E, Moriyón I, Blasco JM, Gorvel JP, López-Goñi I. 1998. A two-component regulatory system playing a critical role in plant pathogens and endosymbionts is present in *Brucella abortus* and controls cell invasion and virulence. *Mol Microbiol* 29:125–138. <http://dx.doi.org/10.1046/j.1365-2958.1998.00913.x>.
60. Uzureau S, Godefroid M, Deschamps C, Lemaire J, De Bolle X, Letesson JJ. 2007. Mutations of the quorum sensing-dependent regulator VjbR lead to drastic surface modifications in *Brucella melitensis*. *J Bacteriol* 189:6035–6047. <http://dx.doi.org/10.1128/JB.00265-07>.
61. Silva TM, Mol JP, Winter MG, Atluri V, Xavier MN, Pires SF, Paixão TA, Andrade HM, Santos RL, Tsolis RM. 2014. The predicted ABC transporter AbcEDCBA is required for type IV secretion system expression and lysosomal evasion by *Brucella ovis*. *PLoS One* 9:e114532. <http://dx.doi.org/10.1371/journal.pone.0114532>.
62. Zygmunt MS, Blasco JM, Letesson JJ, Cloeckaert A, Moriyón I. 2009. DNA polymorphism analysis of *Brucella* lipopolysaccharide genes reveals marked differences in O-polysaccharide biosynthetic genes between smooth and rough *Brucella* species and novel species-specific markers. *BMC Microbiol* 9:92. <http://dx.doi.org/10.1186/1471-2180-9-92>.
63. Vizcaino N, Caro-Hernandez P, Cloeckaert A, Fernandez-Lago L. 2004. DNA polymorphism in the omp25/omp31 family of *Brucella* spp. identification of a 1.7-kb inversion in *Brucella cetaceae* and of a 15.1-kb genomic island, absent from *Brucella ovis*, related to the synthesis of smooth lipopolysaccharide. *Microbes Infect* 6:821–824. <http://dx.doi.org/10.1016/j.micinf.2004.04.009>.
64. Mancilla M, López-Goñi I, Moriyón I, Zárrega AM. 2010. Genomic island 2 is an unstable genetic element contributing to *Brucella* lipopolysaccharide spontaneous smooth-to-rough dissociation. *J Bacteriol* 192:6346–6351. <http://dx.doi.org/10.1128/JB.00838-10>.
65. Thalmann O, Shapiro B, Cui P, Schuenemann VJ, Sawyer SK, Greenfield DL, Germonpré MB, Sablin MV, López-Giráldez F, Domingo-Roura X, Napierala H, Uerpmann HP, Loponte DM, Acosta AA, Giemsch L, Schmitz RW, Worthington B, Buikstra JE, Druzhkova A, Graphodatsky AS, Ovodov ND, Wahlberg N, Freedman AH, Schweizer RM, Koepfli KP, Leonard JA, Meyer M, Krause J, Pääbo S, Green RE, Wayne RK. 2013. Complete mitochondrial genomes of ancient canids suggest a European origin of domestic dogs. *Science* 342:871–874. <http://dx.doi.org/10.1126/science.1243650>.
66. Maquart M, Zygmunt MS, Cloeckaert A. 2009. Marine mammals *Brucella* isolates with different genomic characteristics display a differential response when infecting human macrophages in culture. *Microbes Infect* 11:361–366. <http://dx.doi.org/10.1016/j.micinf.2008.12.012>.
67. Larsen AK, Nymo IH, Briquemont B, Sorensen KK, Godfroid J. 2013. Entrance and survival of *Brucella pinnipedialis* hooded seal strain in human macrophages and epithelial cells. *PLoS One* 8:e84861. <http://dx.doi.org/10.1371/journal.pone.0084861>.